2014-01-17

Phase Behavior Modeling of Complex Hydrocarbon Systems Applicable to Solvent Assisted Recovery Processes

Bayestehparvin, Bita

UNIVERSITY OF CALGARY

Phase Behavior Modeling of Complex Hydrocarbon Systems Applicable to Solvent Assisted Recovery Processes

by

Bita Bayestehparvin

A THESIS

SUBMITTED TO THE FACULTY OF GRADUATE STUDIES

IN PARTIAL FULFILMENT OF THE REQUIREMENTS FOR THE

DEGREE OF MASTER OF SCIENCE

DEPARTMENT OF CHEMICAL AND PETROLEUM ENGINEERING

CALGARY, ALBERTA

JANUARY, 2014

Abstract

Solvent assisted recovery processes have taken significant attention recently. It has been shown that co-injection of solvent and steam can increase bitumen production to a rate higher than steam injection alone. The major shortcoming in this area is the lack of basic knowledge relevant to the solvent/heat assisted recovery processes. The objective of this project is to develop an understanding of the phase behaviour of bitumen/solvent systems with four milestones. First, a phase behaviour model based on the Peng-Robinson equation of state has been developed and validated for simple systems. Second, the available mixing rules for computing the co-volumes of polar and non-polar mixtures were evaluated. Third, bitumen was characterized in order to estimate its critical properties based on the boiling point distribution from the simulated distillation data. The boiling point distribution was modeled using probability distribution functions. Finally, the results for the phase behaviour of solvent (e.g. methane, ethane and carbon dioxide)/bitumen (Athabasca, Cold Lake) systems were modeled with an EoS for different operating conditions.

Acknowledgments

This thesis would not have been possible without the generous contributions of many people through academic advising, mentoring, research guidance, and the moral support that is so indispensable for the focus and resilience of all graduate students.

I would like to express my profound gratitude to my supervisor, Dr. Jalal Abedi for his support, patience, and encouragement throughout my graduate studies. It is not often that one finds an advisor and colleague who always find the time to listen to the little problems and roadblocks that crop up in the period of performing research. Without his technical and editorial advice, this study would never have been completed.

I wish to thank the members of my examining committee, Dr. Jocelyn L Grozic, Dr. Gordon R. Moore, and Dr. Long X Nghiem, for their valuable time and comments. The constructive comments and support provided by Dr. Hassan Hassanzadeh are also highly appreciated.

Special thanks go to my colleague and friend in the SHARP (Solvent Heated Assisted Recovery Process) research group, Hossein Nourozieh, for his valuable discussion on technical issues and PVT modeling throughout my project. I appreciate the resources, direction, and penetrating criticism he provided.

I also wish to express thanks for all of the administrative support offered by the Department of Chemical and Petroleum Engineering staff at the University of Calgary and for their kind and friendly attitude. I had the pleasure of working with colleagues at the University of Calgary. The assistance and moral support from my friends and fellow graduate students in the Department of Chemical and Petroleum Engineering is highly appreciated. I would like to thank all of my friends, in particular; Vahid Asili, Bahareh Azinfar, Mingxu Ma, Maryam Moghadasi, Saina Nourozieh, Hashem Salari, Fakhry Seyedeyn-Azad, AmirAhmed ShirazиManesh, Saeed Taheri and Mohsen Zirrahi for their continued friendship and support. Our friendships are one of the most important treasures in my life.

I wish to express my appreciation for the financial support of all of the member companies in the SHARP Research Consortium: Alberta Innovates Energy and Environment Solutions, Chevron Energy Technology Co., Computer Modelling Group Ltd., ConocoPhillips Canada, Devon Canada Co., Foundation CMG, Husky Energy, Japan Canada Oil Sands Ltd., Laricina Energy, Brion Energy Corp., Nexen Inc., Natural Sciences and Engineering Research Council of Canada (NSERC), OSUM Oil Sands Co., Penn West Energy, Statoil Canada Ltd., Suncor Energy, and Total E&P Canada.

Finally, I would like to thank my family for their continued moral support, especially my parents and my brother, Babak, who continuously supported me during my studies. My deepest gratitude goes to my husband Mohammad for his understanding, cooperation, and patience. Thank you for being there for me on this difficult road. It means so much to have you by my side in all moments and thank you for believing in me and showing me the possibility of making the impossible, possible.

For Mohammad

Table of Contents

List of Tables

List of Figures

List of Symbols, Abbreviations, and Nomenclature

Uppercase

A	Dimensionless attractive term parameter of equation of state
$\tilde{A}$	Helmholtz free energy
B	Dimensionless repulsive term parameter of equation of state
C	Numerical constant for Wong-Sandler
D	Summation term defined in Wong-Sandler mixing rule
E	Excess property
G	Gibbs energy
I_{ij}	Second binary interaction coefficient
I_{ij}^{0}	Temperature independent second binary interaction coefficient parameter
I_{ij}^{1}	Temperature dependent second binary interaction coefficient parameter
I_{ij}^{2}	Temperature dependent second binary interaction coefficient parameter
J	Jacobian
K	Equilibrium ratio
K_{ij}^{0}	Temperature independent first binary interaction coefficient parameter
K_{ij}^{1}	Temperature dependent first binary interaction coefficient parameter
K_{ij}^{2}	Temperature dependent first binary interaction coefficient parameter
N_g	Number of pseudo-components
P	Pressure
Q	Quadratic sum of second virial coefficient
R	Gas constant
S	Total entropy
S_E	Volume shift parameter
S_E^{1}	Temperature dependent volume shift parameter
S_E^{2}	Temperature dependent volume shift parameter
T	Temperature
V	Volume
Z	Compressibility factor

Lowercase

A	Attractive term parameter of equation of state
B	Repulsive term (co-volume) parameter of equation of state
c_i	Correction term for volume shift
F	Fugacity
G	Local composition factor for the NRTL model
N	Mole or carbon number
n_c	Number of component
n_p	Number of data point
V	Molar volume
Wt	Weight fraction
X	Solvent mole fraction in liquid phase
Y	Mole fraction in gas phase
Z	Initial mole fraction

Scripts

∞	Infinite pressure state
B	Boiling point (subscript)
C	Critical
Cal	Calculated value
Cor	Corrected
Exp	Experimental data
G	Gas phase
L	Liquid phase
M	Mixture
T	Matrix transpose

Greek

ξ	Parameter in Twu (1983) correlation
ζ	Parameter in Twu (1983) correlation

τ	NRTL model binary interaction parameter
φ	Fugacity coefficient
α	Temperature dependency coefficient of attractive term
Ψ	Regression parameter in volume shift correlation
ρ	Saturated density
χ	Temperature independent volume shift parameter
μ	Chemical potential
μ_c	Damping parameter in Levenberg-Marquardt algorithm
B	Mean value parameter of gamma distribution function
Γ	Shape factor parameter in gamma distribution function
E	Error
H	Lowest molecular weight in gamma distribution function
Θ	Regression parameter in Chueh and Prausnitz (1967) model
Ω	Acentric factor

Abbreviation

AARD	Absolute average relative deviation
BI	Binary interaction coefficient
EoS	Equation of state
LLE	Liquid-liquid equilibrium
L_{Mw}	Limiting molecular weight
Mw	Molecular weight
NRTL	Non-random two-liquid model
OF	Objective function
PC	Pseudo-component
PR	Peng-Robinson equation of state
SCN	Single carbon number
SG	Specific gravity
SSI	successive substitution iteration
TBP	True boiling point
TPG	Three-parameter gamma function

VDW1P	Van der Waals mixing rule with one regression parameter
VDW2P	Van der Waals mixing rule with two regression parameters
VLE	Vapour-liquid equilibrium
WS	Wong-Sandler mixing rule

Chapter 1: Introduction

Among the energy sources, crude oils provide 34% of the world's energy needs and are considered a vital source of energy (International Energy Agency 2008). In spite of the growth in alternative energy sources, crude oils are expected to remain essential to industry. However, depending on the properties of crude oil, the production and processing can be different. The United States Geological Survey (2006) classified crude oils into the following three main categories:

Table 1-1: Definition of crude oils based on viscosity, density and API gravity at 15.6 ^{o}C at atmospheric pressure (USGS)

Type	Viscosity(cp)	Density(kg/m^3)	API Gravity (^{o}API)
Conventional oil	$<10^2$	<934	>20
Heavy oil	10^2-10^5	934-1000	10-20
Bitumen	$>10^5$	>1000	<10

Currently, 90% of world's oil production is from conventional oils. The global demand for oil is increasing, but the rate of discovery of new conventional oil reserves is decreasing. Thus Heavy oil and bitumen reserves have been considered as an alternative candidate to conventional oil reserves. Canada is a pioneer in bitumen production and 98% of Canadian oil reserves are oil sands. Canada's oil sands reserves are the third largest in the world after Saudi Arabia and Venezuela. However, bitumen production is challenging and requires specialized techniques.

Although heavy oil is available, it is not easy to produce. In order for the oil to be mobile it must have a low enough viscosity to move along production wells (Gates 2010). For example, in Expanding-Solvent SAGD (ES-SAGD), the solvent reduces the viscosity of the oil by diluting the bitumen and changing its composition (Gates 2010).

The design and development of heavy oil processes, including separation and upgrading of petroleum products and enhanced oil recovery techniques, require accurate predictions of phase equilibria and mutual solubility of different solvents e.g. light gases in heavy hydrocarbons (Fink 2011). Solvent-based recovery processes suffers from limited fundamental and basic data.

Experimental measurements, molecular simulation, empirical correlations, and equation of state (EoS) modeling are examples of approaches used to obtain phase equilibrium information and overcome this lack of data. Experiments in spite of their accuracy are expensive and time-consuming and it is not feasible to obtain experimental data for all possible mixtures over wide ranges of pressures and temperatures. Molecular simulation is a theoretical approach that is hindered by high computational complexity. Depending on the system under study, the execution time is a function of the molecular size and structure. This issue makes molecular simulation impractical for the chemical and petroleum industries. Empirical correlations are commonly developed on the basis of experimental data and are only applicable for a specified system over a limited range of conditions.

The most popular approach for phase behaviour study is the application of equations of state (EoS). EoSs are developed for three purposes. The first is to generate phase equilibrium data for interpolation, and to calculate integration and differential. Then they can be used to predict the volumetric properties of substances and finally to describe vapour-liquid equilibrium (Tsonopoulos, 1969). EoSs can be applied to calculate properties in one phase, two phase, or even multiphase systems. Their application and simplicity have led to proposal of a variety of empirical, semi empirical, and even theoretical EoSs during the past couple of decades (Wang 2002). Among the EoSs, the Peng Robinson (PR) and Soave Redlich Kwong (SRK) have the widest applications to industry. This can be attributed to their ability to define the relationship between temperature, pressure, and phase composition in binary and multiphase systems with sufficient accuracy with a simple function. Limited input data of a few numbers for the critical properties and acentric factors, making these EoSs popular for use in a wide range of components with short execution time (Wang 2002).

Bitumen consists of hundreds of components, which have different structural and chemical properties. Its fractions can be saturated (paraffin, cycloparaffin), aromatics, and even more complex components like resins, which are aromatics that are soluble in *n*-pentane but insoluble

in propane. Bitumen also contains asphaltene, which consists of thousands of chemical components and has a structure that is not yet defined (Speight 2010). The properties of the constituents of bitumen must be defined as input data for any model used to predict phase behaviour. However, there is no separation technique capable of identifying all of these components. Additionally, phase behaviour prediction of such a huge system using an EoS requires a strong processor and long execution time. These two reasons limit the number of identified components. Nevertheless, bitumen is defined as a mixture of pseudo-components with a defined boiling point interval.

To model the phase behaviour of a bitumen containing system, bitumen must be characterized into pseudo-components with defined physical and chemical properties. During characterization, the original fluid is separated into groups with specified properties, which represent the behaviour of the original fluid. The acentric factor and critical properties of the heavy pure components (n>100) are unknown. Thus, the characterization is not limited to fractions and should be completed for heavy pure components as well (Riazi 2005).

Experimental methods for the characterization of heavy oils and bitumen include gas chromatography, simulated distillation, and vacuum distillation. These methods are time consuming, costly, and may cause cracking or decomposition of the bitumen's components by increasing the temperature. Gas chromatography (GC) is a cheaper alternative to the TBP test and can identify the mass of the C_{7+} fraction (Whitson and Brule 2000). A correlation must be used to calculate key properties such as the specific gravity and the normal boiling point. The bitumen can be partially characterized by the experimental method and modeling is required for complete characterization.

Discrete and continuous methods are two different approaches used to describe heavy oil fluid (Danesh 1998). The discrete description method like the single carbon number (SCN) function models the heavy portion of the oil by a number of SCNs and is only valid for integer carbon

numbers. Continuous models focus on all SCN groups and can be used in both characterization and continuous thermodynamics.

The main goal of this study is to generate a stepwise bitumen characterization scheme and phase behaviour study of different solvent/bitumen systems. My research as part of the solvent heated recovery process (SHARP) research consortium aims at providing thermodynamic data needed in solvent-assisted bitumen recovery processes.

This chapter presents a brief introduction about the importance of phase behaviour. The difficulties for modeling bitumen containing systems and the objectives of the study are explained. The second chapter presents a comprehensive literature review. The history of EoS creation from the simple van der Waals EoS to more complex multiparameter equations is investigated. The problems and limitations of different EoSs and their modifications for different conditions are discussed. Finally, a summary of the background of phase behaviour modeling for bitumen containing systems and characterization schemes is presented.

The concept of equilibria and its criteria for any system is discussed in the third chapter. The chapter explains the PR EoS and its application for mixtures using different random and non-random mixing rules. Different correlations for the binary interaction coefficient and volume shift are proposed to improve the vapour-liquid equilibria (VLE) prediction of the EoSs. The application of these correlations in the flash calculation is investigated and the Levenberg-Marquardt regression method algorithm was used for finding the regression parameters. The molar distribution of conventional and heavy oils is compared and a stepwise scheme for bitumen characterization is presented. Finally, the developed code is validated and the simple binary systems are examined.

The gamma distribution function was used to extrapolate the TBP curve for Athabasca and Cold Lake bitumen in the fourth chapter. The efficiency of different critical properties, correlations, and lumping schemes were compared and, based on the best selected correlation, the characterization of Athabasca and Cold Lake bitumen is presented. The proposed

characterization, coupled with different mixing rules, was used to model the phase behaviour of different solvent/bitumen systems. The volume shift concept was used for modeling the saturated density and the temperature dependent volume shift correlation is proposed. Finally, by considering bitumen as one pseudo-component, the efficiency of the Wong-Sandler mixing rule is analyzed. In the last chapter, the results are summarized and the conclusion is presented. Some ideas are suggested for future works.

Chapter 2: Literature Review

Van der Waals equation of state (EoS) (1873) was followed by several other attempts to improve phase behaviour prediction via EoS. The produced EoS models can be categorized into different groups including cubic EoS. Despite its two parameter simplicity, the Peng Robinson (PR) cubic EoS model is able to successfully model the phase behaviour of different systems. Unfortunately, the phase behaviour prediction of heavy oils and bitumen is not straightforward and the bitumen must be characterized. This chapter reviews the development of different EoS models with a focus on cubic EoS. Previous efforts to characterize heavy oil and bitumen are also summarized. Finally the applications of each method for different systems have been reviewed.

2.1. Equation of State (EoS)

Van der Waals (1873) modified the ideal gas law and developed his EoS based on the assumption of non-zero volume and a pairwise attractive inter-particle force. After the development of the van der Waals EoS, Onnes (1909) proposed virial EoS, which defined the compressibility factor as a power function of density. Despite its advantages, virial EoS was unable to predict multiphase behaviour. Beattie and Bridgeman (1927) developed a five parameter EoS which successfully predicted volumetric behaviour except in critical regions (Atilhan 2004). Benedict et al. (1940) presented the Benedict-Webb-Rubin (BWR) multiparameter EoS, which was accurate in the critical region and for the supercritical components. In spite of its successful application, the large number of adjustable parameters made their EoS impractical for mixtures (Wei and Sadus 2000).

Redlich and Kwong (1949) proposed a two parameter EoS that was based on the addition of a temperature dependent term to the van der Waals EoS. The Redlich and Kwong EoS was tested by many researchers (Chueh and Prausnitz 1967 (a, b), Carnahan and Starling 1972, Abbott 1979

and Spear et al. 1971) for different pure, binary, and ternary systems of polar or symmetric components. The results determined that the Redlich and Kwong EoS accurately models the phase behaviour of both vapour and liquid phases. The contribution of the repulsive parameter of the van der Waals EoS to entropy is accurate only at low density. Therefore, Guggenheim (1965) tested four different functions for the repulsive parameter to improve the prediction. Carnahan and Starling (1969) modified the virial series of rigid spheres by considering geometric form and modifying the repulsive term to propose an EoS that is more accurate for hard sphere molecules.

Later, Soave (1972) modified the Redlich-Kwong EoS by suggesting a general temperature-dependent parameter to improve the calculation of saturated pressure for pure substances. In spite of its strength, the modified EoS faced some weaknesses. One of the major problems was its failure to predict liquid densities. In fact, it always predicts specific volumes, greater than the experimental values (Peng and Robinson 1976). Peng and Robinson (1976) modified the Redlich-Kwong EoS and proposed an EoS model to improve the liquid density and vapour pressure predictions of the van der Waals EoS. The predicted critical compressibility was closer to the experimental value leading to improved density calculation near the critical point. The PR EoS is equally or more accurate than the Soave-Redlich-Kwong (SRK) for the prediction of the phase and volumetric behaviour of binary, ternary, and multi-component systems (Wei and Sadus 2000).

Han et al. (1988) compared the VLE prediction of seven different EoS models and found that the PR EoS provides superior predictions for mixtures containing hydrogen or nitrogen. Stryjek and Vera (1986) modified the temperature dependent function in the PR EoS to make it applicable to systems containing polar components. Introducing a third parameter to van der Waals's attraction term resulted in an EoS model proposed by Patel and Teja's (1982), with the ability to predict an adjustable critical compressibility factor rather than fixed values. Their proposed EoS showed improved saturation pressure prediction for polar fluids.

Christoforakos and Franck (1986) proposed an EoS applicable for use in elevated temperature and pressure regions and for highly polar molecules. Their model was based on the van der Waals EoS with the Carnahan and Starling (1969) modification for the repulsive term. (Wei and Sadus 2000)

Based on molecular theories, more complicated EoS models were developed for structurally complex molecules. Beret and Prausnitz (1975) and Donohue and Prausnitz (1978) developed a three parameter Perturbed-Hard-Chain-Theory applicable to large, structurally complex molecules. Their proposed EoS considered molecules as chains of segments as proposed by Prigogine et al. (1957) and Flory (1965) and can be used to model long and convex molecules. Later, Chapman et al. (1990) and Huang and Radosz (1990) proposed the Statistical Associating Fluid Theory (SAFT), based on molecular principals in real fluids and mixtures. Their model was developed by advances in statistical mechanics and computer power which can be applied for pure fluids and mixtures containing associated fluids (Wei and Sadus 2000).

These EoSs despite their high accuracy in phase behaviour modeling suffer from some practical issues. The complexity, large number of input data and large execution time are some of those. The simplicity, less number of input data make PR EoS a good candidate for phase behaviour modeling of bitumen containing systems. In addition to these advantages, this EoS can easily be used for calculating other thermodynamic properties like Helmholtz free energy.

The EoS models were originally developed for pure systems but can be applied for mixtures by employing the mixing rules. Mixing rules are used to calculate the EoS input parameters for mixtures. In 1873, van der Waals proposed the classical mixing rule to calculate the constant EoS parameters. The classical mixing rule is the most common mixing rule that is coupled with other EoS models. Han et al. (1988) tested the van der Waals mixing rule with different EoSs and showed that the van der Waals mixing rule with one adjustable parameter can describe the phase behaviour of mixtures containing non-polar or slightly polar molecules with sufficient accuracy.

Anderko (1990) investigated the weaknesses of the van der Waals mixing rule for the prediction of the properties of non-ideal mixtures. Despite successfully predicting the phase behaviour of systems with no specific interaction between their molecules, the one parameter classical mixing rule could not accurately determine the phase diagram of polar systems.

Many attempts (Adachi and Surgie, 1986, Panagiotopoulos and Reid, 1986, Stryjek and Vera, 1986, Schwartzentruber et al., 1987, Sandoval et al., 1989) have been made to modify the attractive parameter mixing rules. Adachi and Sugie (1986) and Iwai et al. (1988) concluded that mixtures with polar components, such as alkanol + alkanol and water + lower alkanol binary systems can be modeled with classical mixing rules with two parameters. Voros et al. (1993) compared the results of different EoSs coupled with different mixing rules. They found that the EoS with temperature and pressure dependent binary interaction coefficients provides more accurate predicted values. Voros et al. (1993) determined that the one-parameter mixing rule provides poorer results than other mixing rules for very asymmetric systems. Both the one-parameter and two-parameter mixing rules showed convergence problems in the vicinity of the critical point. The two-parameter mixing rule produced more accurate predictions in some cases but is not accurate enough for compressed gasses and liquids (Rowlinson and Swinton 1982). Foster et al. (2005) used the two-parameter mixing rule coupled with the PR EoS to predict the VLE of binary and ternary systems of carbon dioxide, hydrogen, and methanol. They found that the solubility of hydrogen in the liquid phase was underestimated when the pressure is higher than the critical point in the carbon dioxide and methanol binary system.

For highly non-ideal mixtures, Huron and Vidal (1979) suggested a mixing rule method derived from the excess Gibbs energy models. Their model was significantly more accurate than the quadratic mixing rules for highly non-ideal systems, but was unable to predict low pressure data (Wei and Sadus 2000). In 1992, Wong and Sandler developed a mixing rule based on the equivalences of excess Helmholtz energy of an EoS with an activity coefficient model at infinite pressure. As with other mixing rules, the Wong-Sandler mixing rule can be applied to any EoS

but it has primarily been used in conjunction with the PR EoS. The Wong-Sandler mixing rule was highly successful for predictions in polar + nonpolar systems.

Huang and Sandler (1993) and Orbey and Sandler (1994) tested the Wong-Sandler mixing rule for different binary systems containing polymer-solvent systems. They concluded that the Wong-Sandler mixing rule can successfully model vapour-liquid equilibria for various mixtures with high accuracy over a range of pressures and temperatures. This mixing rule has become popular for phase behaviour studies of polar systems. For instance, Lopez et al (2009) and Elizalde et al (2007) used the Wong-Sandler mixing rule to model asymmetric binary mixtures of carbon dioxide and *n*-alkanols. They determined that the Wong-Sandler mixing rule predicts the VLE of highly asymmetric binary mixtures with sufficient accuracy. In this study, one-parameter, two-parameter and Wong-Sandler mixing rules will be compared in bitumen containing phase behaviour modeling.

Despite these improvements to phase behaviour modeling, there are still limitations in the prediction of volumetric behaviour. Volume translation was developed to improve volumetric behaviour prediction.

Martin (1967) first used volume translation for the molar volume coordinate in volumetric EoS (Frey 2009). Peneloux et al. (1982) stated that the equilibrium condition does not change by translation as long as there is no volume dependency in the translation function. They applied their method to the two-parameter SRK EoS and tested the proposed method for pure liquids, mixtures of liquids, and vapour-liquid equilibrium conditions. The predicted results were satisfactory in all cases except for the pure component in the vicinity of critical points and liquids under high pressure.

Jhaveri and Youngren (1988) successfully applied the Peneloux model for PR EoS. Several temperature dependent volume shift correlations have been proposed (Watson et al., 1986, Chou and Prausnitz, 1989, Magoulas and Tassios, 1990, Tsai and Chen, 1998, and Twu and Chan,

2009). Tsai and Chen (1998) considered the volume shift as a function of reduced temperature and found good agreement with experimental data for both pure components and binary systems.

Voros et al. (1994) tested volume shift in three different scenarios; constant value, as a function of reduced temperature and acentric factor, and as a function of the acentric factor. They found that the translation technique gives better results when the acentric factor is greater than 0.3. As the acentric values increase, the improvement increases and as the reduced temperature of one component decreases towards unity, the importance of the temperature dependent term increases. Later, new volume shift correlations were developed that are a function of volume and temperature (Mathias et al. 1989, Kutney et al. 1997). In this study, saturated bitumen density will be modeled with volume shift. Different scenarios will be considered for volume shift which will be explained in the next chapter.

2.2. Equation of State (EoS) Modeling for Heavy Oil and Bitumen Systems

Modeling of bitumen containing system begins in 1977 when Bishnoi et al. tried to model solubility of methane and carbon dioxide in bitumen and typical bitumen density. They modeled bitumen with 5 pseudo-components and calculate the molecular weight and specific gravity by Bergman (1976) equation. They used PR EoS for density prediction and found their value higher than experimental data in all temperature conditions. Improvement in critical properties and acentric factor of bitumen pseudo-components can improve the prediction which shows the importance of a good characterization scheme. They also used PR EoS and Chao-Seader (Chao and Seader 1961) method for prediction of methane and carbon dioxide solubility in bitumen. PR EoS needs fewer pure component properties but it needs interaction parameters for each pair components in system, while Chao-Seader method cannot calculate liquid phase density. They didn’t have any experimental data for solubility and so they couldn’t compare their results with experimental data.

In 1985, Mehrotra et al. modeled the saturated density and gas solubility of carbon dioxide in Athabasca and solubility of ethane and carbon dioxide in Peace-River bitumen. They modeled the solubility data with PR EoS considering four and five pseudo-components for Athabasca and Cold Lake bitumen respectively. They found the predicted values generally in good agreement with experimental data.

Fu et al. (1986a) measured the vapour-liquid equilibrium of methane and ethane in Cold Lake bitumen. They used the PR and the modified Soave-Redlich-Kwong (MSRK) EoSs to estimate VLE data and correlated the binary interaction coefficients with temperature. They used the estimated critical properties and acentric factors already reported by Fu et al. (1986b) and considered bitumen as one pseudo-component. They also conducted a comparison with the "EQUI-PHASE" package, developed by Robinson et al. (1981), containing the properties and binary interaction coefficients for different gases and Cold Lake bitumen. Their minimized objective function for finding the binary interaction coefficients was the difference between the saturation pressure of the modeled and experimental data. They found that the binary interaction coefficients decrease as temperature increases and were close to zero for both systems under study. They concluded that the MSRK produces more accurate predictions than the PR of the "EQUI-PHASE" software; however, they indicated it could be due to the bitumen properties which are available in this package and cannot be interpreted as the weakness of the PR EoS.

In a subsequent study, Fu et al. (1986c) used the MSRK EoS to determine the binary interaction coefficients of bitumen containing systems. The systems included carbon dioxide-Athabasca bitumen, carbon dioxide-Cold Lake bitumen, nitrogen-Athabasca bitumen, methane-Athabasca bitumen, methane-Cold Lake bitumen, and ethane-Athabasca bitumen. They investigated the binary interaction coefficients in each isotherm and modeled the data as a function of temperature. For simplicity and due to a lack of data, they considered a linear temperature dependent function and compared their results with the PR EoS and found good agreement with experimental data.

In another attempt, Fu et al. (1987) studied the sensitivity of the prediction of the VLE properties of gas-containing bitumen systems by critical properties, binary interaction coefficients, and acentric factors. They used available literature data for the properties of bitumen and applied both the PR and MSRK EoS models. They studied three binary systems of methane-Cold Lake bitumen, carbon dioxide-Athabasca bitumen, and carbon dioxide-Cold Lake bitumen. They determined that the phase equilibrium calculation is more sensitive to critical pressures and temperatures than to acentric factors and binary interaction coefficients. The same behaviour was observed for the liquid density leading the researchers to conclude that critical pressure and temperature have a huge effect on the results. Changing the acentric factor and the binary interaction coefficient (even by 50%) did not significantly influence the results. They also discovered that the model is least sensitive to binary interaction coefficients in the systems of methane-Athabasca bitumen.

In 1988, Mehrotra and Svrcek measured the properties of Cold Lake bitumen saturated with gases (1988a). Mehrotra and Svrcek (1988b) modeled Cold Lake bitumen with three pseudo-components. They used the PR EoS to predict light gas (methane, ethane, carbon dioxide, nitrogen) solubility in Cold Lake bitumen. They applied the Kesler-Lee estimations to calculate the critical properties and acentric factors of the Cold Lake bitumen pseudo-components. The binary interaction coefficients were determined by matching the experimental gas solubility data with the calculated PR EoS values. They modeled the bitumen with three pseudo-components but ignored the interaction between pseudo-component/pseudo-component pairs due to lack of data. They found their scheme of three pseudo-component bitumen more accurate than the one-component

In 1989, Yu et al. measured the solubility of carbon dioxide in the Cold Lake bitumen system. They applied the Perturbed Hard Chain (PHC), Soave and PR EoS models to predict the measured data. For flash calculation, they applied a different approach for calculating the binary interaction coefficient for different EoSs. For the PHC and Soave models, the binary interaction

coefficients were considered constant with respect to the different components but may vary with temperature. In contrast, for the PR EoS, the binary interaction coefficients were considered to be temperature independent but differed with respect to the different components. The results of this research showed that the PHC model can predict solubility data with excellent accuracy. However, this result may be changed at lower temperatures. At low temperatures, other EoS model predicts phase behaviour more accurately than the PHC model due to its predictive weaknesses near the critical point.

In 1989, Mehrotra et al. modeled Wabasca bitumen with three pseudo-components containing distillable maltenes, undistillable maltenes, and asphaltene. They predicted the solubility of nitrogen, carbon monoxide, methane, ethane, and carbon dioxide in Wabasca bitumen using the PR EoS and assuming constant binary interaction coefficients independent of temperature. They determined that a three pseudo-component scheme originally developed for viscosity prediction can be applied to solubility modeling with sufficient accuracy.

Kokal et al. (1990) modeled the VLE and liquid-liquid equilibria (LLE) behaviour of carbon dioxide with Saskatchewan heavy oil and its fractions. They used the PR EoS to match the experimental data by optimizing the binary interaction coefficients. They also modeled the carbon dioxide system with normal alkanes that have the same molecular weight as heavy oil and attempted to match the density data by volume translation.

In 1991, Jamaluddin et al. used the Martin EoS to model the solubility and saturated density of carbon dioxide in bitumen and heavy oils. The solvents consisted of *n*-decane, 9 different oils, and Athabasca, Cold Lake, Peace River, and Wabasca bitumen. They considered heavy oil as one pseudo-component and calculated the critical properties using the Kesler-Lee correlation. They determined that both the Martin and PR EoS can predict solubility with similar accuracy. However, the Martin EoS can model saturated density better than the PR EoS. In another attempt, Huang et al. (1991) used statistical associating fluid theory (SAFT) to model the solubility of bitumen in CO_2. They used eleven pseudo-components for Cold Lake bitumen and

three different cuts. They compared the SAFT, PHC, and Soave EoS models and discovered that cubic EoS models such as the Soave EoS can predict phase behaviour better than other EoS models near the critical point.

Deo et al. (1991) measured the solubility of carbon dioxide in the Tar Sand Triangle, the PR Spring Rainbow I, and the Athabasca tar sand bitumen. They used the PR and Schmidt-Wenzel (SW) EoSs to model their experimental data and correlate binary interaction coefficients as a function of the specific gravity and UOP K factor. Bitumen was considered as one pseudo-component and the Kesler-Lee correlation was used to calculate the critical properties. They obtained binary interaction coefficients by minimizing the square difference of the experimental and calculated solubility values. They concluded that the binary interaction coefficients for SW EoS are more temperature dependent than that of the PR Eos.

Eastick et al. (1992) employed the PR EoS to model the phase behaviour of Cold Lake bitumen with carbon dioxide over a temperature range of 25^{o}C to 150^{o}C at pressures up to 10 MPa. They considered 5 different cuts of bitumen and investigated the VLE and LLE data of each cut and the whole bitumen. They developed a generalized correlation for Cold Lake bitumen binary interaction coefficient as a function of critical temperature and molar mass. In addition, the binary interaction coefficients between the cuts were correlated as a function of temperature and the difference in molar mass. The model could predict experimental data with an error of less than 7%.

In 1995, Salim and Trebble used a modified PR EoS to model the solubility of carbon dioxide in Cold Lake bitumen. They generalized the critical properties and binary interaction coefficients as a function of the molecular weight and aromaticity. They used the bitumen characterization method proposed by Huang and Radosz (1990) and applied gamma distribution to the molecular weight. They found that their generalized PR EoS underpredicted the solubility of carbon dioxide in whole bitumen at higher temperatures. This discrepancy was interpreted as the difference between the reported molecular weight and the distribution molecular weight. They also

concluded that the data matching errors for the SAFT and PR EoSs are close while the SRK and PHC models predict the solubility with a greater percent error.

Frauenfeld et al. (2002) modeled the systems of ethane and propane + Cold Lake/Lloydminster oil; and carbon dioxide, methane, ethane, and propane + Lloydminster Aberfeldy oil. They predicted the solubility of the above-mentioned solvents in oil with the PR EoS considering the binary interaction coefficients as regression parameters with an AARD of less than 5%.

Yazdani and Maini (2007) modeled the Frog-Lake heavy oil and butane system by means of the PR EoS. They characterized the bitumen into two pseudo-components, maltenes and asphaltenes, and considered critical temperature, pressure, acentric factor, omega a and b, and the binary interaction coefficient as regression parameters. This method allowed them to match the saturation pressure. They used volume shifts to predict the saturation density.

Kariznovi et al. (2011a) measured the solubility of propane in extra heavy oil in temperature between 100^{o}C and 200^{o}C as well as the saturated phase density and viscosity. They modeled the literature experimental data using the PR EoS and bitumen characterized by six pseudo-components.

Li et al. (2013) experimentally and theoretically investigated the phase behaviour of propane-*n*-butane-heavy oil at temperatures up to 396.15 K and pressures up to 5030 kPa. They used the volume translated PR EoS with modified alpha. They also defined two binary interaction coefficients for propane-heavy oil and *n*-butane-heavy oil as a function of reduced temperature and successfully matched their results to the experimental saturation pressure data.

Whitson and Ghasemi (2013) used the PR EoS with the volume shift to model a system of light solvents (nitrogen, carbon monoxide, carbon dioxide, methane, and ethane) with Athabasca bitumen. They used the gamma distribution function for crude assay data as presented by Ghasemi et al. (2011) and characterized bitumen with five pseudo-components. Their results were in good agreement with the experimental data.

Badamchi-Zadeh et al. (2013) described the phase behaviour of carbon dioxide, propane, and Athabasca bitumen using oil characterization and EoS methods. They modeled the solubility and density of binary and ternary mixtures of solvents and bitumen with a two-parameter EoS. The bitumen was characterized using the characterization method provided by VMGSim to 28 pseudo-components and lumped to 4 PCs. They determined that a third parameter of volume shift is required to accurately predict the saturated density of the mentioned systems.

2.3. Characterization

Characterization of pure components began when Watson and Nelson (1933) presented two graphical charts to define molecular weight as a function of boiling point and Watson or universal oil products (UOP) characterization factor (K_W) or boiling point and API gravity. Their research was followed by extensive work on the characterization of pure hydrocarbon and fractions. Between 1930 and 1960, most of the developed methods were graphical such as the Winn monogram. Since then, most of the methods have been analytical in nature (Riazi 2005).

When the amount of data available from a sample is increased, the characterization becomes more accurate and is capable of describing the reservoir with greater precision. However, taking reliable downhole samples for heavy oils and bitumen is difficult (Zabel et al. 2010 and Memon et al. 2010). At high temperature, bitumen fractions may crack or decompose meaning that the experimental method can only cover a portion of the bitumen fractions. For this reason, characterization modeling methods are essential.

Generally, bitumen characterization has been done following a stepwise scheme (Whitson 1983, Kumar and Okuno. 2012). In the first step, the characterization data from an experimental method is extended, while in the next step, the critical properties, acentric factors, and other necessary data are calculated using correlations. Later, the components must be grouped to reduce the number of pseudo-components, modeling complexity, and execution time. The properties may need to be modified to match the phase behaviour experimental data.

2.3.1. Description of Fluid Heavy End

The first characterization scheme was developed by Lohrenz et al. (1964). Their research indicated that the heptane plus fraction can be characterized by pseudo-components with carbon numbers of 7 to 40. Following the Lohrenz et al. (1964) study, Katz (1983) presented his logarithmic correlation based on his investigation of six condensate systems (Ahmed 1989).

Whitson (1983) proposed a characterization method to extend the partially molar distribution to the heavier components. Whitson considered five conditions to develop a probability function. The function needed to be accomplished, easy to use, and show consistent matching. In addition, it needs to be able to extend the partial analysis without requiring too many unknown or initial parameters. Whitson chose the gamma distribution as his probability function.

Another applicable distribution is the Chi-Square used by Quinones et al. (Quinones-Cisneos 2004) for the first time. The Chi-Square is a special case of the gamma distribution. In fact, gamma distribution can be used for mole fraction modeling and the Chi-Square is applicable for describing the weight fraction.

Dhulesia (1984) used cumulative form of the Weibull distribution for petroleum fractions' distribution. Later, Riazi (1989) used a developed form of the Weibull distribution (Dhulesia 1984) as his molar distribution function for the phase behaviour modeling of 68 different crude oils. He applied the two-parameter model for heavy oil data of Rodgers et al. (1987) and compared the result of his own method with those of the gamma distribution model.

Pedersen et al. (1992) proposed a new model with a linear relation between the SCN and the logarithm of concentration. They tested their model for 17 North Sea reservoir oil compositional analyses obtained with high-pressure gas chromatography. They showed that compositional analysis above C_{20+} is not required for their calculation. Their discrete model, in spite of its simplicity, could not successfully model the left-skewed SCN curve.

Sanchez et al. (2007) tested 25 different distribution models for more than 137 samples. They concluded that the Weibull extreme, Weibull, and Kumaraswamy distributions successfully

described the behaviour of their samples. In another attempt, Xavier et al. (2011) compared the performance of five different distribution functions for characterizing the TBP curve including Beta, Gamma, Riazi, Weibull, and Weibull extreme. They used a large database of Brazilian oil and determined that the Weibull extreme predicted the molar distribution with greater accuracy comparing to the other distribution functions.

In addition to the gamma (Whitson 1983) distribution, the chi-square (Quinones-Cisneos 2003) and logarithmic distributions (Pedersen et al. 1983a, 1984) are the most common molar distributions in the literature. However, gamma is the most general distribution that can be reduced to two other molar distributions under specific conditions. While the logarithmic distribution is sufficiently accurate for conventional oils, this simple model does not work for heavy oils and bitumen, where a more complicated model like gamma or chi-square is required (Ghasemi et al. 2011). Regardless of how complicated the distribution is, the accuracy of the predictions is dictated by the amount of uncertainty in the compositional analysis.

2.3.2. Critical Properties Estimation

Kesler and Lee (1976) correlated the critical pressure, temperature, and acentric factor as a function of true boiling point (TBP) and specific gravity (SG). Their correlations for critical pressure and temperature are valid below 1200^{o}F (650 ^{o}C). Several modifications have been proposed to extend these correlations above 1200^{o}F (650 ^{o}C) (Ahmed 1989). In another attempt, Riazi and Daubert (1980) generated a correlation that is applicable for components with a molecular weight of 300 g/mol to 700 g/mol. Their correlation was simple, required few constant parameters, and could reasonably predict the properties over a boiling point range of 40 ^{o}C -455 ^{o}C (Jabr 1990).

Twu (1984) developed perturbation expansion correlations based on the difference between the specific gravity of the hydrocarbon fraction and normal paraffin with the same boiling point. In

his method, the properties for a normal alkane are calculated and then extended to the petroleum fractions (Danesh 1998).

Riazi and Al-Sahhaf (1996) presented their correlation as a function of SCN for C_6-C_{50}. Their correlations can be altered depending on the PNA analysis of the component for different properties including normal boiling point, critical properties, and acentric factors.

In 2007, Sancet presented his correlation for critical properties as a function of the fraction's molecular weight. He tested his correlations coupled with cubic EoS models and compared his results with the Riazi-Daubert (1980) correlations. His results showed that both correlations are equally accurate in the prediction of VLE prediction and that his correlations offer improved density prediction in high molecular weight hydrocarbons. Other equations for critical properties and acentric factor of petroleum fractions were developed by Cavett (1962), Lin-Chao (1984), Winn-Sim-Daubert (1980) and Edmister (1958).

Duan et al. (2013) compared the available correlations and indicated that for critical pressure, the Kesler-Lee (1976), Sancet (2007), and Twu (1984) correlations evaluate the data with sufficient accuracy in the carbon number range from 7 to infinity, while Ahmed (1985) correlation can be used in the range of 7-40. For critical temperature, Ahmed (1985) correlation is not applicable, except in the carbon number range from 7-60, while the other correlations can be used for any carbon number. He also recommended the use of the Sancet (2007) and Twu (1984) correlations for boiling point temperature evaluation.

2.3.3. Lumping and Averaging Properties

Lumping and reducing the number of pseudo-components should not affect the accuracy of the predicted data and can significantly reduce the execution time. Salim and Trebble (1995) increased the number of pseudo-components in Cold Lake bitumen and supercritical carbon dioxide system until no change in the results of the flash calculation was observed. They found

that increasing the number of pseudo-components does not significantly affect the equilibrium results when the number is greater than fifteen.

In 1981, Lee et al. proposed a simple scheme for lumping components with similar physicochemical properties. The similarity of these properties is verified by the slopes of the properties along the normal boiling point curve. Whitson (1983) also provides a lumping scheme which defines the number of pseudo-components as a function of number of carbons in the first SCN in the C_{n+} fraction and the last SCN generated by the characterization scheme. Other lumping schemes have been proposed by Mehra et al., 1982, Montel-Gouel, 1984, Schlijper, 1986, Behrens-Sandler, 1986, and Gonzalez et al. 1986.

The properties of the fractions must be averaged by means of the mixing rules. Hong (1982) suggested a weight fraction average for the mixing parameters, while Kay (1936) proposed his mixing rules based on mole average.

2.4. Characterization for Heavy Oil and Bitumen Systems

Kokal and Sayegh (1990) applied a continuous distribution function for obtaining molar composition of high molecular weight fractions in their modeling of Lone Rock heavy oil containing systems. They considered three pseudo-components, where the last one described asphaltene. They also used the Kesler-Lee and Twu correlations to calculate the critical properties and acentric factor.

Huang and Radosz (1991a) focused on a system of Cold Lake bitumen and carbon dioxide. They distilled the bitumen into five cuts. However, only cut 1 and 2 were completely distillable, cut 3 and 4 were partly distillable, and cut 5 was not distillable at all. They matched the whole bitumen with two gamma fits. In the first model, the distillable portion was matched, while in the second approach, the total bitumen including the non-distillable cut 5 was fit. The William and Teja approach (1987) was used to match the data. They attempted to reconstruct the distillation curve by applying a material balance to the distilled curve. The results were not perfectly

matched. This may have been the result of the small number of cuts used in the experiment. Hopefully, by increasing the number of cuts, the two diagrams can be matched to each other.

They also attempted to match the data for the mixture of bitumen and supercritical carbon dioxide. They used the PHC EoS and compared the results of four different approaches. The data were taken from Huang and Radosz (Radosz 1990) and Yu, Huang and Radosz (1989). They found that the previous approach by Huang and Radosz (1991b) of modeling bitumen by discrete pseudo-components gave the best results.

Salim and Trebble (1995) studied the phase behaviour prediction of Cold Lake bitumen and supercritical carbon dioxide. They used the same data as Huang and Radosz (1991b) research and their analyzed cuts for bitumen. They utilized a simple cubic PR EoS and compared their results with the relatively complicated SAFT EoS used by Huang and Radosz (1991b). They used Sigmund and Trebble's method (1992) to calculate the critical properties and acentric factor, which was found by matching the data for 38 aromatic compounds. They used the gamma distribution with a similar procedure to Huang and Radosz (1991a) and considered 12 pseudo-components for whole bitumen. This number was determined by trial and error and by flash calculations.

They determined that it is impossible to match the whole bitumen using a single gamma distribution. In this case, they considered a single pseudo-component for the last fraction and modeled the rest using gamma distribution. They also conducted a sensitivity test to determine the effect of different parameters on observed error. They discovered that the number of pseudo-components does not have a significant effect on phase behaviour prediction but the fraction with the greatest molecular weight can influence the error significantly. They concluded that despite the lesser AARD for SAFT than for the PR EoS, the simplicity of the PR EoS makes it superior to the SAFT model.

Riazi (1997) studied the use of different distribution functions for 48 different oils containing condensate, crude oils, and heavy fractions reported by Rodgers et al. (1987). He modeled this

distribution using three different models; exponential, gamma, and Riazi molar distributions. He concluded that for heavy fractions, his model is better than the gamma distribution. This can be explained by the exponential component of his proposed model, which offers more flexibility in the prediction of the molar distribution. He also indicated that the exponential model is not appropriate for heavy fractions and heavy ends under any circumstances.

Rodriguez et al. (2010) assumed that each single carbon number which has a fixed molecular weight contains not only normal carbon numbers but other hydrocarbon constituents such as cyclo or aromatics. Under this assumption, they proposed a method for finding the limiting molecular weights in the integration of the cumulative density function. Additionally, they employed a new method for determining the shape factor (γ) and tested their modification on 6 different samples including heavy oils. The SCN and mole fraction of at least two previous fractions are required for their method. In their method, L_{Mw} is the regression parameter found by fitting the experimental data and the three-parameter gamma (TPG) function for mole fraction. Their results were in good agreement with experimental data however they differ from one sample to another, which they concluded; it was due to different molecular weights for different SCNs.

Ghasemi et al. (2011) proposed a method for fitting the measured mole fraction, specific gravity data, and boiling point data for 16 different samples containing Athabasca and Cold Lake bitumen. They used three models simultaneously to match the named data including the gamma distribution model, Soreide (1989), and Twu (1984) correlations. In the gamma distribution model, they considered the shape factor (γ), minimum molecular weight (η), and the molecular weight of the plus fraction (M_{n+}) as the regression parameters. In addition, they considered two regression parameters, C_f and n in the Soreide correlation, which is used to relate specific gravity to molecular weight. They also used Twu correlation factor to relate molecular weight to specific gravity and the normal boiling point. In total, six regression parameters were considered.

Castellanos Diaz et al. (2011) modeled a mixture of Athabasca bitumen, propane, and carbon dioxide. They used a conventional characterization coupled with PR cubic EoS. They used simulated distillation (SimDis) data, which was available up to 63.7 wt% and extrapolated the NBP curve with six different cases. Overall, the gamma distribution and linear extrapolation for asphaltene gave the most accurate results.

Kumar and Okuno (2012) applied two different approaches to the phase behaviour modeling of different conventional and heavy oil samples. They used a conventional characterization method with logarithmic distribution and a new characterization method with chi-square distribution. They concluded that both distribution methods are good candidates for modeling the molar distribution of heavy oils and bitumen.

Duan et al. (2013) used gamma distribution to define the mole fraction as a continuous function of molecular weight. They studied 14 different samples containing gas condensate, volatile, black, and heavy oils. They used the classic Peng-Robinson cubic EoS to predict the saturation pressure with an accuracy of 2.23% to 9.8% comparing to experimental data.

Chapter 3: Modeling and Methodology

3.1. Phase Behaviour Modeling

This study investigated the phase behaviour of non-condensable gases and bitumen systems. A two-phase flash calculation code was developed for this purpose in C++. The PR EoS was modified to improve the prediction of vapour-liquid equilibrium properties and saturated liquid density. The bitumen characterization methods are also explained and the proposed modification on gamma distribution function mentioned. Finally the EoS code has been validated by means of literature data and commercial software of CMG-WinProp. In the next section, the developed code has been applied to binary systems of (methane + methanol, ethanol, and 1-propanol), (methane + *n*-tetradecane and *n*-octadecane), (ethane + *n*-tetradecane and *n*-octadecane), (carbon dioxide + methanol, ethanol, and 1-propanol), (carbon dioxide + *n*-decane, *n*-tetradecane, and *n*-octadecane).

3.1.1. Equilibrium Condition

In spontaneous processes, the Gibbs energy of a system tends to decrease and reaches a minimum value at equilibrium conditions:

$$(\partial G)_{P,T} = 0 \qquad 3\text{-}1$$

$$(\partial^2 G)_{P,T} > 0 \qquad 3\text{-}2$$

G indicates the Gibbs energy and T and P represent the temperature and the pressure of the system. The above criteria are necessary for equilibrium but are not sufficient because the energy of the system must be at its minimum value. The Gibbs energy of an open system is a function of the number of moles of the chemical species present in the system as well as the temperature and pressure. The Gibbs energy is presented by (Smith, et al. 2005):

$$nG = g(P, T, n_1, n_2, ...) \tag{3-3}$$

$$d(nG) = \left[\frac{\partial(nG)}{\partial P}\right]_{T,n} dP + \left[\frac{\partial(nG)}{\partial T}\right]_{P,n} dT + \sum_i \left[\frac{\partial(nG)}{\partial n_i}\right]_{P,T,n_{j\neq i}} dn_i \tag{3-4}$$

n_j indicates that all mole numbers are held constant except the mole number of the i^{th} component. The chemical potential of the i^{th} component is defined as the deviation of Gibbs energy with respect to the mole number of the i^{th} component while temperature, pressure, and the mole number of all of the other components are constant. By this definition Equation 3-4 becomes the following:

$$d(nG) = (nV)dP - (nS)dT + \sum_i \mu_i dn_i \tag{3-5}$$

V and S are the volume and entropy of the system and μ_i represents the chemical potential.

$$\mu_i \equiv \left[\frac{\partial(nG)}{\partial n_i}\right]_{P,T,n_j} \tag{3-6}$$

In a closed system with no chemical reaction that consists of θ phases at constant temperature and pressure, the equilibrium requirement is as follows:

$$d(nG) = \sum_{k=1}^{\theta} \left(\sum_i \mu_i dn_i \right)_k = 0 \tag{3-7}$$

The total mole number of each component is constant because the system is closed. Therefore, the chemical potential of each component in all phases is equal.

$$\mu_i^{(1)} = \mu_i^{(2)} = ... = \mu_i^{(\theta)} \tag{3-8}$$

The chemical potential of one component is related to its fugacity by the following simple equation:

$$d\mu_j = RTd(\ln f_i) \tag{3-9}$$

R is the universal gas constant and f_i is the fugacity of the i^{th} component. The fugacity of an ideal gas is equal to its pressure and is defined as a measure of the non-ideality of a system. The

chemical potential in different phases at equilibrium condition is equal and therefore, the fugacity in different phases is also equal. In the present study, the systems under study are at their VLE conditions and the following equation applies:

$$f_j^{\,G} = f_j^{\,L} \qquad 3\text{-}10$$

The fugacity can be calculated in each phase by:

$$\ln \frac{f_j}{y_j p} = \frac{1}{RT} \int_{\infty}^{V} \left[\frac{RT}{V} - \left(\frac{\partial p}{\partial n_j}\right)_{T,V,n_i} \right] dV - \ln z \qquad 3\text{-}11$$

As Equation 3-11 indicates, the fugacity of each component can be calculated by determining the relationship between volume, pressure, and temperature. Equation 3-10 represents the equilibrium condition, which is the main criterion for describing bitumen-containing systems.

3.1.2. Peng-Robinson EoS

Van der Waals (1873) considered attractive and repulsive forces when he proposed his well-known EoS. His EoS features two major improvements over previous models; the assumption that molecules are particles with volume and a consideration of the attraction forces between molecules. Prior to this it was assumed that the molecules behave like ideal gases and there is no attraction between them. Van der Waals (1873) proposed the following equation.

$$P = \frac{RT}{(v-b)} - \frac{a}{v^2} \qquad 3\text{-}12$$

v, $\frac{a}{v^2}$ and *b* represent the molar volume, attractive and repulsive term respectively. *b* is an apparent volume and as the pressure approaches to infinity, the volume approaches *b*. Therefore, *b* should always be less than the molar volume and is called the co-volume. The above correlation can be rearranged as a function of volume or compressibility factor and presented by the following equations.

$$v^3 - (b + \frac{RT}{P})v^2 + (\frac{a}{P})v - \frac{ab}{P} = 0 \quad \text{3-13}$$

$$Z^3 - (1+B)Z^2 + AZ - AB = 0 \quad \text{3-14}$$

A and B are dimensionless parameters and defined below:

$$A \equiv \frac{aP}{(RT)^2} \quad \text{3-15}$$

$$B \equiv \frac{bP}{RT} \quad \text{3-16}$$

$$Z \equiv \frac{Pv}{RT} \quad \text{3-17}$$

The van der Waals equation has a cubic form of molar volume and compressibility factor. This type of equations is called a cubic EoS. Later, Peng and Robinson (1976) determined that choosing an appropriate function for the attractive term improves the predicted compressibility factor so that it approaches a more realistic value. They also found that defining the attractive term as a function of reduced temperature in addition to acentric factor considerably improved the vapour pressure prediction of the pure substances and mixtures. Based on the above considerations, they proposed the following equation:

$$P = \frac{RT}{v-b} - \frac{a(T)}{v(v+b)+b(v-b)} \quad \text{3-18}$$

The Equation 3-18 can be rearranged in cubic form of compressibility factor.

$$Z^3 - (1-B) + (A - 3B^2 - 2B)Z - (AB - B^2 - B^3) = 0 \quad \text{3-19}$$

where *A*, *B*, and *Z* are defined by Equations 3-15 to 3-17. Solving the above equation for temperatures less than the critical temperature results in three roots. The smallest one is the compressibility factor of the vapour, the largest one is the compressibility factor of the liquid and the middle root does not have any physical meaning. These roots are shown in Figure 3-1.

The attractive and repulsive parameters can be found by applying the horizontal inflection point at the critical point (Figure 3-1).

$$(\frac{\partial P}{\partial v})_{T=T_c} = (\frac{\partial^2 P}{\partial v^2})_{T=T_c} = 0 \qquad 3\text{-}20$$

where subscript *c* corresponds to the critical point. Applying above criteria to Equation 3-18 produces the following attractive and repulsive terms:

$$a(T_c) = 0.45724 \frac{R^2 T_c^{\ 2}}{P_c} \qquad 3\text{-}21$$

$$b(T_c) = 0.07780 \frac{RT_c}{P_c} \qquad 3\text{-}22$$

$$Z_c = 0.307 \qquad 3\text{-}23$$

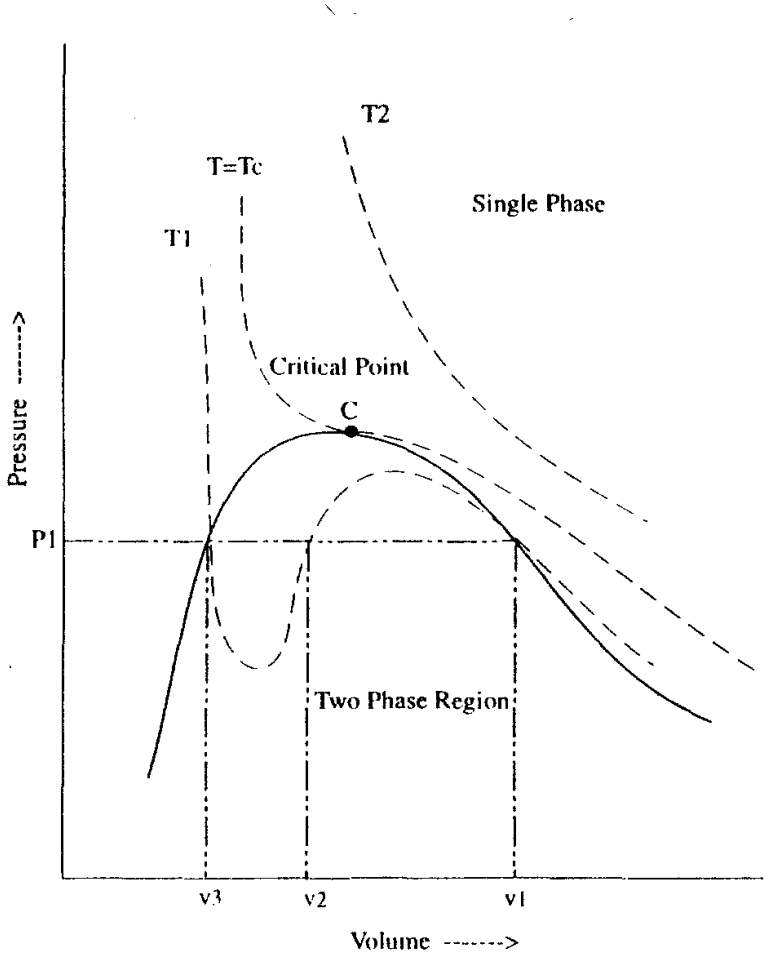

Peng and Robinson improved the vapour pressure prediction by defining temperature dependent attractive and repulsive parameters

$$a(T) = a(T_c).\alpha(T_r, \omega) \quad \text{3-24}$$

$$b(T) = b(T_c) \quad \text{3-25}$$

Applying the thermodynamic relationship, the expression for the fugacity of a pure component is as follows.

$$\ln \frac{f}{P} = Z - 1 - \ln(Z - B) + \frac{A}{2\sqrt{2}B} \ln \frac{Z + (1 - \sqrt{2})B}{Z + (1 + \sqrt{2})B} \quad \text{3-26}$$

3.1.2.1. Modification of α

Different correlation has been proposed which correlated α parameter as a function of reduced temperature to improve the vapour pressure prediction for different systems. Peng and Robinson (1976) proposed an equation for α as a function of ω and T_r. The form of their equation is similar to that proposed by Soave (1972) for the SRK EoS. The Peng and Robinson (1976) equation for α is as follows.

$$\alpha^{1/2} = 1 + (0.37464 + 1.54226\omega - 0.26992\omega^2)(1 - T_r^{1/2}) \quad \text{3-27}$$

Peng and Robinson (1978) extended their equation for α to improve heavy fraction prediction and developed the following equation.

$$\alpha^{1/2} = 1 + (0.379642 + 1.48503\omega - 0.1644\omega^2 + 0.016667\omega^3)(1 - T_r^{1/2}) \quad \text{3-28}$$

Twu et al. (1995) demonstrated that α changed linearly with respect to the acentric factor at a constant reduced temperature. They suggested the modification below:

$$\alpha = \alpha^{(0)} + \omega(\alpha^{(1)} - \alpha^{(0)}) \quad \text{3-29}$$

$\alpha^{(0)}$ and $\alpha^{(1)}$ are a function of reduced temperature. This equation provides the ability to predict the parameter for components with a high acentric factor. Twu et al. (1995) provide two sets of correlations for Equation 3-29. When the reduced temperature is less than one $\alpha^{(0)}$ and $\alpha^{(1)}$ are calculated by the following correlations:

$$\alpha^{(0)} = T_r^{-0.171813} \exp[0.125283(1 - T_r^{1.77634})] \quad \text{3-30}$$

$$\alpha^{(1)} = T_r^{-0.607352} \exp[0.511614(1 - T_r^{2.20517})] \quad 3\text{-}31$$

Nji et al. (2009) used experimental vapour pressure data from the National Institute of Standard (NIST) and presented the following correlation:

$$\alpha^{1/2} = 1 + (0.388187 + 1.56132\omega - 29.014\omega^2 + 0.0617513\omega^3)(1 - T_r^{1/2}) \quad 3\text{-}32$$

Li and Yang (2010) proposed a correlation based on matching the vapour pressure of different hydrocarbon and non-hydrocarbon systems up to *n*-treterraoctane (*n*-$C_{43}H_{88}$). Their correlation is as follows.

$$\begin{aligned}\alpha = \exp\{&(1.13280 - 0.05052\omega + 0.25948\omega^2)(1 - T_r) \\ &+ 0.81769 \ln[1 + (0.31355 + 1.86745\omega - 0.52604\omega^2)(1 - \sqrt{T_r})]^2\}\end{aligned} \quad 3\text{-}33$$

The appropriate α parameter can significantly improve the VLE prediction. This effect becomes more significant in systems with a high acentric factor (ω>0.5). As bitumen consists of heavy components, the α parameter is expected to have a significant effect. This is investigated in the next chapter.

3.1.2.2. Mixing Rules

The EoSs were originally developed for pure components but they can be applied for mixtures by employing the mixing and combining rules. Mixing rules are used to calculate the EoS input parameters for mixtures. In 1873, van der Waals proposed the classical mixing rule to calculate the attractive and repulsive parameters for mixtures. The following two equations show the mixing rules for calculating attractive and co-volume terms for EoSs.

$$a_m = \sum_i \sum_j x_i x_j a_{ij} \quad 3\text{-}34$$

$$b_m = \sum_j x_j b_j \quad 3\text{-}35$$

The *b* parameter is obtained from the average molecular volume, which is based on an arbitrary assumption and a simple mathematical formula (Prausnitz 1999). In systems containing similar

sized molecules of moderate densities, the mixing rule for parameter *b* does not have a significant effect on the EoS results. However, the parameter *a* considerably changes the fugacity (Prausnitz 1999). The attractive parameter *(a)* reflects the strength of the attraction and is related to the attraction parameter of the pure components by the following combining rule:

$$a_{ij} = \sqrt{(a_i a_j)}(1 - K_{ij}) \qquad 3\text{-}36$$

where K_{ij} indicates binary interaction between molecules *i* and *j*. Equation 3-36 is called the geometric mean assumption and was proposed by Berthelot (Prausnitz 1999). The one-parameter mixing rule cannot provide accurate predictions near critical regions or for complicated systems containing polar components or molecules with complex structures (Prausnitz 1999). The following is the general equation for the fugacity coefficient calculation using the one-parameter mixing rule.

$$\ln \varphi_i = -\ln(z - B) + (Z - 1)B_j^{'} - \frac{A}{2\sqrt{2}B}(A_j^{'} - B_j^{'}) \ln\left[\frac{z + (\sqrt{2}+1)B}{z - (\sqrt{2}-1)B}\right] \qquad 3\text{-}37$$

x_i is the molar fraction, *z* is compressibility factor, and φ_j is the fugacity coefficient.

The two-parameter classical mixing rule can predict the phase equilibrium data in the vicinity of the critical point. The most common method of expressing the adjustable parameter is a quadratic dependence on composition.

$$a_m = \sum_i \sum_j x_i x_j a_{ij} \qquad 3\text{-}38$$

$$b_m = \sum_i \sum_j x_i x_j b_{ij} \qquad 3\text{-}39$$

where,

$$a_{ij} = \sqrt{(a_i a_j)}(1 - K_{ij}) \qquad 3\text{-}40$$

$$b_{ij} = \sqrt{(b_i b_j)}(1 - I_{ij}) \qquad 3\text{-}41$$

and,

$$b_{ij} = \frac{b_i + b_j}{2}(1 - I_{ij}) \qquad 3\text{-}42$$

K_{ij} and I_{ij} are two regression parameters. The composition quadratic dependency of repulsive equation coupled with equation 3-42 is equivalent to the linear composition dependency. The fugacity coefficient is calculated with quadratic composition dependency using the following equation.

$$\begin{aligned} \ln\varphi_i = & \left(\frac{2\sum x_i b_{ij} - b}{b}\right)(Z-1) - \ln(Z-b) \\ & - \left(\frac{A}{2\sqrt{2}B}\right)\left(\frac{2\sum x_j a_{ij}}{a} - \frac{2\sum x_j b_{ij} - b}{b}\right)\left\{\ln\left(\frac{Z + (1+\sqrt{2})B}{Z + (1-\sqrt{2})B}\right)\right. \end{aligned} \qquad 3\text{-}43$$

The derivation of the fugacity coefficient is explained in Appendix I. The van der Waals mixing rules are relatively successful for modeling the hydrocarbon system but cannot accurately represent asymmetric systems. Different random mixing rules have been proposed to overcome this problem for highly polar and asymmetric components. Wong and Sandler (1992) combined an EoS with a free-energy model and developed a mixing rule, which can be applied to any EoS, but has been primarily used with the PR EoS. The details of this mixing rule are summarized in Appendix II and briefly presented below:

$$b_m = \frac{Q}{(1-D)} \qquad 3\text{-}44$$

$$\frac{a_m}{RT} = Q\frac{D}{(1-D)} \qquad 3\text{-}45$$

D and Q are defined as:

$$Q = \sum_i \sum_j x_i x_j \left(b - \frac{a}{RT}\right)_{ij} \qquad 3\text{-}46$$

$$D = \sum_i x_i \frac{a_i}{b_i RT} + \frac{A^E{}_\infty}{CRT} \qquad 3\text{-}47$$

Different activity coefficient models can be used to obtain excess Helmholtz energy. In this study, the non-random two-liquid (NRTL) model was used to calculate the Helmholtz energy

because this model was originally developed for strongly non-ideal systems. The fugacity coefficients for PR EoS coupled with NRTL model, are calculated with the following equation.

$$\ln \varphi_i = -\ln[\frac{P(\overline{V} - b_m)}{RT}] + \frac{1}{b_m}(\frac{\partial n b_m}{\partial n_i})(\frac{P\overline{V}}{RT} - 1) + \frac{1}{2\sqrt{2}}(\frac{a_m}{b_m RT})[\frac{1}{a_m}(\frac{1}{n}\frac{\partial n^2 a_m}{\partial n_i}) - \frac{1}{b_m}\frac{\partial n b_m}{\partial n_i}]\ln[\frac{\overline{V} + b_m(1-\sqrt{2})}{\overline{V} + b_m(1+2\sqrt{2})}] \quad 3\text{-}48$$

In this study three different mixing rules and combining rules are used to model solvent bitumen systems. Bitumen consists of polar asphaltene molecules, therefore the Wong-Sandler equation is used for bitumen containing systems. The Wong-Sandler mixing rule was investigated where bitumen is considered as one pseudo-components.

3.1.2.3. Binary Interaction Parameter

The binary interaction coefficients between the components *i* and *j* is dependent on the size of molecules (Peng and Robinson 1976). The binary interaction between hydrocarbons increases as the relative difference between their molecular weights increases (Slot et al. 1989). Chueh and Prausnitz (1967) proposed the following two-parameter binary interaction coefficient correlation.

$$K_{ij} = \upsilon_i \left[1 - \left(\frac{2(V_{ci}^{1/3} V_{cj}^{1/3})^{1/2}}{V_{ci}^{1/3} + V_{cj}^{1/3}} \right)^{\theta} \right] \quad 3\text{-}49$$

Nikos et al. (1986) proposed a binary interaction coefficient correlation as a function of the temperature and acentric factor.

$$K_{ij} = \delta_2 T_{rj}^{\ 2} + \delta_1 T_{rj} + \delta_0 \quad 3\text{-}50$$

They suggested different equations for δ_0, δ_1 and δ_2 for different systems of methane, nitrogen and, carbon dioxide with hydrocarbons as a function of the acentric factor. Gao (1992) presented a correlation based on critical temperature.

$$K_{ij} = 1 - \left(\frac{2\sqrt{T_{ci} T_{cj}}}{T_{ci} + T_{cj}} \right)^{\theta} \quad 3\text{-}51$$

θ is the tuning parameter. Meanwhile, Agrawal (2012) presented the following binary interaction coefficient as a function of temperature.

$$K_{ij} = K_{ij}{}^{0} \left(1 + \frac{K_{ij}{}^{1}}{T} + K_{ij}{}^{2} \ln T\right) \quad 3\text{-}52$$

$K_{ij}{}^{0}$ is a temperature independent term and can be calculated using the previously mentioned binary interaction coefficient models. The efficiency of temperature dependent correlations for phase behaviour prediction is studied in the next chapter.

3.1.2.4. Volume Translation

The PR EoS successfully predicts the equilibrium compositions of mixtures but is not accurate in the prediction of phase densities. For this reason, different methods have been developed to improve the volumetric behaviour of the PR EoS. Peneloux et al. (1982) introduced a third parameter, called volume shift, to the two-parameter SRK EoS. Applying this parameter has no influence on the equilibrium calculation and does not change the equilibrium compositions. This parameter only affects the volume calculation, leading to improved density prediction. Peneloux et al. (1982) tested their proposed method for pure liquids, mixtures of liquids, and vapour-liquid equilibrium conditions. The predicted results were satisfactory in all cases except for pure components near the critical points and for liquids under high pressure. The Peneloux et al. (1982) volume correction is as follows:

$$\tilde{V} = V - C \quad 3\text{-}53$$

C is the correction term and is calculated using a linear mixing rule,

$$C = \sum_{i} z_i c_i \quad 3\text{-}54$$

This formula is applied to liquid and gas phases with the following equations:

$$\tilde{V}_l = V_l - \sum_{i=1}^{n} c_i x_i \qquad 3\text{-}55$$

$$\tilde{V}_g = V_g - \sum_{i=1}^{n} c_i x_i \qquad 3\text{-}56$$

Peneloux et al. (1982) correlated the volume translation parameter as a function of Racket compressibility. To correct for a lack of compressibility factor data, they used the Spencer and Adler (1978) correlation and developed an equation as a function of acentric factor:

$$c_i = 4.43797878(0.29441 - Z_{RA})\frac{T_{ci}}{P_{ci}} \qquad 3\text{-}57$$

$$c_i = 4.43797878(0.00261 + 0.0928\omega_i)\frac{T_{ci}}{P_{ci}} \qquad 3\text{-}58$$

As the translation function has no volume dependency or composition dependency, there will be no change in the equilibrium. The function multiplies the fugacity of each component by an equal amount in both phases (Danesh 1988) which has no effect on the equilibrium calculations.

$$\phi_i^{Cor} = \phi_i \exp(-c_i P / RT) \qquad 3\text{-}59$$

φ_i^{cor} is the fugacity coefficient after applying the volume translation. Jhaveri and Youngern (1984) applied the Peneloux approach to the PR EoS and defined a dimensionless shift parameter:

$$S_E = c / b \qquad 3\text{-}60$$

In spite of its success, the constant volume shift approach is impractical for multi-component systems. Different volume shifts are introduced as a function of reduced temperature. Watson et al. (1986) proposed the first temperature dependent correlation shown below.

$$c_i = c_0 + c_1 \exp\left(c_2\left(\left|1 - T_r\right|\right)\right) \qquad 3\text{-}61$$

In this study, a volume shift parameter correlation similar to Equation 3-52 was used to predict the density. Danesh (1998) defined volume shift as a function of molecular weight:

$$S_E = 1 - \frac{\Psi}{M^{\chi}} \qquad 3\text{-}62$$

Where Ψ and χ are positive constant that can be used as regression parameters for heavy fractions. Similar to Agrawal (2012) model for binary interaction coefficient, temperature dependent volume shift correlation is proposed:

$$S_E = \left(1 - \frac{\Psi}{M^{\chi}}\right)\left(1 + \frac{SE^1}{T} + SE^2 \ln(T)\right) \qquad 3\text{-}63$$

This correlation, with two regression parameters, can improve the density prediction over a wide range of pressures and temperatures.

3.1.2.5. Flash Calculation

Different numerical methods have been proposed for the VLE calculation when the system approaches the equilibrium condition. The most common one is successive substitution. This method begins with an initial estimate of the equilibrium ratio (K_i). The *K*-values are related to the fugacity coefficients ϕ_{iL} and ϕ_{iV} as follows:

$$K_i = \frac{\phi_{iL}}{\phi_{iV}} = \frac{\frac{f_{iL}}{(x_i P)}}{\frac{f_{iG}}{(y_i P)}} \qquad 3\text{-}64$$

K_i is the equilibrium ratio of i^{th} component. At equilibrium condition, the fugacities of the components are equal in both the vapour and liquid phases. Therefore the Equation 3-64 becomes:

$$K_i = \frac{y_i}{x_i} \qquad 3\text{-}65$$

The *K*-values and initial mole fraction can be used to calculate the mole fractions of components in the liquid and vapour phases.

$$x_i = \frac{z_i}{1+(K_i-1)n_v} \tag{3-66}$$

$$y_i = \frac{z_i K_i}{1+(K_i-1)n_v} \tag{3-67}$$

n_v is the number of moles in the vapour phase. n_v can be determined by an iterative method via the vapour and liquid mole fraction definition:

$$\sum_{i=1}^{N} x_i = \sum_{i=1}^{N} y_i = 1 \tag{3-68}$$

Rachford and Rice (1952) suggested using a monotonic function instead of the above equation to make the solving algorithm more robust.

$$f(n_v) = \sum_{i=1}^{N}(y_i - x_i) = \sum_{i=1}^{N} \frac{(K_i-1)z_i}{(K_i-1)n_v+1} = 0 \tag{3-69}$$

The Newton-Raphson equation is used to solve the above equation. The deviation of the Rachford-Rice equation is defined follows:

$$f(n_v)' = -\sum_{i=1}^{N}\left[\frac{z_i(K_i-1)^2}{\left[n_v(K_i-1)+1\right]^2}\right] \tag{3-70}$$

As Figure 3-2 indicates, the deviation of the Rachford-Rice equation is always negative, allowing its root to be found more easily. The Wilson equation (1968) is more widely used to initialize K values.

$$K_i = \left(\frac{P_{ci}}{P}\right)\exp\left[5.37(1+\omega_i)(1-\frac{T_{ci}}{T})\right] \tag{3-71}$$

These K-values are used to calculate the liquid and vapour composition. The K-values are reevaluated by calculating the fugacity using the equations below:

$$\sum_i (1-\frac{f_{iL}}{f_{iV}})^2 < \varepsilon \tag{3-72}$$

$$\sum_i \frac{(K_i' - K_i)^2}{K_i' K_i} < \varepsilon \tag{3-73}$$

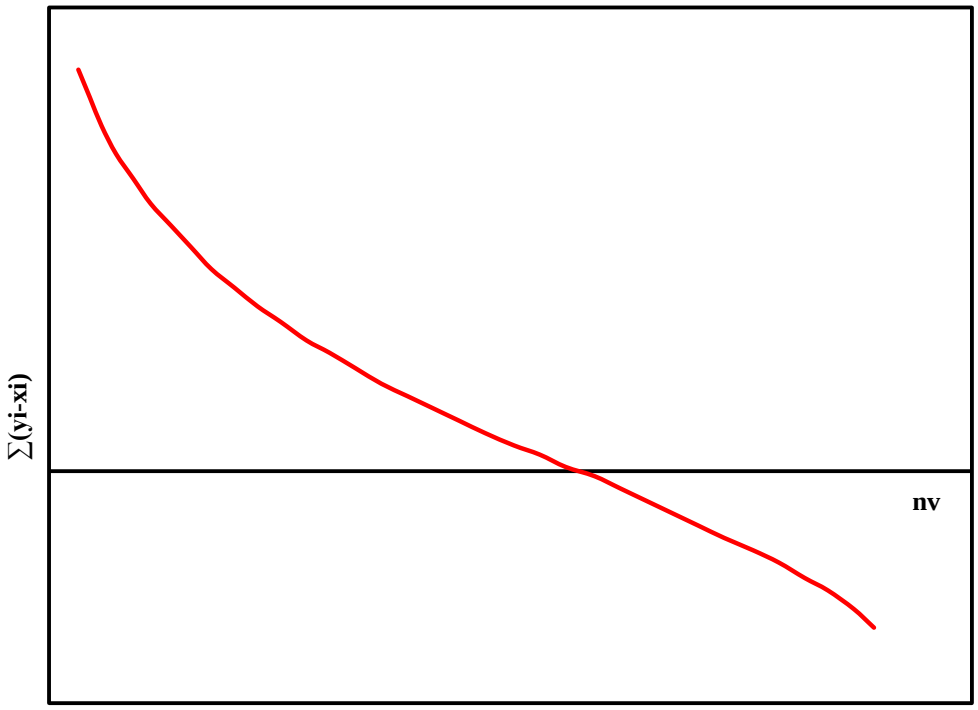

Figure 3-2: Monotonically decreasing Equation 3-69

Figure 3-3 is a schematic algorithm for the flash calculation. In this algorithm, the successive substitution iteration (SSI) method is used for the flash calculation. In addition to simplicity, this method reduces the Gibbs free energy in every iteration (Firoozabadi 1999). This method also does not need good initial K-values unlike Newton's method however its convergence is slow. The conjunction of Newton and SS method can be a good choice which contains both stability and speed in convergence.

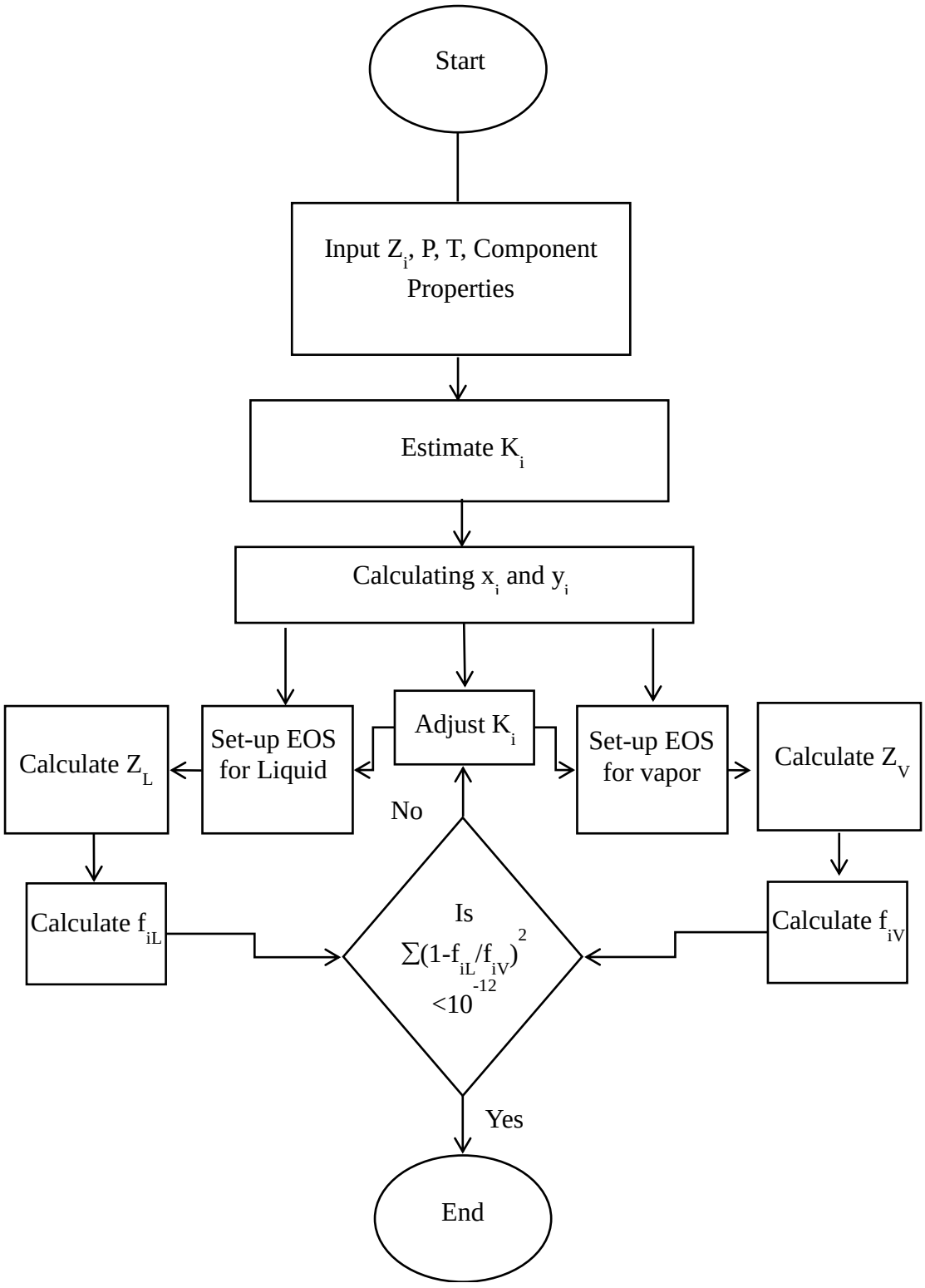

Figure 3-3: Two phases flash calculation flowchart (Danesh 1998)

3.2. Optimization

An optimization algorithm is required to obtain the tuning parameters for the PR EoS and NRTL models. The optimization for finding the least square of the deviations is related to the unconstrained minimization. Dennis et al. (1983) presented a more detailed explanation of unconstrained minimization. The nonlinear least problem is as follows:

$$\min_{x \in R^n} f(x) = \frac{1}{2} R(x)^T R(x) = \frac{1}{2} \sum_{i=1}^{m} r_i(x)^2 \qquad 3\text{-}74$$

where m>n, the first derivative of f(x) is:

$$\nabla f(x) = \sum_{i=1}^{m} r_i(x).\nabla r_i(x) = J(x)^T R(x) \qquad 3\text{-}75$$

Similarly, the second derivative is

$$\nabla^2 f(x) = \sum_{i=1}^{m} (\nabla r_i(x).\nabla r_i(x)^T + r_i(x).\nabla^2 r_i(x)) = J(x)^T J(x) + S(x) \qquad 3\text{-}76$$

$$S(x) = \sum_{i=1}^{m} r_i(x) \nabla^2 r_i(x) \qquad 3\text{-}77$$

$$x_+ = x_c - (J(x_c)^T J(x_c) + \mu_c I)^{-1} J(x_c)^T R(x_c) \qquad 3\text{-}78$$

μ_c is the damping parameter. This equation, known as the Levenberg-Marquardt method, was first suggested by Levenberg (1944) and Marquardt (1963). The damping parameter is critical to the optimization efficiency; thus if the damping parameter be large, the minimum value cannot be found correctly, while a small amount leads to a very slow rate of convergence. An optimum value for the damping parameter can be determined for each problem. An optimization method was proposed where the damping factor at each level of regression was changed considering the closeness to the answer. In regions far from the answer, the damping factor was enlarged while in the vicinity of the solution, its value is reduced. This method can be considered as a combination of the steepest descent and Gauss-Newton methods. When the first guess is far from the solution, the algorithm behaves like the steepest descent and converges at a slow linear

convergence rate. On the other hand, when the first guess is close to the solution, it behaves like the Gauss-Newton method with a greater speed of convergence (a quadratic rate). The Levenberg-Marquardt algorithm may still be slow and locally convergent in problems with large residual value or for very nonlinear problems.

Two different scenarios were considered in defining the objective function (*OF*). In the first scenario, the parameters have been regressed to minimize the objective function of solvent solubility. Then the volume translation technique was applied to match the saturated liquid densities. Thus, the objective functions are as follows:

$$OF = \sum_{i=1}^{np} \sum_{j=1}^{nc} \left[\frac{x^{cal} - x^{\exp}}{x^{\exp}} \right]^2 \qquad 3\text{-}79$$

$$OF = \sum_{i=1}^{np} \left[\frac{\rho^{cal} - \rho^{\exp}}{\rho^{\exp}} \right]^2 \qquad 3\text{-}80$$

In the second scenario, all adjustable parameters including volume shifts and mixing rule parameters are simultaneously regressed to minimize the square error of the saturated liquid compositions and densities. The objective function in this case is,

$$OF = \sum_{i=1}^{np} \left[\frac{\rho^{cal} - \rho^{\exp}}{\rho^{\exp}} \right]^2 + \left[\frac{x^{cal} - x^{\exp}}{x^{\exp}} \right]^2 \qquad 3\text{-}81$$

where n_p is the number of points and n_c is the number of components in each studied system. The *cal* and *exp* superscript refer to the calculated and experimental values, respectively. In the first scenario, the program has fewer regression parameters and requires less iteration for convergence than it does in the second case.

The following figure (Figure 3-4) is a schematic algorithm for the modified Levenberg-Marquardt method.

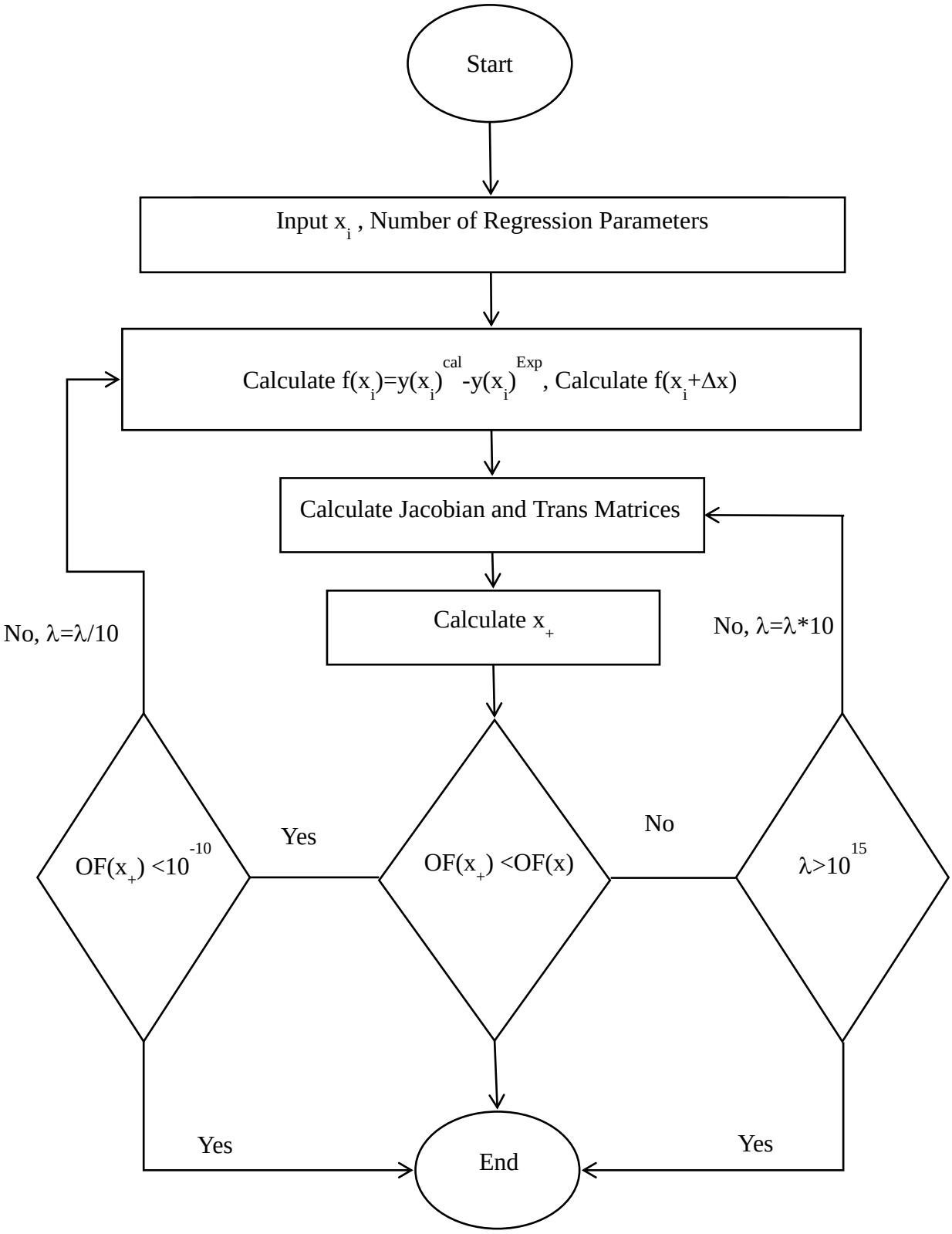

Figure 3-4: Levenberg-Marquardt regression flowchart

The deviation of the *OF* with respect to the regression parameters is calculated numerically. The Jacobian matrix which consists of all of the first order partial variations of the *OF* is defined as follows:

$$J = \begin{bmatrix} \frac{\partial F_1}{\partial x_1} & \cdot & \cdot & \cdot & \frac{\partial F_1}{\partial x_n} \\ \cdot & \cdot & & & \cdot \\ \cdot & & \cdot & & \cdot \\ \cdot & & & \cdot & \cdot \\ \frac{\partial F_m}{\partial x_1} & \cdot & \cdot & \cdot & \frac{\partial F_m}{\partial x_n} \end{bmatrix} \qquad 3\text{-}82$$

In our case, m=1 which means that there is one *OF* and n is the number of regression parameters. In the next step the transpose of the Jacobian matrices are defined and (x^+) is calculated. When the modified answer is far from the solution, the damping factor is enlarging. In the vicinity of the solution, the speed of convergence decreases.

3.3. Characterization Scheme

As mentioned in the previous section, prior to phase behaviour modeling using EoS, the properties of the system must be defined as an input. These properties include the critical properties and acentric factors. Bitumen is a complex mixture of different components, some of which are impossible to characterize. Several approaches have been proposed for bitumen characterization using experimental data. As a result of recent research, experimental data for the true boiling point (TBP) and SCN weight fractions are available. This data is the most common set of data used for bitumen characterization in the petroleum industry. This section reviews the application of these methods to heavy oil and bitumen.

3.3.1. Molar Distribution Functions

Several experimental methods have been proposed to distill bitumen to a higher weight percent. In spite of improvements, bitumen cannot be distilled completely as it often cracks or

decomposes. For this reason additional modeling schemes are required to extend the molar distribution of molecular weight, SCN, and other characteristics of the C_{n+} fraction. There is no superior scheme and each system is modeled appropriately by one specific scheme. The molar distributions of condensate systems exhibit an exponential distribution, while heavy oils and bitumen exhibit left-skewed distributions (Ahmed 1989). This behaviour can be observed in Figure 3-5. Different exponential distributions have been developed for the characterization of the condensate fluids. Katz (1983) proposed the following correlation, based on the compositional behaviour of six condensate systems.

$$Z_n = 1.38205 Z_7 + e^{-0.25903n} \qquad 3\text{-}83$$

Z_{7+}=mole fraction C7+

n=carbon number of the pseudo-component

Z_n=mole fraction of the pseudo-component with carbon number of *n*

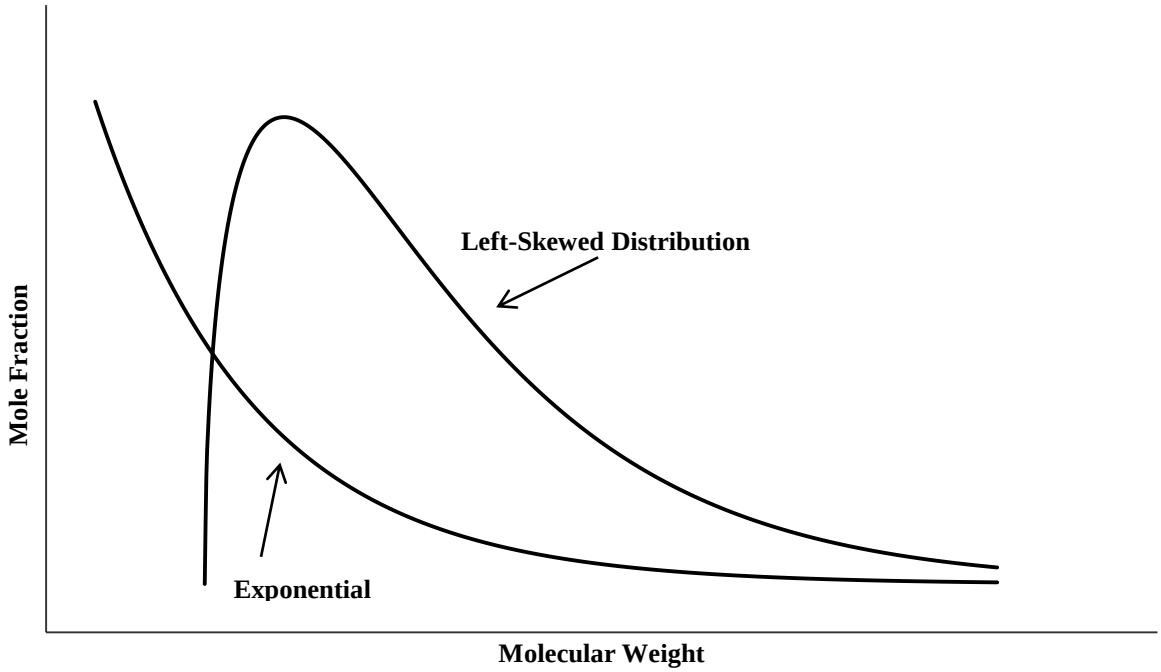

Figure 3-5: Exponential and left-skewed molar distributions

Other methods employ exponential type functions include those developed by Lohrenz (1964) and Pedersen (1982). However, these methods are not applicable in the case of heavy oils and

bitumen, which have a left-skewed molar distribution function. The SCN distribution of Athabasca bitumen shows a left-skewed behaviour which cannot be modeled by the exponential distribution with sufficient accuracy (Figure 3-5). As Equation 3-83 indicates, the Katz approach is a discrete approach to modeling the phase behaviour of different carbon numbers; however it has been shown that continuous models are more applicable and flexible.

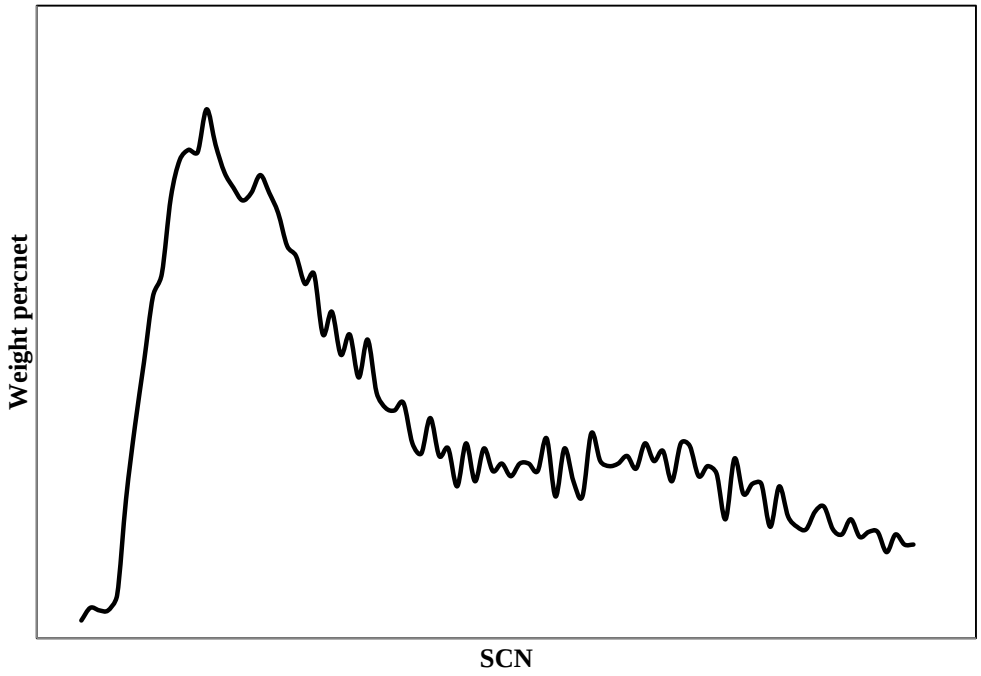

Figure 3-6: SCN distribution of Athabasca bitumen

The distribution functions which show left-skewed behaviour are summarized in Table 3-1. The number of regression parameters for each distribution and their literature application for heavy oils and bitumen are also summarized in the table.

Among the left-skewed distribution functions, Chi-square, Weibull, and Gamma have greatest application to heavy oil and bitumen modeling. Among them, the gamma function has a more general form, which can be altered in the form of the Weibull and Chi-square distribution. In addition, the gamma function can consider different values for shape factor, and illustrate exponential behaviour, making it a good candidate for the characterizing of both heavy and light oils.

Table 3-1: Left-skewed distribution functions

Distribution Name	Number of Parameters	Used for Heavy Oils
Riazi	3	Riazi (1989)
Gamma	3	Whitson (1983)
Chi-Square	2	Quinones-Cisneros (2003)
Weibull	2	
Gaussian	2	
Log-normal	2	
t distribution	3	Used for other type
F distribution	2	
Beta	4	Used for other type
Levy	2	
Burr Type XII	4	Used for other type
Fisk	3	Used for other type
Frechet	3	Used for other type
Gumble	2	Used for other type

3.3.1.1. Gamma Distribution Function

Whitson (1983) chose the third type of Pearson (1958) distribution system, which is a three-parameter gamma (TPG) function. Adjusting the value of the shape factor (γ) can transform this function into other types of distributions. For instance, if the factor equals to one, the gamma function has an exponential shape. For value greater than one, the function has a left skewed distribution. The probability function of this distribution can be calculated by,

$$p(x) = \frac{(x-\eta)^{\gamma-1}\exp[(x-\eta)/\beta]}{\beta^{\gamma}\Gamma(\gamma)} \qquad 3\text{-}84$$

where *p(x)* is the probability function and *x* is the parameter under study, which can be molecular weight. η, β and γ are the gamma distribution parameters. η represents the minimum molecular weight, which is included in the C_{n+} fraction. The occurrence probability for the components with a molecular weight of less than η is zero. γ is the shape factor and β is calculated directly from γ and η. The cumulative probability function is calculated via the following equation,

$$P(X \le x) = \int_{\eta}^{x} p(x)dx \qquad 3\text{-}85$$

This cumulative function shows the occurrence frequency over the interval of η to x. The parameters must be defined with respect to the experimental data. However, in the lack of experimental data, correlations can be used to estimate the TPG parameters. Whitson (1983) expressed an approximation correlation for minimum molecular weight.

$$\eta = 14n - 6 \qquad 3\text{-}86$$

n is the carbon number in the SCN group in C_{n+}. β can be found directly from α and η with following formula:

$$M_{n^+} - \eta = \gamma\beta \qquad 3\text{-}87$$

γ describes the shape of the probability function. The effect of different values of γ on the shape of the probability is shown in Figure 3-7. As this figure illustrates, a value greater than 1 is appropriate for heavy oils and bitumen.

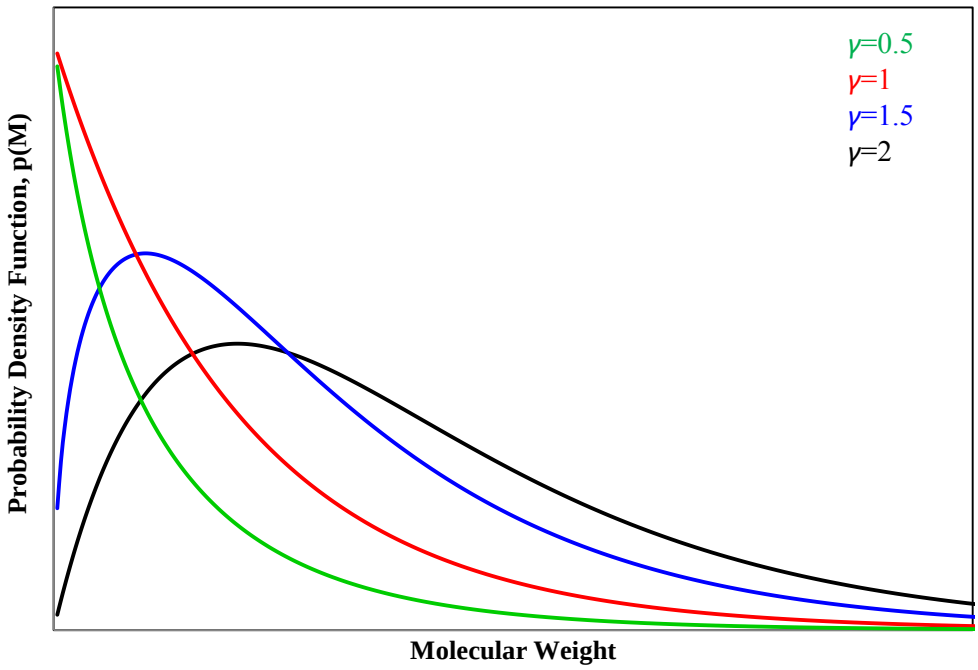

Figure 3-7: Effect of different α values on the shape of probability function

Whitson (1983) proposed a method for converting the above diagram to mole fraction versus molecular weight. The components, which have a molecular weight between M_{i-1} and M_i, occurred with a frequency, defined by the following equation:

$$f_i = \int_{M_{i-1}}^{M_i} p(x)dx = P(r)(M \le M_i) - P(r)(M \le M_{i-1}) \qquad 3\text{-}88$$

The mole fraction, weight fraction and molecular weight of the components having f_i frequency is calculated by Equations 3-89, 3-90, and 3-91.

$$z_i = f_i z_{n^+} \qquad 3\text{-}89$$

$$\overline{M}_i = \eta + \gamma\beta \frac{P(M \le M_i, \gamma+1) - P(M \le M_{i-1}, \gamma+1)}{P(M \le M_i, \gamma) - P(M \le M_{i-1}, \gamma)} \qquad 3\text{-}90$$

$$f_{wi} = z_i \overline{M}_i / (z_{n^+} M_{n^+}) \qquad 3\text{-}91$$

The following is the cumulative probability function obtained from Equations 3-84 and 3-85:

$$P(X \le x) = e^{-y} . \sum_{j=0}^{\infty} [y^{\gamma+j} / \Gamma(\gamma + j + 1)] \qquad 3\text{-}92$$

where $y = (x - \eta)/\beta$, the summation can be ceased when,

$$\sum_{j+1} - \sum_{j} \le 10^{-6} \qquad 3\text{-}93$$

Equations 3-84 to 3-93 will be used to model experimental data of Athabasca and Cold Lake bitumen.

3.3.1.2. Estimation of γ

γ has a significant effect on the shape of the distribution and different approaches have been developed for its calculation. Greenwood et al. (1960) presented different correlations for the estimation of γ. They tested different polynomial and rational approximations and found that the following two correlations were superior to the others.

$$\gamma = Y^{-1}(0.5000876 + 0.1648852\ Y - 0.0544274\ Y^2); \quad 0 \le Y \le 0.5772 \qquad 3\text{-}94$$

$$\gamma = \frac{8.898919 + 9.059950Y + 0.9775373Y^2}{Y(17.79728 + 11.968477Y + Y^2)}; 0.5772 \le Y \le 17.0 \quad 3\text{-}95$$

where

$$Y = \ln[(M_{n^+} - \eta)/m_G] \quad 3\text{-}96$$

$$m_G = \left[\prod_{i=n}^{N}(M_i - \eta)^{z_i}\right]^{1/z_{n^+}} \quad 3\text{-}97$$

Any application of the above correlations requires fully analyses of the molecular weight and SCN mole fractions. While above method is applicable for light oils, complete analysis of heavy oils is not possible. Optimization is another method for the estimation of γ, in which a regression scheme is used to fit the experimental composition.

$$E(\gamma) = \sum_{i=n}^{N}(z_i - \bar{z})^2 \quad 3\text{-}98$$

$$E(\gamma) = \sum_{i=n}^{N}(f_{wi} - \tilde{f}_{wi})^2 \quad 3\text{-}99$$

Rodriguez et al. (2010) tested different values of γ and determined that the best fit occurred when the experimental molecular weight with the maximum mole fraction (Mw_{max}) and the TPG have the same value. Duan et al. (2013) used the Rodriguez approach and generated an equation for the value of the molecular weight with the maximum mole fraction Mw_{max}. The derivative of the probability function with respect to molecular weight is calculated by Equation 3-100.

$$\frac{dp(M)}{dM} = \frac{(\gamma-1)(M-\eta)^{\gamma-2}\exp[-(M-\eta)/\beta]}{\beta^{\gamma}\Gamma(\gamma)} - \frac{(M-\eta)^{\gamma-1}\exp[-(M-\eta)/\beta]}{\beta^{\gamma+1}\Gamma(\gamma)} \quad 3\text{-}100$$

The derivative of a curve at its maximum is equal to zero:

$$\left.\frac{dp(M)}{dM}\right|_{Mw_{\max}} = 0 \quad 3\text{-}101$$

The Duan et al. correlation is used to obtain the shape factor. However because the value of Mw_{max} is not known in our case, a new approach has been proposed that is explained in section 3.3.4. Each SCN group with *n* carbon atoms consists of different components (saturated,

aromatic and etc.). Thus, the molecular weight of each SCN cannot be accurately calculated using correlations. Rodriguez et al. (2010) changed the boundary for the cumulative frequency of the SCN occurrence in Equation 3-88. Their new method is based on the best fit between the TPG and GC mole fraction of each SCN.

$$z_{char}(C_n) = z_{C_{n+}} \int_{Mw_{\min}}^{LMw} p(M)dM \qquad 3\text{-}102$$

In the above correlation, Mw_{min} and L_{Mw} (limiting molecular weight) indicate the minimum and maximum molecular weight in a SCN group. The relationship between the mole fraction of the TPG and the experimental data is found by iteration and at least two previous carbon numbers and their respective mole fractions are required. In the next step, the relationship between L_{Mw} and SCN is obtained and can be used for further SCN groups. Rodriguez et al. (2010) presented their procedure in a stepwise scheme, which consider a relationship between L_{Mw} and Mw_{min}:

$$L_{Mw} = M_{w_{\min}} + dM \qquad 3\text{-}103$$

dM can accept a different value but is normally 0.1, 0.01 and 0.001. The effect of changing the value of dM is addressed in the next chapter. The first step in applying the Rodriguez et al. (2010) procedure is calculating an elementary L_{Mw} using Equation 3-86. Next Equation 3-102 is used to calculate the mole fraction of SCN. If this value was smaller than the experimental data then:

$$L_{M_w} = L_{M_w} + dM \qquad 3\text{-}104$$

L_{Mw} will be updated using the above equation until the calculated mole fraction is higher than the experimental data. Then, L_{Mw} will be defined as a function of the carbon number and will be used to extrapolate to the region where no experimental data is available.

3.3.2. Physical Properties Calculation

Calculations of physical properties are made possible by means of correlations that are generally functions of boiling point, specific gravity, molecular weight and SCN. These

correlations basically generate the physical properties for components with low SCN. However, caution must be exercised in the application of these correlations for fractions with high SCN. The physical properties of interest are critical pressure, temperature, volume, acentric factor, boiling point and specific gravity. Kesle and Lee (1976) correlated the critical pressure, critical temperature and acentric factor as a function of the normal boiling point and specific gravity.

$$T_c[R] = 341.7 + 811SG + (0.4244 + 01174SG)T_b[R] + \frac{(0.4669 - 3.2623SG)\times 10^5}{T_b[R]} \quad \text{3-105}$$

$$\ln P_c[psia] = 8.3634 - \frac{0.0566}{SG} - (0.24244 + \frac{2.2898}{SG} + \frac{0.11857}{SG^2})\times 10^{-3} T_b[R] + (1.4685 + \frac{3.648}{SG} + \frac{0.47227}{SG^2})\times 10^{-7} T_b{}^2[R] - (0.42019 + \frac{1.6977}{SG^2})\times 10^{-3} T_b{}^3[R] \quad \text{3-106}$$

$$\omega = \frac{(\ln P_{br} - 5.92714 + \frac{6.09648}{T_{br}} + 1.28862\ln T_{br} - 0.169347 T_{br}{}^6)}{(15.2518 - \frac{15.6875}{T_{br}} - 13.4721\ln T_{br} + 0.4357 T_{br}{}^6)} \; for T_{br} \le 0.8 \quad \text{3-107}$$

$$\omega = -7.904 + 0.1352K_w - 0.007465K_w{}^2 + 8.359T_{br} + \frac{(1.408 - 0.01063K_w)}{T_{br}} \; for T_{br} \ge 0.8 \quad \text{3-108}$$

Twu (1984) presented his model based on perturbation theory in which the physical properties for a reference system are calculated and then expanded to real systems. They chose *n*-alkanes to act as the reference system. Twu (1983) correlated physical properties as a function of the normal boiling point.

$$P_{cp}{}^o[psia] = (3.83354 + 1.19629\xi^{1/2} + 34.8888\xi + 36.1952\xi^2 + 104.193\xi^4)^2 \quad \text{3-109}$$

$$\xi = 1 - \frac{T_b[R]}{T_{cp}{}^o[R]} \quad \text{3-110}$$

$$T_c{}^o[R] = T_b[R](0.533272 + 0.191017\times 10^{-3} T_b[R] + 0.779681\times 10^{-7} T_b{}^2[R] - 0.284376\times 10^{-10} T_b{}^3[R] + 0.959468\times 10^{28}/T_b{}^{13}[R])^{-1} \quad \text{3-111}$$

$$V_c{}^o[\frac{ft^3}{lbmol}] = [1 - (0.419869 - 0.505839\xi - 1.56436\xi^3 - 9481.70\xi^{14})]^{-8} \quad \text{3-112}$$

$$SG^o = 0.843593 - 0.128624\xi - 3.36159\xi^3 - 13749.5\xi^{12} \quad 3\text{-}113$$

$$T_b = \exp(5.71419 + 2.71579\zeta - 0.286590\zeta^2 - 39.8544/\zeta - 0.122488/\zeta^2) - 24.7522\zeta + 35.3155\zeta^2 \quad 3\text{-}114$$

$$\zeta = \ln Mw^o \quad 3\text{-}115$$

Equation 3-114 has an explicit functionality of normal boiling point. Therefore Twu (1984) suggested the equation below as a first guess:

$$Mw^o = T_b/(10.44 - 0.0052T_b) \quad 3\text{-}116$$

Equations 3-109 to 3-116, enable the calculation of the physical properties of real fluids using the following general equation.

$$g = g^o[(1+2f)/(1-2f)]^2 \quad 3\text{-}117$$

g can be the critical pressure, critical temperature, critical volume, and molecular weight. For critical pressure the equation would be:

$$P_c[psia] = P_c^o[psia](T_c[R]/T_c^o[R])(V_c[\frac{ft^3}{lbmol}]/V_c^o[\frac{ft^3}{lbmol}])[(1+2f_P)/(1-2f_P)]^2 \quad 3\text{-}118$$

$$f_P = \Delta SG_P[(2.53262 - 46.1955/T_b^{1/2}[R] - 0.00127885T_b[R]) + (-11.4277 + 252.140/T_b^{1/2}[R] + 0.00230535T_b[R])\Delta SG_P] \quad 3\text{-}119$$

$$\Delta SG_P = \exp[0.5(SG^o - SG)] - 1 \quad 3\text{-}120$$

Critical temperature:

$$T_c[R] = T_c^o[R][(1+2f_T)/(1-2f_T)]^2 \quad 3\text{-}121$$

$$f_T = \Delta SG_T[-0.362456/T_b^{1/2}[R] + (0.0398285 - 0.948125/T_b^{1/2}[R])\Delta SG_T] \quad 3\text{-}122$$

$$\Delta SG_T = \exp[5(SG^o - SG)] - 1 \quad 3\text{-}123$$

Critical volume:

$$V_c[\frac{ft^3}{lbmol}] = V_c^o[\frac{ft^3}{lbmol}][(1+2f_V)/(1-2f_V)]^2 \quad 3\text{-}124$$

$$f_V = \Delta SG_V[0.466590/T_b^{1/2}[R] + (-0.182421 + 3.01721/T_b^{1/2}[R])\Delta SG_V] \quad 3\text{-}125$$

$$\Delta SG_V = \exp[4(SG^o - SG^2)] - 1 \quad \text{3-126}$$

Molecular weight:

$$\ln Mw = \ln Mw^o[(1+2f_M)/(1-2f_M)]^2 \quad \text{3-127}$$

$$f_M = \Delta SG_M[|x| + (-0.0175691 + 0.193168/T_b^{1/2}[R])\Delta SG_M] \quad \text{3-128}$$

$$|x| = \left|0.0123420 - 0.328086/T_b^{1/2}[R]\right| \quad \text{3-129}$$

$$\Delta SG_M = \exp[5(SG^o - SG)] - 1 \quad \text{3-130}$$

The above equations require the knowledge of the normal boiling point and specific gravity. In the absence of specific gravity data, where the molecular weight is known, it can be calculated using the molecular weight correlation equations.

Ahmed (1985) correlated the physical properties presented by Katz and Firoozabadi (1978). Their equation is a function of carbon number and has the following generalized form.

$$\theta = a_1 + a_2 n + a_3 n^2 + a_4 n^3 + \frac{a_5}{n} \quad \text{3-131}$$

In this equation, n is the carbon number and a_1 to a_5 are the coefficients of the equation. θ represents the physical properties and can be the molecular weight, normal boiling point, specific gravity, acentric factor, critical temperature, critical pressure, and critical volume.

Sancet (2007) presented his correlations based on molecular weight. He showed that his correlations produce better liquid density predictions in the presence of high molecular weight hydrocarbons than Riazi-Daubert's (1980) correlation does.

$$P_c[psia] = 82.82 + 653e^{-0.00742M} \quad \text{3-132}$$

$$T_c[R] = -778.5 + 383.5\ln(MW - 4.075) \quad \text{3-133}$$

$$T_b[R] = 194 + 0.001241(T_c[R])^{1.869} \quad \text{3-134}$$

The application and difference of the mentioned correlation are studied in the next chapter. Additionally, a sensitivity analysis of saturated liquid density and solubility with respect to each parameter is presented.

3.3.3. Lumping Scheme

Lee et al. (1981) proposed a lumping method for oil fractions with relatively close physiochemical properties. They suggested that when the properties are plotted versus a characteristic independent variable, the slope of these curves shows the closeness of the property of interest. Since almost all of the physical properties are calculated and defined based on the normal boiling point, the average value of the boiling point was used as the characteristic parameter. They proposed their lumping method in five steps.

In the first step the available physiochemical properties must be plotted versus the normal boiling point. Second, the slope of these curves for each fraction is calculated numerically while in the third step, this value must be normalized using the following equation:

$$\overline{m_{ij}} = \frac{\left|m_{ij}\right|}{\max_{i=1\ldots n_f}\left|m_{ij}\right|} \qquad 3\text{-}135$$

In Equation 3-135, m_{ij} is the slope for each fraction at each $\overline{T_b}$ and n_f and n_p refer to the number of original oil fractions and the number of available properties, respectively. In the next step, the slopes are averaged. Finally, the calculated values are considered and the fractions with close physiochemical properties are lumped together.

Whitson (1983) also proposed a lumping scheme based on Sturges' rule, a law for choosing bars when data is represented in a histogram. He also considered gamma distribution similar to the folded log-normal distribution and calculated the number of pseudo-components using Equation 3-136:

$$N_g = Int\left[1 + 3.3\log_{10}(N - n)\right] \qquad 3\text{-}136$$

n and *N* are the minimum and maximum carbon number in the characterized sample, respectively. The pseudo-components are separated by molecular weight.

$$M_I = M_{C_n}\left(\frac{M_{N^+}}{M_{C_n}}\right)^{\frac{1}{N_H}} \qquad 3\text{-}137$$

In Equation 3-137, N_H is the pseudo-component of interest. The applicability of these two lumping schemes and the effect of decreasing the number of pseudo-components on phase behaviour modeling are investigated in the next chapter.

3.3.4. Characterization Algorithm

In the present study, two different sets of data are available; the TBP and SCN curves of Athabasca bitumen (Figure 3-8 and Figure 3-9) obtained by the SHARP group and the TBP curve of Cold Lake bitumen presented by Eastick (1986).

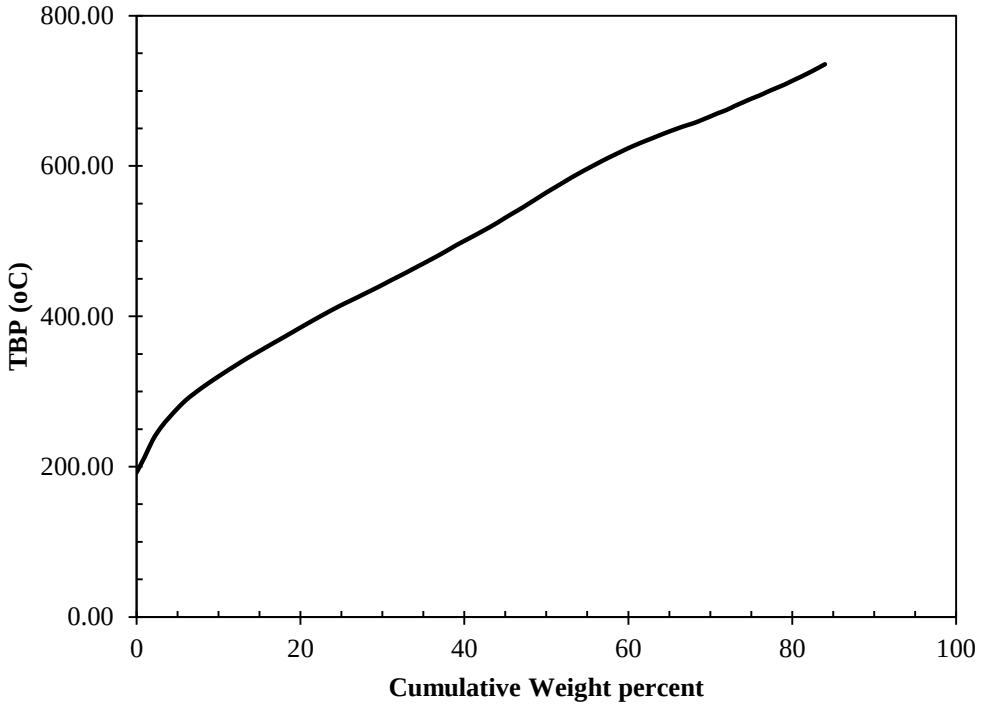

Figure 3-8 : Normal boiling point for Athabasca bitumen

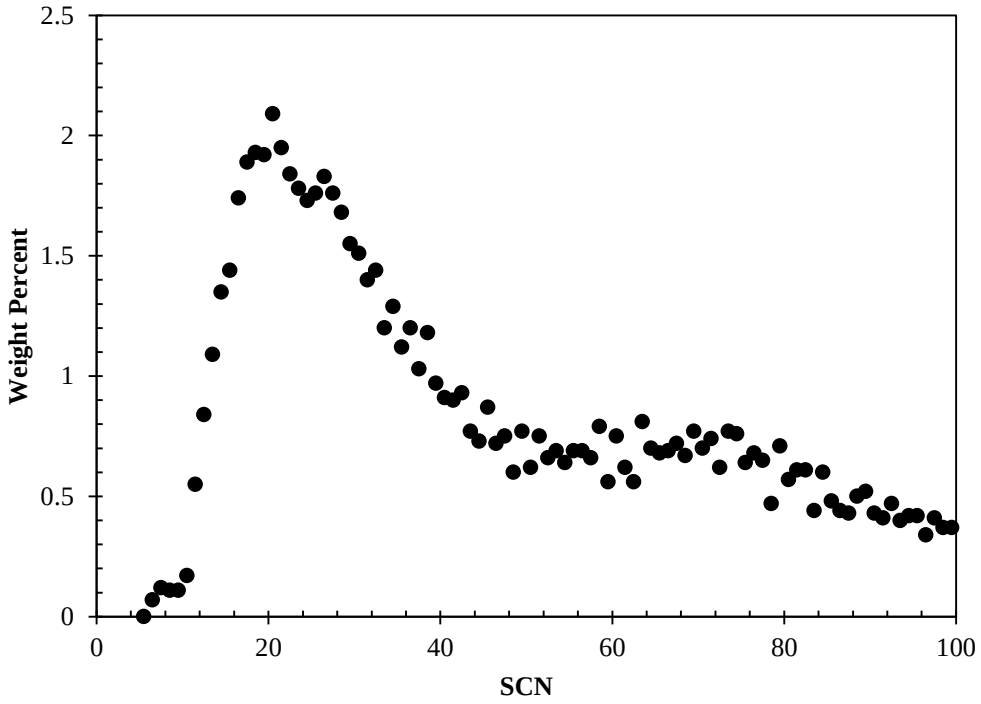

Figure 3-9: Weight percent for each SCN in Athabasca bitumen

In addition to these curves, the average molecular weight and specific gravity of whole bitumen is also available. The characterization scheme in this study is presented in a schematic algorithm (Figure 3-13). The main goal in this section is to extrapolate the TBP curve by extrapolating the SCN curve using the molar distribution. The extrapolated SCN curve must be changed to a TBP curve using a correlation. The TBP and SCN curves of Athabasca bitumen have been used to determine the best correlation to relate the two diagrams. For this purpose, the TBP of each SCN is calculated by the interest correlation and the weight percent for each SCN is then calculated and compared with the TBP curve. Duan et al. (2013) compared the Ahmed (1985), Sancet (2007) and Twu (1984) correlations for different SCNs and indicated Ahmed (1985) correlation cannot be used in SCNs higher than 40 and 60 for critical temperature and pressure calculation respectively while Sancet (2007) and Twu (1984) correlations are applicable over a wide range of SCNs. The Twu (1984) correlation can reconstruct the TBP curve from the SCN curve with an AARD of 1.58% (Figure 3-10).

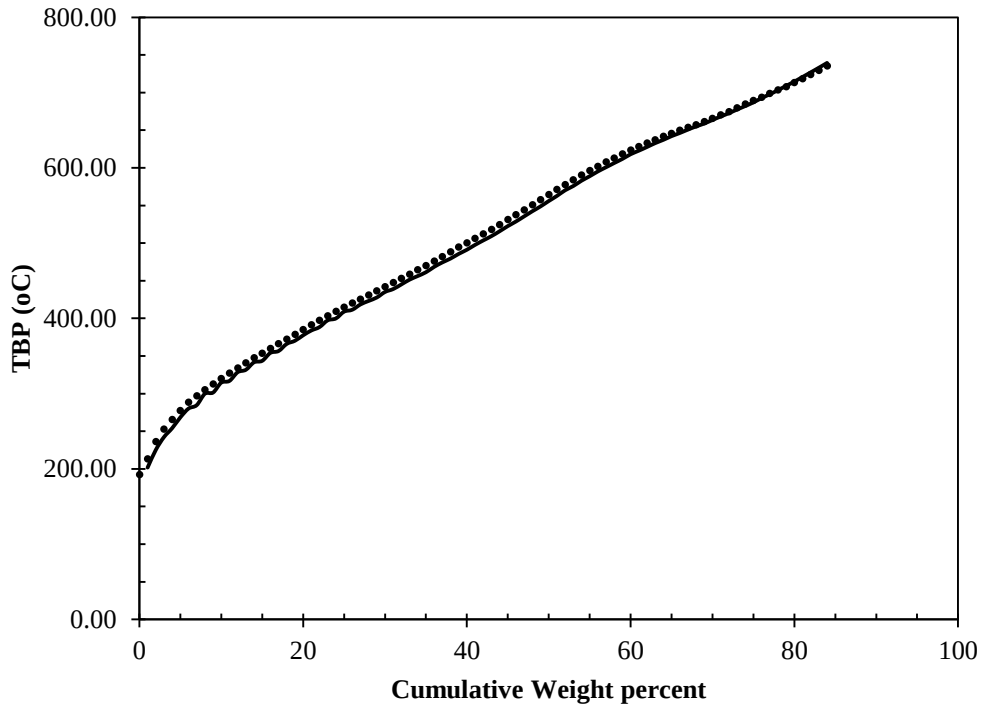

Figure 3-10: Predicted and experimental normal boiling points of Athabasca bitumen, the dots are experimental points and the line is modeling.

In the next step, the molar distribution is modeled with the gamma distribution function. In this study, a lack of experimental molar distribution data means that Mw_{max} is unknown and cannot be used to find the shape factor (γ). A trial and error method was proposed to overcome this lack of data. The method assumed the Mw_{max} is in relation with SCN_{max} which will be obtained with Figure 3-11 and its molecular weight can then be calculated using the gamma distribution. This value is used as an initial guess and will be corrected in further steps. Figure 3-11will be reconstructed using the limiting molecular weight.

In following step, Mw_{max} will be compared to the assumed value and its value will be modified until it is close enough to the assumed value. The limiting molecular weight versus SCN will be used to extrapolate to higher carbon numbers and will be used to extrapolate the TBP curve. The algorithm of the gamma distribution function for heavy oil is shown in Figure 3-13.

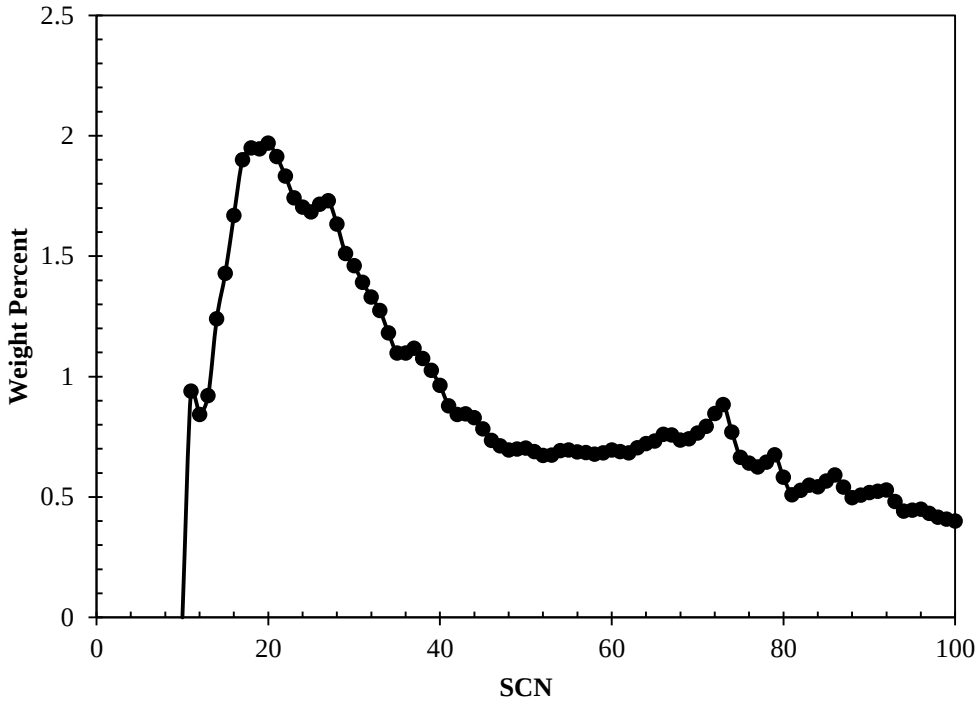

Figure 3-11: The predicted and experimental data for weight percent of each SCN. The dots are experimental points and the line is modeling

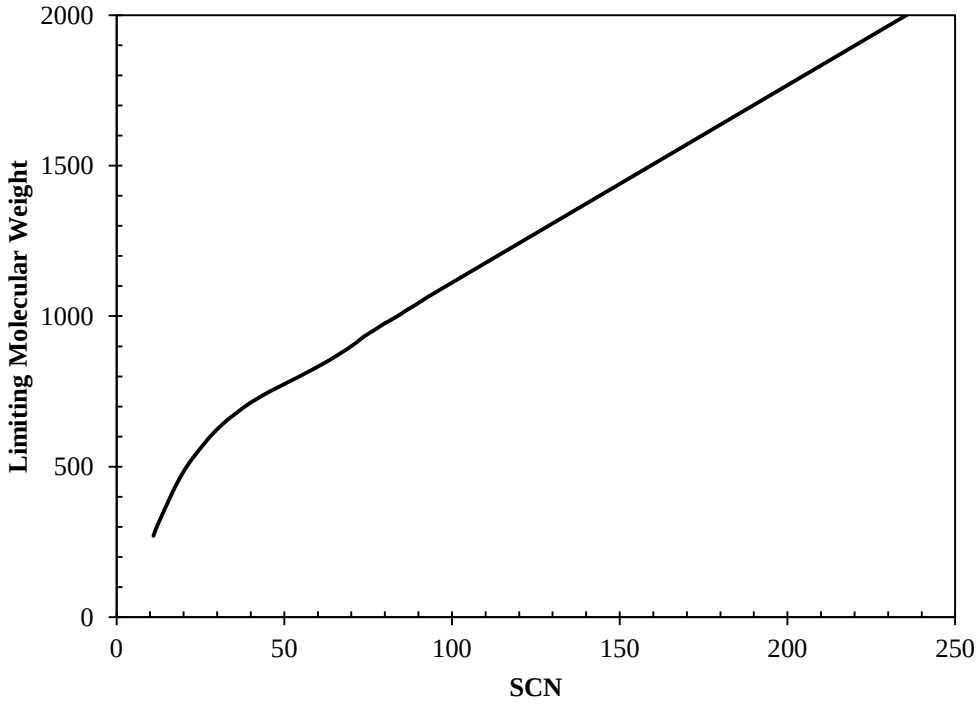

Figure 3-12: Limiting molecular weight for SCNs and the extended values

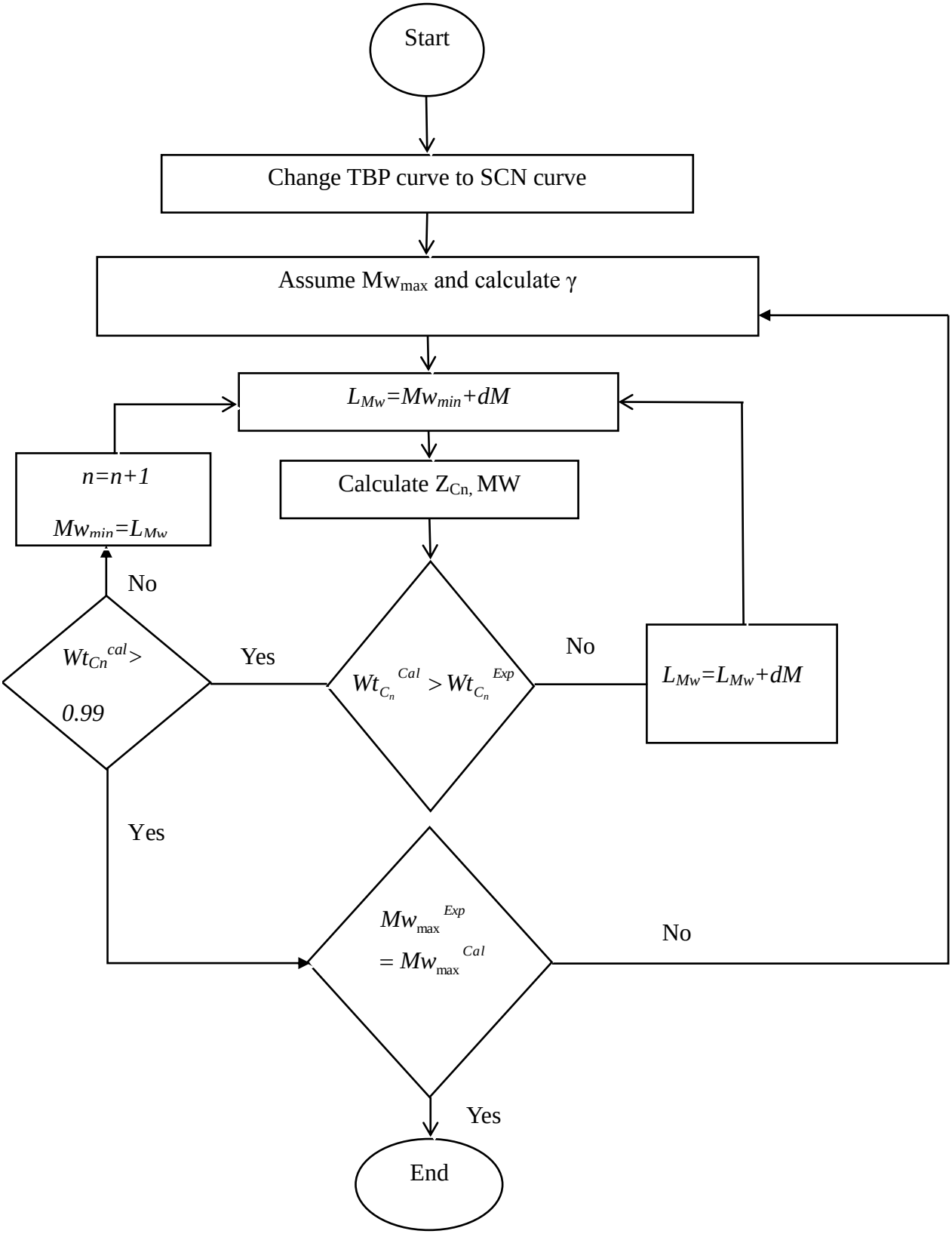

Figure 3-13: Bitumen characterization by gamma distribution model

3.4. Code Validation

After the code is developed in the C^{++} environment, it must to be validated using literature results and commercial software. For this purpose, the ternary system of carbon dioxide, ethanol, and *n*-decane was selected. Nourozieh et al. (2013) reported the VLE data for this ternary system over the pressure range of 1 MPa to 6 MPa and two different temperatures (303.2 and 323.2 K). Nourozieh et al. (2013) used two different EoSs of the PR and SRK and used the binary interaction parameters and volume shifts as regression parameters. The critical properties and acentric factors of the pure components are reported in Table 3-2. In the present study, the mole fraction of carbon dioxide in the ternary system was modeled by means of the PR EoS coupled with the van der Waals mixing rules. The binary interaction coefficients of Nourozieh et al. (2013) are also applied and the resulting AARD was compared to validate the code. The OF and AARD of the mole fraction are defined as follows.

$$OF = \sum_{i=1}^{np} \left[\frac{x^{cal} - x^{\exp}}{x^{\exp}} \right]^2 \qquad 3\text{-}138$$

$$AARD(x) = \frac{100}{np} \sum_{i=1}^{n_p} \frac{\left| x^{\exp} - x^{cal} \right|}{x^{\exp}} \qquad 3\text{-}139$$

x is mole fraction and *exp* and *cal* represent the experimental and calculated values, respectively. The coefficients in Nourozieh et al. (2013), the binary interaction coefficients in this study, and the associated AARDs are reported in Table 3-2. When the binary interaction coefficients in Nourozieh et al. (2013) are applied in the developed program, the AARD is 5.66% which is exactly the same as their reported value. In addition, the table below shows that our program predicts the mole fraction more successfully. This may be due to different *OF* which is defined by *K*-values in the WinProp program instead of the mole fraction.

Table 3-2: Binary interaction coefficient and AARD for ternary system of carbon dioxide, ethanol and *n*-decane.

	k_{12}	k_{13}	k_{23}	**AARD**
Nourozieh et al. (2013)	0.0848	0.1246	-0.0484	5.66
Present study	0.1764	0.1189	0.0838	4.17

The mole fraction of the components in the liquid and vapour phase and the vapour mole fraction are also compared with the WinProp program to validate our code (Table 3-3). As the table indicates, the values calculated by our program are exactly the same as those calculated with WinProp.

Table 3-3: Comparison of two phases flash calculation of developed code and WinProp, x and n_v are carbon dioxide liquid mole fraction and vapour mole fraction respectively.

P/Mpa	Developed Code		WinProp	
	10^2x	n_v	10^2x	n_v
0.96	10.948	0.1621	10.948	0.1621
1.94	21.643	0.1890	21.644	0.1890
2.94	32.157	0.2328	32.159	0.2328
3.94	42.499	0.3090	42.505	0.3090
4.87	52.343	0.4586	52.347	0.4586
5.84	63.897	0.8088	63.905	0.8088

The density prediction of the program was also validated. The AARD and *OF* for density are defined by the following equation.

$$OF(\rho) = \left(\frac{\rho^{\exp} - \rho^{xal}}{\rho^{\exp}} \right)^2 \qquad 3\text{-}140$$

$$AARD(\rho) = \frac{100}{np} \sum_{i=1}^{n_p} \frac{\left| \rho^{\exp} - \rho^{cal} \right|}{\rho^{\exp}} \qquad 3\text{-}141$$

The volume shifts and resulting AARDs are presented in Table 3-4. The volume shift parameters reported by Nourozieh et al. (2013) is tested and the same AARD was obtained.

The experimental and predicted carbon dioxide solubility in a binary mixture of ethanol and *n*-decane is shown in Figure 3-14. As the figure indicates, increasing the molar composition of ethanol in a binary mixture of ethanol and *n*-decane, decreases the solubility of carbon dioxide. The saturated densities of the mixture are also shown in Figure 3-15. Nourozieh et al. (2013) found that applying the volume shift for the solvent as well, significantly improves the prediction.

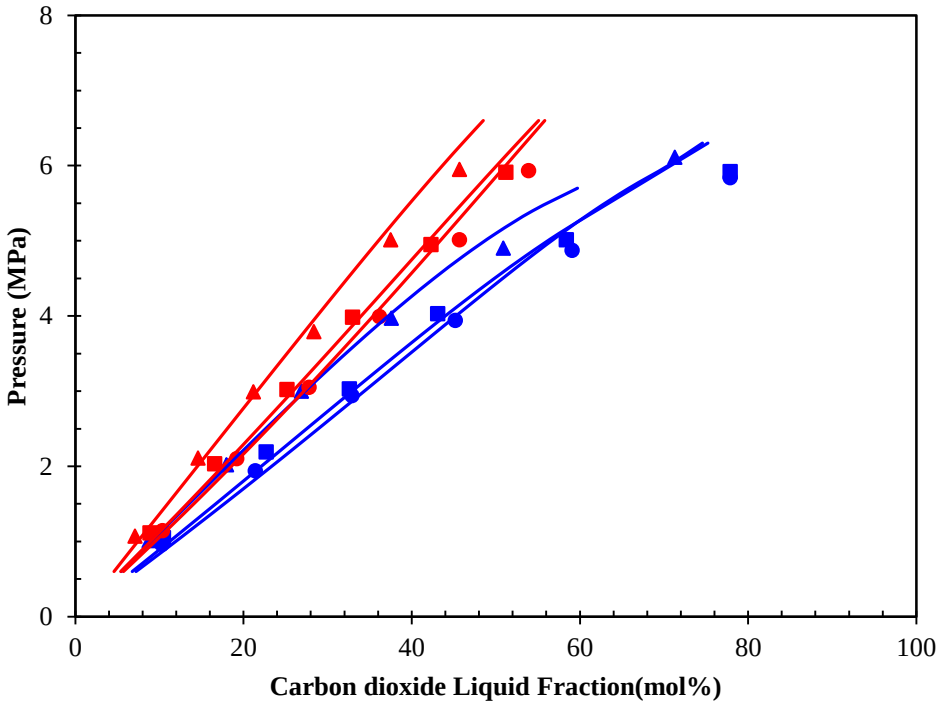

Figure 3-14: Carbon dioxide mole fraction in binary mixture of ethanol and *n*-decane, ●, ■, ▲ are x_2/x_1=0.25, x_2/x_1=0.5 and x_2/x_1=0.75. The blue and red lines are 303.2 K and 323.2 K.

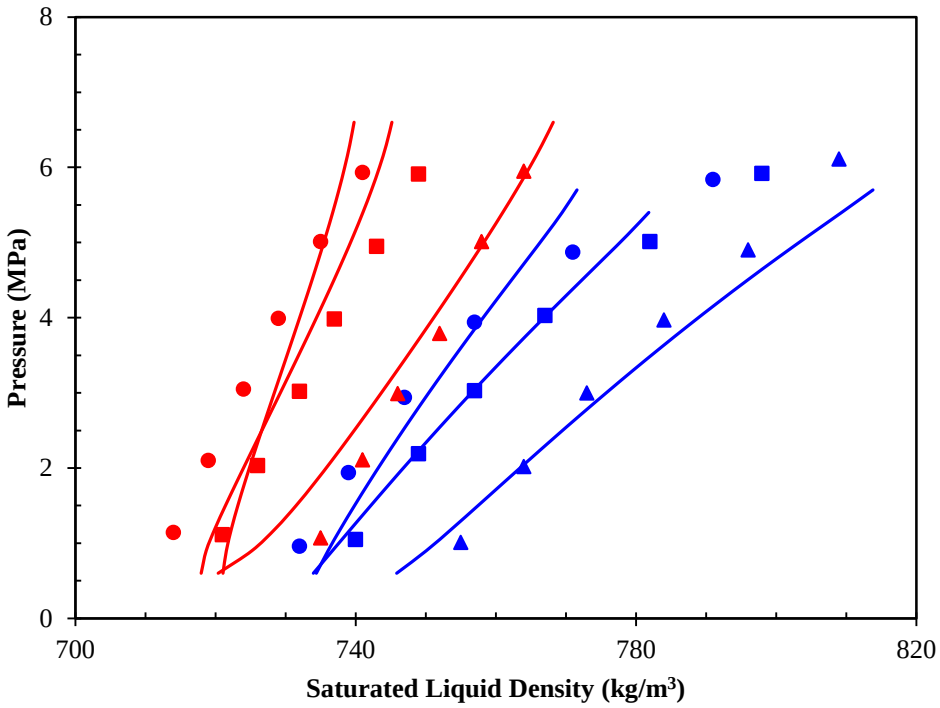

Figure 3-15: Liquid density of carbon dioxide, ethanol and *n*-decane, ternary system. ●, ■, ▲ are x_2/x_1=0.25, x_2/x_1=0.5 and x_2/x_1=0.75. The blue and red lines are 303.2 K and 323.2 K.

Table 3-4: Carbon dioxide, ethanol and *n*-decane volume shifts in ternary mixture

	V_s			*AARD*
	CO_2	C_2H_6O	$nC_{10}H_{22}$	
Nourozieh et al. (2013)	0	-0.0084	0.0746	1.03
Present study	0	0.0604	0.0907	0.468

Following the validation of the van der Waals mixing rule, the developed code for the Wong-Sandler rule has been validated. A system of propane-methanol system was selected for this purpose and is modeled by Wong and Sandler (1992). The experimental data were taken from Galivel-Solastiouk et al. (1986) which contains 12 points over the pressure range 0.35 MPa to 1.4 MPa at 313.1 K. The presented study and the Wong and Sandler (1992) results are presented in Table 3-5. The predicted value of the binary interaction coefficient and the NRTL parameter of the present study and the Wong and Sandler (1992) are in good agreement. The experimental data and calculated values are presented in Figure 3-16.

Table 3-5: Binary interaction coefficient and NRTL parameters for binary mixture of propane and methanol.

	k_{12}	τ_{12}	τ_{12}	AAD*(K)%*
Wong and Sandler (1992)	0.16	4.03	1.85	0.65
Present study	0.16	4.09	1.82	0.61

The *OF* and AARD are defined as a function of K-values:

$$OF(K) = \left[\frac{K^{\exp} - K^{xal}}{K^{\exp}} \right]^2 \qquad 3\text{-}142$$

$$AAD(K) = \frac{100}{np} \sum_{i=1}^{n_p} \left| K^{\exp} - K^{cal} \right| \qquad 3\text{-}143$$

As Figure 3-16 indicates, the binary system of methanol and propane is highly non-ideal. The Wong-Sandler results are in good agreement with the experimental data.

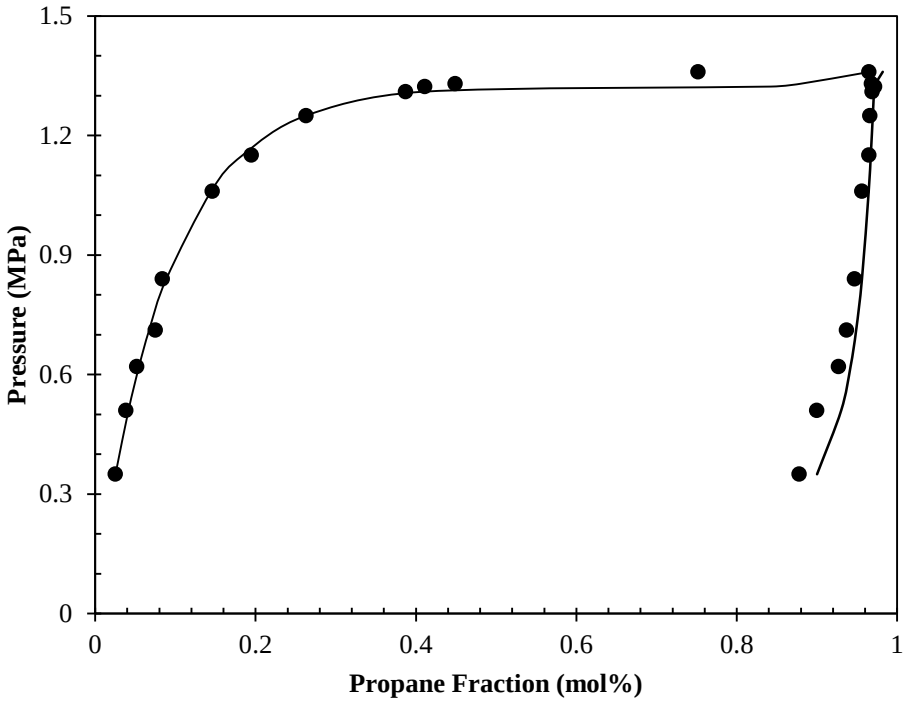

Figure 3-16: Liquid and vapour mole fraction of propane in binary mixture of propane and methanol. The lines are predicted value and the dots are experimental data.

3.5. Simple Systems

The main objective of this study is to improve the phase behaviour modeling of solvent (methane, ethane, carbon dioxide) and bitumen systems. For better understanding, binary mixtures of the mentioned solvents and different components including *n*-alkanols and *n*-alkanes were studied. For this purpose, the experimental data from previous studies in our group was used to conduct a comprehensive EoS modeling of binary polar and non-polar systems utilizing the van der Waals and Wong-Sandler mixing rules, and the volume translation technique. Two different combining rules were considered for the repulsive parameter in the application of the van der Waals mixing rules. The binary systems (methane + methanol, ethanol, and 1-propanol), (methane + *n*-tetradecane and *n*-octadecane), (ethane + *n*-tetradecane and *n*-octadecane), (carbon dioxide + methanol, ethanol, and 1-propanol), (carbon dioxide + *n*-decane, *n*-tetradecane, and *n*-octadecane) are of interest. The experimental phase equilibrium data used in this section are summarized in Table 3-6. The temperature and pressure ranges for each binary system are also

presented in this table. As Table 3-6 indicates, more than 300 data points were considered. The critical properties (temperature, pressure and volume), boiling point, molecular weight, and acentric factors of the components under study are reported in Table 3-7. To predict the saturated liquid compositions and densities of different binary systems, the mixing rules and combining rules coefficients were used as adjusting parameters.

Table 3-6: Experimental data used for the phase behaviour modeling study; n_p, number of data points; T, temperature; P, pressure.

System	n_p	T/K	P/MPa	Reference
Methane +				
Methanol	8	294.6	1.05-7.99	Nourozieh et al. (2012) a
Ethanol	8	295.0	1.02-7.99	Nourozieh et al. (2012) a
1-Propanol	8	294.9	0.99-8.02	Nourozieh et al. (2012) a
n-Tetradecane	6	294.7	2.05-9.49	Nourozieh et al. (2012) b
	6	324.0	2.07-9.54	
	6	373.4	2.10-9.50	
	6	447.6	1.99-9.47	
n-Octadecane	6	323.0	2.08-9.49	Kariznovi et al. (2012)
	6	347.9	2.09-9.47	
	6	398.0	2.03-9.59	
	6	447.6	1.92-9.51	
Ethane +				
n-Tetradecane	6	323.2	1.05-5.94	Kariznovi et al. (2011)
	7	373.4	1.01-7.07	
	8	422.6	1.08-8.00	
n-Octadecane	6	323.2	1.15-5.89	Nourozieh et al. (2012) c
	8	372.8	0.94-7.98	
	8	422.6	0.95-8.17	
Carbon dioxide +				
Methanol	5	303.2	102-505	Kariznovi et al. (2013) a
	6	323.2	1.11-5.95	
Ethanol	6	303.2	1.14-5.94	Kariznovi et al. (2013) a
	6	323.2	102-6.07	
1-Propanol	5	303.2	0.90-499	Kariznovi et al. (2013) a
	6	323.2	0.77-6.00	
n-Decane	6	323.2	1.02-5.96	Kariznovi et al. (2013) b
	6	373.2	1.12-6.19	Nourozieh et al. (2013) a
n-Tetradecane	6	323.2	0.98-5.97	Kariznovi et al. (2013) b
	6	373.2	0.96-5.97	Nourozieh et al. (2013) a
n-Octadecane	6	372.8	0.95-5.99	Kariznovi et al. (2013) c

Table 3-7: Thermodynamic properties of components (Yaws 1990)

Component	CAS No.	MW	T_b/K	T_C/k	P_C/MPA	V_C	ω
Carbon dioxide	124-38-9	44.01	194.67	304.19	7.382	94	0.228
Methanol	67-56-1	32.042	337.85	512.58	8.096	117.8	0.566
Ethanol	64-17-5	46.069	351.44	516.25	6.384	166.9	0.637
1-Propanol	71-23-8	60.096	370.35	536.71	5.17	218.5	0.628
Methane	74-82-8	16.043	111.66	190.58	4.604	99.3	0.011
Ethane	74-84-0	30.07	184.55	305.42	4.88	147.9	0.099
n-Decane	124-18-5	142.285	447.3	618.45	2.123	603.1	0.484
n-Tetradecane	629-59-4	198.392	526.73	692.4	1.621	842.8	0.662
n-Octadecane	593-45-3	254.5	589.86	745.26	1.214	1070	0.795

Two different approaches were tested which demonstrate the effect of the solubility results on saturated density prediction. The use of two different objective functions enables the creation of a parametric regression for solubility and density prediction both simultaneously and separately.

3.5.1. First Approach

In this section, the binary interaction coefficients and NRTL parameters were regression to predict the solubility of the binary mixtures. The obtained parameters were used to model saturated density by means of volume shifts. The isotherm conditions were also modeled.

3.5.1.1. Temperature Independent Parameters

The best fit parameters for one-parameter, two-parameter, and Wong-Sandler mixing rules are presented in Table 3-8. In addition to the parameters, the average absolute relative deviations (AARD) between the experimental compositions and calculated values were calculated using the following equation and are summarized in Table 3-8.

$$AARD(x) = \frac{100}{np}\sum_{i=1}^{n_p}\frac{\left|x_{\exp} - x_{cal}\right|}{x_{\exp}} \qquad 3\text{-}144$$

n_p is the number of experimental data, x_{exp} and x_{cal} are the experimental and calculated composition of the gaseous solvent in the saturated liquid phase. The binary interaction coefficients for non-polar systems are small and their value increases for mixtures containing

polar components (Kontogeorgis 2009). Table 3-8 illustrates that increasing the non-polar chain length in alcohols increases the binary interaction coefficient of (methane + alkanol). Table 3-8 also indicates that the binary interaction coefficient of methane + 1-propanol is greater than its interaction with heavy hydrocarbons. This is a result of the non-polar behaviour of heavy hydrocarbons. For the binary systems of methane + ethane + heavy hydrocarbons, four different temperatures were studied and the binary interaction coefficients and NRTL model parameters for different mixing rules were found to be independent of temperature. The results indicate that for hydrocarbons heavier than *n*-tetradecane, the change in the binary interaction coefficient of methane + *n*-alkane with the carbon number is too small. Kordas et al. (1995) developed a correlation for the binary interaction parameters of methane + alkanes systems as a function of their carbon number. As Table 3-8 illustrates, the binary interaction coefficients of methane + *n*-tetradecane and methane + *n*-octadecane systems are similar which is in agreement with the results reported by Kordas et al. (1995).

Carbon dioxide is a quadrupolar molecule; it has no dipole but contains a dipole moment causing its properties to differ from those of nonpolar molecules (Prausnitz 1999). Table 3-8 indicates that the binary interaction for carbon dioxide + alkanol systems is larger than that of methane + alkanol systems with the same alkanol. Since carbon dioxide is not a polar component, increasing the length of the non-polar chain of alkanol results in an increase in the binary interaction coefficient. Increasing the molecular weight in heavy alkanes decreases the binary interaction coefficient. This can be explained by the properties of the quadrupolar moment of carbon dioxide. Kordas et al. (1994) generated a correlation for the binary interaction parameter of carbon dioxide + alkane systems which has a U-type temperature dependency. Kordas et al. (1994) indicated that the binary interaction coefficients decrease when the number of carbons is increased. The best fit parameters presented in Table 3-8 for (carbon dioxide + *n*-decane, *n*-tetradecane, and *n*-octadecane) confirmed this trend.

Table 3-8: Binary interaction and NRTL model parameters

System	One-Parameter Mixing Rule		Two-Parameter Mixing Rule			Wong-Sandler Mixing Rule			
	k_{12}	AARD(x)	k_{12}	I_{12}	AARD(x)	k_{12}	τ_{12}	τ_{21}	AARD(x)
Methane+									
Methanol	-0.049	1.99	-0.079	-0.014	1.70	0.688	714.39	1131.8	1.73
Ethanol	-0.009	2.82	-0.103	-0.044	0.40	0.274	1390.5	1853.1	0.45
1-Propanol	0.031	1.31	0.011	-0.008	1.09	0.870	1610.9	-359.31	0.99
n-Tetradecane	0.017	4.82	0.084	0.022	3.98	0.513	3522.4	-1183.3	3.09
n-Octadecane	0.017	3.85	0.103	0.023	2.60	0.636	2559.5	-1011.7	2.29
Ethane+									
n-Tetradecane	0.004	1.69	0.003	0.0003	1.65	0.712	-40.378	420.28	1.80
n-Octadecane	0.003	3.39	0.016	0.010	2.34	0.817	-303.14	665.86	2.07
Carbon dioxide+									
Methanol	0.048	3.54	0.056	0.009	3.16	0.357	43847	1433.8	1.15
Ethanol	0.084	3.55	0.078	-0.006	3.10	0.450	46757	1985.4	2.27
1-Propanol	0.123	5.00	0.086	-0.029	2.13	0.577	1413.2	1327.7	1.93
n-Decane	0.123	2.11	0.109	-0.009	1.45	0.875	2002.8	208.26	5.38
n-Tetradecane	0.110	2.42	0.112	0.002	2.39	0.999	2007.5	-52.662	6.20
n-Octadecane	0.089	2.87	0.138	0.018	2.01	0.894	14445	-2125.8	1.71

The saturated liquid densities were also predicted using the PR EoS. The volume translation technique was considered to improve volumetric predictions. Three different cases were studied; the first case presents the results of the PR EoS without any volume shift. In the second case, the volume translation technique was only applied to the heavy component and in the third case, the volume shift was considered for two components. The volume shift values for the different cases for all three mixing rules as well as the AARD of the saturated liquid densities are summarized in Table 3-9. The absolute average deviation for the saturated liquid density was calculated using the equation below:

$$AARD(\rho) = \frac{100}{np}\sum_{i=1}^{n_p}\frac{\left|\rho_{\exp} - \rho_{cal}\right|}{\rho_{\exp}} \qquad 3\text{-}145$$

n_p is the number of experimental data, ρ_{exp} is the experimental value of the saturated liquid density and ρ_{cal} is the value predicted by the PR EoS. As Table 3-9 indicates, applying the

volume translation technique to both components leads to a lower deviation. The values of the volume translation are bounded within -1 and +1. Table 3-9 also illustrates that the values of the volume shift of the light component in the Wong-Sandler mixing rule are close to the upper and lower limits.

The parameters in Table 3-9 and the Jhaveri et al. (1988) study show that increasing the carbon number of the hydrocarbon systems increases the volume shift parameter. The experimental data and calculated values for the saturated liquid compositions and densities using the one-parameter, two-parameter and Wong-Sandler mixing rules for methane/*n*-octadecane , ethane/*n*-octadecane, and carbon dioxide/alkanes are compared in Figure 3-17 to Figure 3-22. When the system is far from the critical point, all three mixing rules have acceptable predictions while near the critical point, the two-parameter and Wong-Sandler mixing rules are more successful. At higher temperatures, the deviation of the two-parameter mixing rule from the experimental data increases and the results merge with those of the one-parameter mixing rule. Thus, under high temperature conditions, the Wong-Sandler mixing rule predicts the compositions better than the others mixing rules.

Table 3-9: Volume shift parameters, V_S, of different binary systems; [1], gaseous solvent; [2], liquid solute.

System	One-Parameter Mixing Rule			Two-Parameter Mixing Rule			Wong-Sandler Mixing Rule		
	V_S [1]	V_S [2]	AARD(ρ_s)	V_S [1]	V_S [2]	AARD(ρ)	V_S [1]	V_S [2]	AARD(ρ)
Methane+									
Methanol	0	0	13.3	0	0	13.3	0	0	13.3
	0	0.159	0.36	0	0.159	0.29	0	0.159	0.35
	-0.281	0.167	0.03	-0.225	0.166	0.02	-0.947	0.167	0.02
Ethanol	0	0	1.5	0	0	1.8	0	0	3.5
	0	0.018	0.43	0	0.022	0.21	0	0.041	0.53
	-0.376	0.029	0.08	-0.173	0.027	0.06	0.258	0.029	0.06
1-Propanol	0	0	0.84	0	0	0.85	0	0	2.1
	0	0.010	0.42	0	0.011	0.35	0	-0.022	1.6
	-0.389	0.021	0.05	-0.349	0.019	0.05	-0.999	0.010	0.41
n-Tetradecane	0	0	10.5	0	0	9.9	0	0	18.7
	0	0.125	1.3	0	0.117	1.2	0	0.236	4.8
	0.520	0.109	1.0	0.264	0.109	1.1	0.999	0.211	3.8
n-Octadecane	0	0	19.9	0	0	19.3	0	0	25.6
	0	0.230	0.9	0	0.222	0.85	0	0.313	4.2
	0.619	0.217	0.71	0.255	0.216	0.79	0.999	0.295	3.3
Ethane+									
n-Tetradecane	0	0	8.7	0	0	8.4	0	0	7.2
	0	0.122	1.1	0	0.117	0.86	0	0.096	1.4
	0.113	0.108	0.45	0.097	0.107	0.49	-0.191	0.123	1.1
n-Octadecane	0	0	18.5	0	0	17.4	0	0	13.7
	0	0.242	2.2	0	0.229	1.1	0	0.176	3.1
	0.317	0.213	0.45	0.161	0.215	0.36	-0.512	0.230	1.1
Carbon dioxide+									
Methanol	0	0	7.9	0	0	7.65	0	0	7.1
	0	0.121	2.5	0	0.116	2.53	0	0.103	3.2
	-0.302	0.172	0.12	-0.319	0.169	0.14	-0.527	0.171	0.08
Ethanol	0	0	1.9	0	0	1.9	0	0	3.2
	0	-0.008	1.9	0	-0.008	1.9	0	-0.023	3.1
	-0.265	0.031	0.12	-0.257	0.031	0.13	-0.523	0.034	0.09
1-Propanol	0	0	0.78	0	0	0.88	0	0	3.3
	0	0.003	0.77	0	0.009	0.62	0	-0.036	2.6
	-0.195	0.021	0.13	-0.141	0.023	0.11	-0.616	0.024	0.09
n-Decane	0	0	5.4	0	0	5.6	0	0	3.9
	0	0.069	0.51	0	0.072	0.59	0	-0.021	3.8
	0.172	0.059	0.30	0.208	0.061	0.31	-0.999	0.037	1.2
n-Tetradecane	0	0	10.6	0	0	10.5	0	0	5.5
	0	0.125	0.73	0	0.124	0.72	0	0.031	4.5
	0.253	0.117	0.49	0.238	0.116	0.51	-0.999	0.059	2.8
n-Octadecane	0	0	19.9	0	0	19.4	0	0	18.4
	0	0.230	0.46	0	0.223	0.22	0	0.209	0.60
	0.387	0.222	0.01	0.163	0.219	0.03	-0.527	0.221	0.03

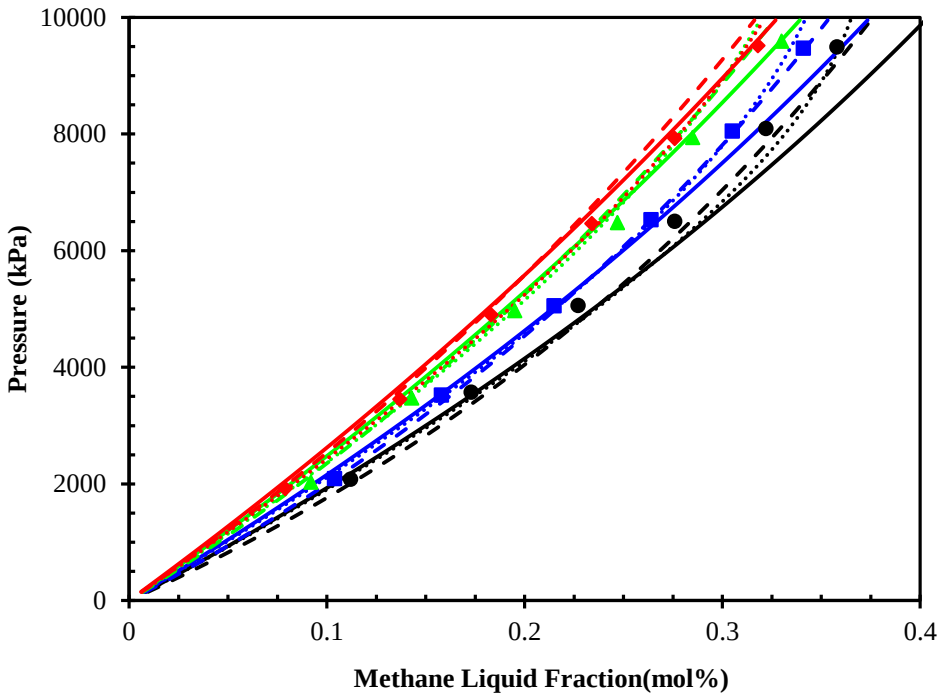

Figure 3-17: Experimental and predicted saturated liquid composition of (methane + *n*-octadecane) binary system; ●, ■, ▲, ♦, experimental data; ●, 323 K; ■, 347.9 K; ▲, 398 K; ♦, 447.6 K; lines, PR EOS; —, one-parameter mixing rule; – – , two-parameter mixing rule; … Wong-Sandler mixing rule.

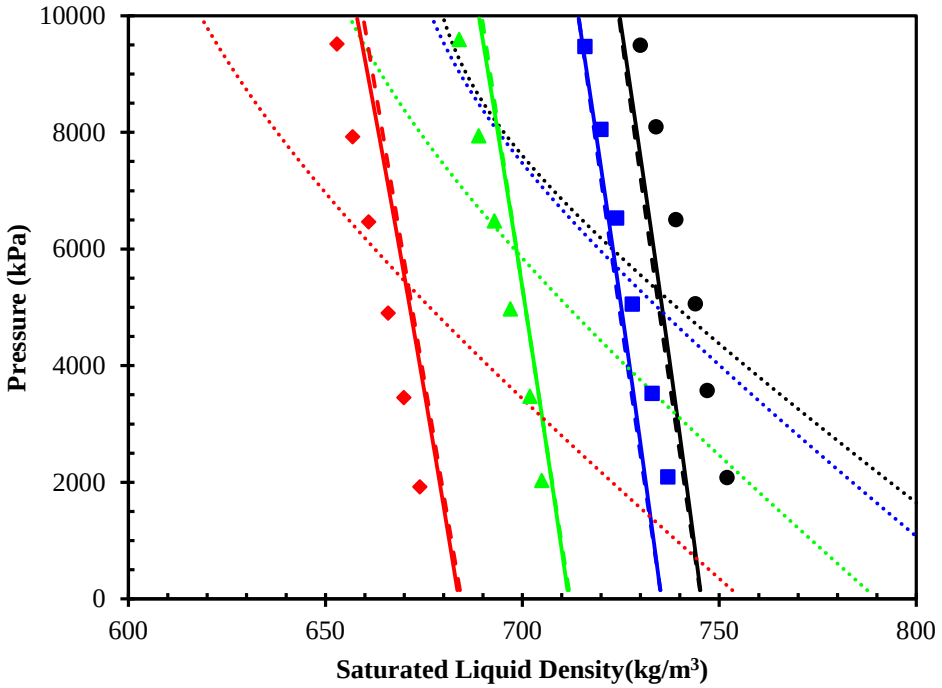

Figure 3-18: Experimental and predicted saturated liquid densities of (methane + *n*-octadecane) binary system; ●, ■, ▲, ♦, experimental data; ●, 323 K; ■, 347.9 K; ▲, 398 K; ♦, 447.6 K; lines, PR EOS; —, one-parameter mixing rule; – – , two-parameter mixing rule; …, Wong-Sandler mixing rule.

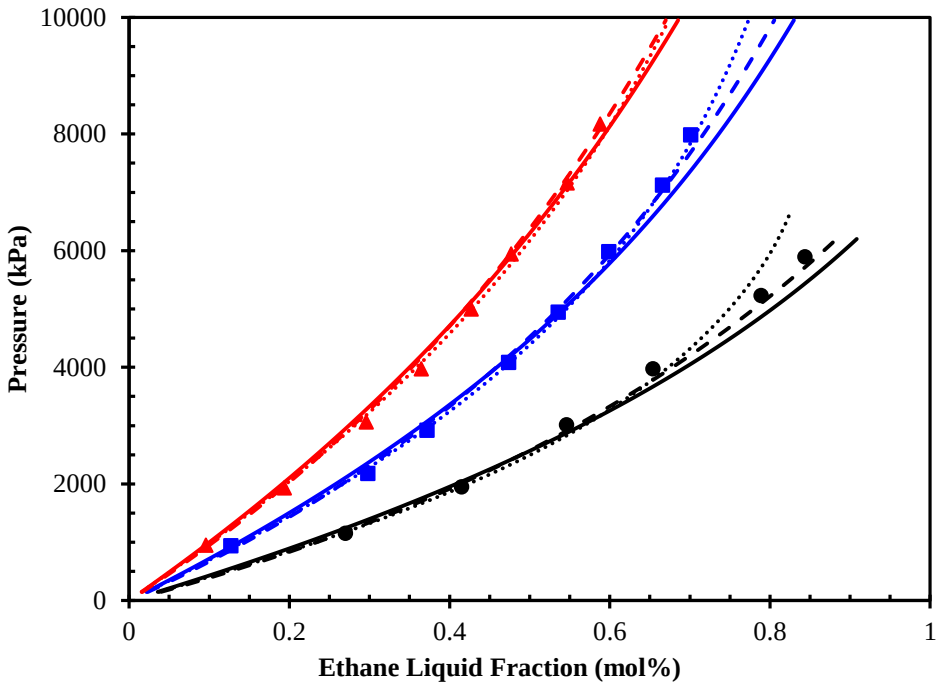

Figure 3-19: Experimental and predicted saturated liquid compositions of (ethane+ *n*-octadecane) binary systems; ●, ■, ▲, experimental data; ●, 323.2 K; ■, 372.8 K; ▲, 422.6 K; lines, PR EOS; —, one-parameter mixing rule; – –, two-parameter mixing rule; …, Wong-Sandler mixing rule.

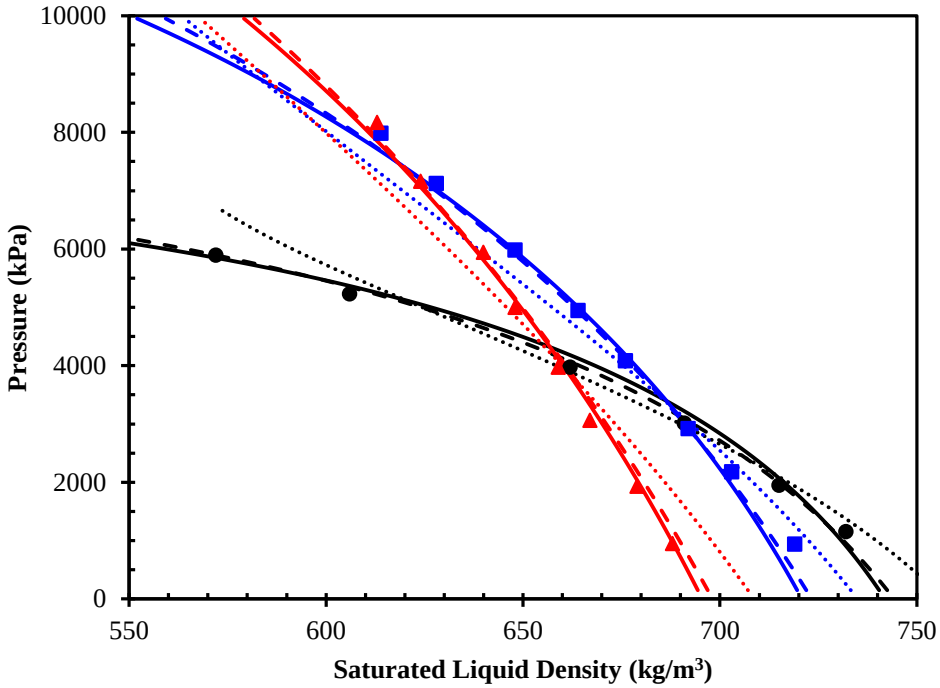

Figure 3-20: Experimental and predicted saturated liquid densities of (ethane+ *n*-octadecane) binary systems; ●, ■, ▲, experimental data; ●, 323.2 K; ■, 372.8 K; ▲, 422.6 K; lines, PR EOS; —, one-parameter mixing rule; – –, two-parameter mixing rule; …, Wong-Sandler mixing rule.

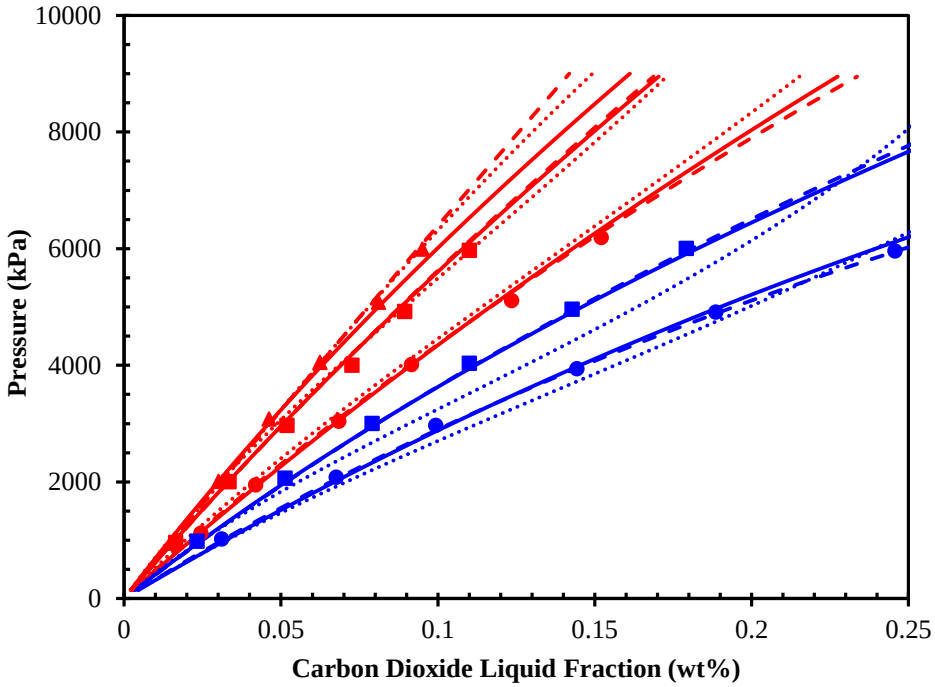

Figure 3-21: Experimental and predicted saturated liquid compositions (in weight fraction) of (carbon dioxide + alkanes) systems; symbols, experimental data; red, 373.2 K; blue, 323.2 K; ●, (carbon dioxide + *n*-decane); ■, (carbon dioxide + *n*-tetradecane); ▲, (carbon dioxide + *n*-octadecane); lines, PR EOS; —, one-parameter mixing rule; – –, two-parameter mixing rule; …, Wong-Sandler mixing rule.

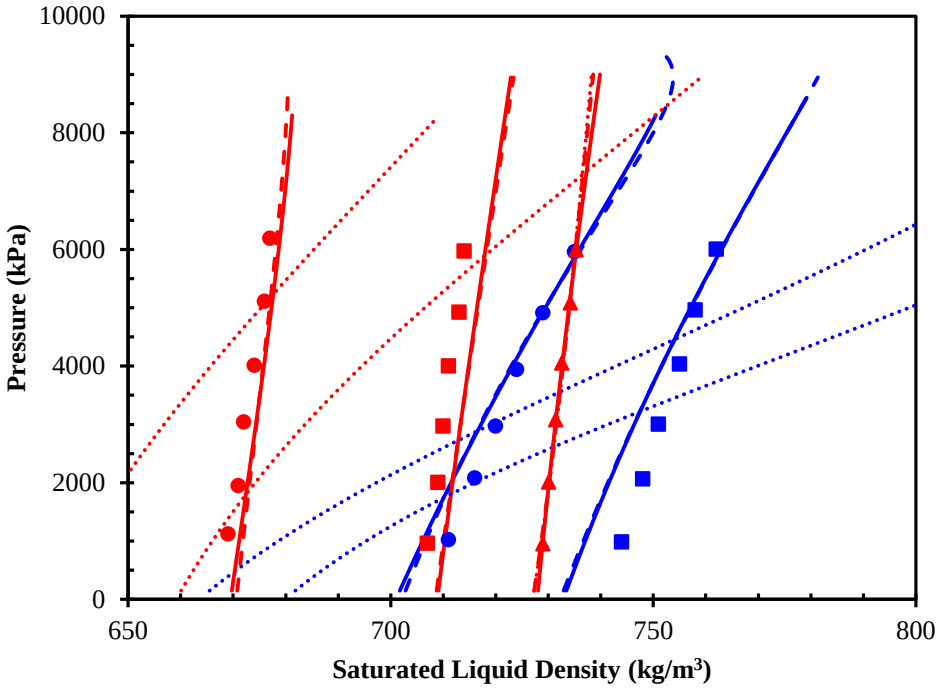

Figure 3-22: Experimental and predicted saturated liquid densities of (carbon dioxide + alkanes) binary systems; symbols, experimental data; blue, 323.2 K; red, 373.2 K; ●, (carbon dioxide + *n*-decane); ■, (carbon dioxide + *n*-tetradecane); ▲, (carbon dioxide + *n*-octadecane); lines, PR EOS; —, one-parameter mixing rule; – –, two-parameter mixing rule; …, Wong-Sandler mixing rule.

3.5.1.2.Temperature Dependent Parameters

The adjustable parameters in the Wong-Sandler mixing rule were determined as a function of temperature for binary systems with experimental data available at different temperatures. The binary interaction coefficients and NRTL model parameters are reported in Table 3-10. The experimental data at four different isotherms were reported for (methane + *n*-tetradecane) and (methane + *n*-octadecane) systems. It has been found that the best-fit parameters are different with the temperature independent parameters.

Table 3-10: Binary interaction coefficients, $k_{12,}$ and NRTL model parameters, τ_{12} and τ_{21}, at different temperatures *T*; *x*, saturated liquid composition; ρ_s, saturated liquid density.

	Methane + *n*-Tetradecane				Methane + *n*-Octadecane			
***T*/K**	294.7	324.0	373.4	447.5	323.1	347.9	398.0	447.6
k_{12}	0.919	0.745	0.911	0.771	0.999	0.999	0.999	0.892
τ_{12}	6314.9	6507.1	6958.3	8377.0	9256.4	9163.7	8589.2	6880.6
τ_{21}	-3165.6	-2972.9	-4179.6	-4366.4	-3811.1	-4154.6	-4721.4	-4132.7
AARD(*x*)	0.64	0.40	0.22	0.64	0.56	0.67	1.11	0.44
AARD(ρ_s)	9.5	13.8	8.0	10.6	17.8	17.4	16.4	18.5
	Ethane + *n*-Tetradecane			Ethane + *n*-Octadecane			CO_2 + Methanol	
***T*/K**	323.2	373.5	422.6	323.2	372.8	422.6	303.2	323.2
k_{12}	0.699	0.735	0.741	0.783	0.833	0.850	0.412	-0.005
τ_{12}	4585.5	-3438.6	-3881.2	8432.7	-3331.6	-4140.1	199500	19547
τ_{21}	-2627.4	5878.0	5786.7	-3578.6	5535.2	6484.1	1417.4	1134.8
AARD(*x*)	0.99	0.85	0.52	0.85	1.07	0.60	0.67	1.31
AARD(ρ_s)	6.8	5.7	5.8	14.6	12.9	13.6	6.6	15.6
	CO_2 + 1-Propanol		CO_2 + *n*-Decane		CO_2 + *n*-Tetradecane		CO_2 + *n*-Octadecane	
***T*/K**	303.2	323.2	303.2	323.2	323.2	373.2	323.2	373.2
k_{12}	0.482	0.087	0.520	0.621	0.784	0.676	0.904	0.884
τ_{12}	172996	18177	3427.3	-357.8	6530.9	10761	7036.0	7672.6
τ_{21}	2067.1	1228.8	330.75	2876.5	-918.07	-1664.9	-1199.4	-2190.7
AARD(*x*)	3.60	0.92	0.80	0.56	0.55	0.94	0.26	0.96
AARD(ρ_s)	7.7	7.7	1.9	4.2	2.7	6.3	5.7	7.2

For binary systems with narrow temperature ranges, the temperature independent parameters are closer to the temperature dependent ones. A comparison of the AARDs in Table 3-8 to Table

3-10 shows that using the temperature dependent parameters with the Wong-Sandler mixing rules produces more accurate predictions for saturated liquid compositions than the temperature independent parameters do. It has been expected that increasing the temperature would reduce the binary interaction coefficients because an increase in temperature decreases the importance of the interaction forces. However this trend may be different in a complex mixture such as bitumen because its prediction is so sensitive to its defined pseudo-components properties.

3.5.2. Second Scenario

In the first scenario, experimental compositions were used to tune the EoS model and the prediction of saturated liquid densities was improved, by adjusting the volume shift values. In other words, the density data were not included in the adjustment of the mixing rule parameters. In this section, the adjustment of the parameters was done based on both the experimental saturated liquid compositions and densities. The best fit parameters and AARDs are reported in Table 3-11 to Table 3-13. As the tables show, for some binary systems, the AARDs of the saturated liquid compositions increase while those of the densities decrease. The reason is the adjustment of parameters using experimental liquid compositions in the first scenario. However, in the second scenario the regression of the model was done with both the experimental densities and compositions.

Table 3-11 summarizes the best fit parameters for the one-parameter mixing rule and Table 3-12 and Table 3-13 represent the parameters for the two-parameter and Wong-Sandler mixing rules, respectively. The results show that for (methane + alkanol) systems, the two-parameter and Wong-Sandler mixing rules have the same AARDs in the prediction of saturated liquid compositions and densities, but the one-parameter mixing rule has the highest deviations. For binary hydrocarbon systems, the two-parameter and Wong-Sandler mixing rules show similar results for saturated liquid compositions, but the density predictions using the two-parameter mixing rule are more accurate. For (carbon dioxide + alkanol) binary systems, the Wong-Sandler mixing rule predicts both the saturated liquid compositions and densities with the lowest

AARDs. For the binary systems (carbon dioxide + alkane), the two-parameter mixing rule is the most accurate for the prediction of the saturated liquid compositions, while the one-parameter mixing rule predicts the densities better than the other mixing rules.

Table 3-11: Binary interaction coefficient, k_{12}, and volume shift parameters, *Vs*, for one-parameter mixing rule.

System	k_{12}	V_S **[1]**	V_S **[2]**	**AARD (*x*)**	**AARD (ρ_s)**
Methane +					
Methanol	-0.049	-0.281	0.167	1.98	0.03
Ethanol	-0.009	-0.378	0.03	2.82	0.08
1-Propanol	0.031	-0.389	0.021	1.31	0.05
n-Tetradecane	0.017	0.559	0.110	4.82	1.0
n-Octadecane	0.017	0.622	0.217	3.85	0.71
Ethane +					
n-Tetradecane	0.004	0.116	0.108	1.69	0.46
n-Octadecane	0.003	0.308	0.213	3.38	0.47
Carbon dioxide +					
Methanol	0.048	-0.300	0.172	3.54	0.12
Ethanol	0.084	-0.261	0.032	3.54	0.12
1-Propanol	0.123	-0.198	0.021	4.99	0.14
n-Decane	0.123	0.183	0.060	2.11	0.31
n-Tetradecane	0.110	0.264	0.117	2.42	0.49
n-Octadecane	0.089	0.384	0.222	2.87	0.01

Table 3-12: Binary interaction coefficients, k_{12} and I_{12}, and volume shift parameters, *Vs*, for two-parameter mixing rule

System	k_{12}	I_{12}	V_S **[1]**	V_S **[2]**	**AARD (*x*)**	**AARD (ρ_s)**
Methane +						
Methanol	-0.079	-0.014	-0.229	0.166	1.70	0.02
Ethanol	-0.103	-0.045	-0.173	0.027	0.40	0.06
1-Propanol	0.011	-0.010	-0.349	0.020	1.09	0.05
n-Tetradecane	0.083	0.022	0.265	0.109	3.98	1.1
n-Octadecane	0.103	0.023	0.252	0.216	2.61	0.79
Ethane +						
n-Tetradecane	0.003	0.001	0.097	0.107	1.66	0.49
n-Octadecane	0.016	0.010	0.160	0.215	2.34	0.36
Carbon dioxide +						
Methanol	0.056	0.010	-0.319	0.169	3.16	0.14
Ethanol	0.077	-0.006	-0.257	0.031	3.10	0.13
1-Propanol	0.086	-0.029	-0.141	0.023	2.13	0.11
n-Decane	0.109	-0.009	0.208	0.061	1.45	0.31
n-Tetradecane	0.112	0.002	0.238	0.116	2.4	0.51
n-Octadecane	0.138	0.018	0.163	0.219	2.01	0.03

Depending on the binary system of interest and the accuracy of the predictions, different mixing rules may be appropriate. The one-parameter mixing rule is not successful in the prediction of saturated liquid compositions but it gives reasonable density results for (carbon dioxide + alkane) systems. The two-parameter and Wong-Sandler mixing rules produce somewhat similar predictions.

Table 3-13: Binary interaction coefficients, $k_{12,}$ NRTL model parameters, τ_{12} and τ_{21}, and volume shift values, *Vs*, for Wong-Sandler mixing rule

System	k_{12}	τ_{12}	τ_{21}	V_S **[1]**	V_S **[2]**	**AARD (*x*)**	**AARD (ρ_s)**
Methane +							
Methanol	0.682	766.03	1108.9	-0.934	0.167	1.72	0.02
Ethanol	0.276	1384.2	1853.1	0.254	0.029	0.45	0.06
1-Propanol	0.761	2782.6	-669.589	-0.999	0.020	0.98	0.05
n-Tetradecane	0.543	3604.4	-1274.4	0.999	0.198	3.35	3.4
n-Octadecane	0.673	2537.6	-1057.21	0.999	0.279	2.43	2.9
Ethane +							
n-Tetradecane	0.710	399.11	1.5394	-0.159	0.122	1.85	1.1
n-Octadecane	0.817	203.14	145.25	-0.498	0.230	2.08	1.1
Carbon dioxide +							
Methanol	0.358	44098	1435.8	-0.531	0.171	1.15	0.07
Ethanol	0.449	46709	1985.1	-0.524	0.034	2.27	0.10
1-Propanol	0.577	1406.4	1331.7	-0.617	0.024	1.93	0.06
n-Decane	0.850	2835.0	-144.84	-0.999	0.058	5.39	0.71
n-Tetradecane	0.998	1497.3	341.43	-0.951	0.071	6.15	3.05
n-Octadecane	0.894	14444	-2125.9	-0.527	0.221	1.71	0.03

Chapter 4: Results and Discussion

In this chapter, the phase behaviour of solvent/bitumen systems has been studied and modeled by proposed code in C++. In bitumen characterization section, based on experimental data obtained from simulated distillation, the bitumen has been characterized into pseudo-components. The effect of different parameters in molar distribution function on obtained results has been investigated. The critical properties and acentric factors of pseudo-components have been calculated by different correlations and different correlations' efficiency for these systems has been studied. The combining rules for critical properties and acentric factor and lumping scheme have been studied as well. After comparing different correlations and schemes by means of best-selected method, the system of non-condensable gases (methane, ethane and carbon dioxide) with Athabasca bitumen has been modeled. The accuracy of cubic EoS regarding to its modification of α and binary interaction coefficient and volume shifts has been compared. The systems of methane, ethane, carbon dioxide and nitrogen with Cold Lake bitumen have been studied as well. Finally, bitumen has been considered as one pseudo-component and the efficiency of Wong-Sandler mixing rule is compared with van der Waals mixing rules.

4.1. Characterization

This study focused on two different types of bitumens; Athabasca and Cold Lake. The TBP and SCN data for Athabasca bitumen was obtained from SHARP data, which was conducted by Nourozieh (2013) and is presented in Figure 4-1 and Figure 4-2. This data was taken using SimDis, which simulated the TBP distillation test via a flame ionization detector (FID). This test provides the TBP curve of bitumen up to 750 ^{o}C and SCN distribution up to carbon number 100. The TBP curve of Cold Lake bitumen is also available (Eastick 1984) which is reported in Table 4-1. The SCN data of Athabasca bitumen will be used in order to find the appropriate correlation for generating the SCN distribution of Cold Lake bitumen.

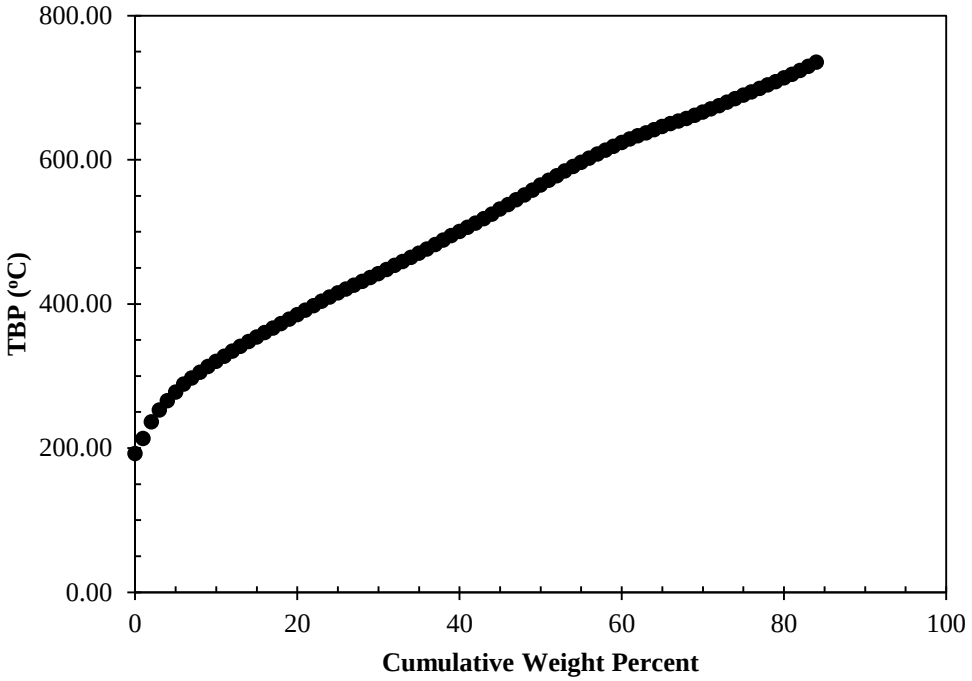

Figure 4-1: TBP curve of Athabasca bitumen (Nourozieh 2013)

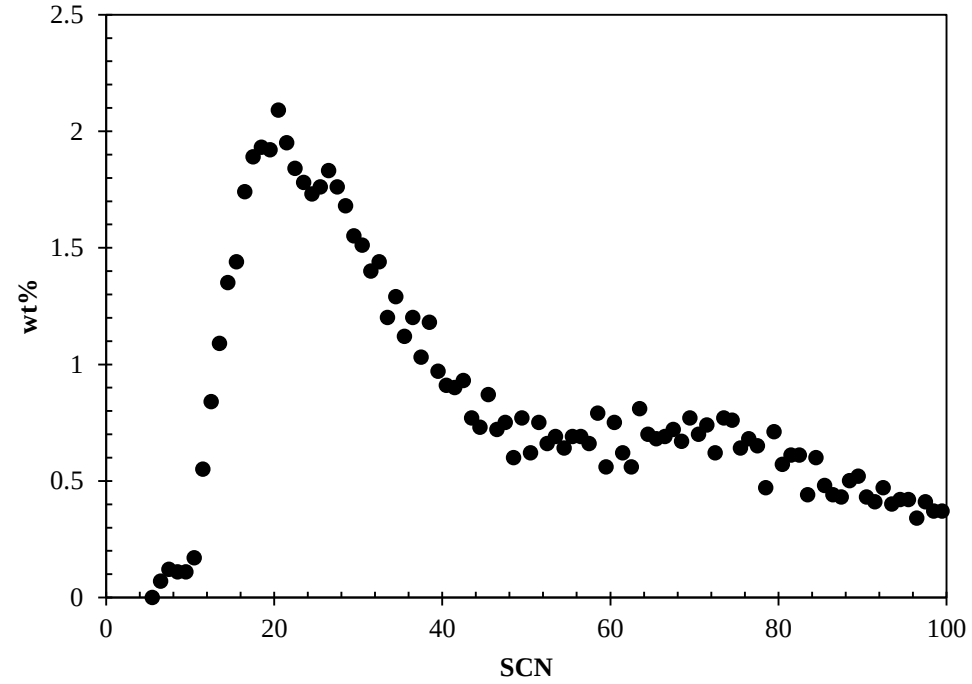

Figure 4-2: SCN data of Athabasca bitumen (Nourozieh 2013)

Table 4-1: SIMDIST distillation data of Cold Lake bitumen (Eastick 1984)

Mass percent Distilled	TBP (^{o}C)	Mass percent Distilled	TBP (^{o}C)
0	236	29	415
1	252	30	420
2	263	31	425
3	272	32	429
4	279	33	434
5	285	34	439
6	292	35	444
7	299	36	448
8	305	37	453
9	312	38	458
10	317	39	463
11	323	40	468
12	328	41	473
13	333	42	478
14	339	43	483
15	344	44	488
16	349	45	493
17	354	46	498
18	359	47	503
19	364	48	509
20	369	49	514
21	374	50	519
22	379	51	525
23	384	52	531
24	389	53	536
25	394	54	543
26	399	55	548
27	405	56	553
28	410	57	559

4.1.1. SCN Data Prediction

SCN data of Athabasca bitumen was transferred to a TBP curve using different correlations. Four different correlations developed by Twu (1984), Ahmed (1985), Riazi and Al-Sahhaf (1996) and Sancet (2007) were compared. The normal boiling point predictions of the different correlations as a function of SCN are shown in Figure 4-3. The results show that all of the correlations can predict the normal boiling point up to carbon number 70 with the same accuracy. The Ahmed (1985) correlation is not successful in predicting the normal boiling point for carbon

numbers greater than 70. As the figure depicts, the Riazi and Al-Sahhaf (1996) correlation is not appropriate for high carbon numbers. This issue can attributed to the exponential form of the Riazi and Al-Sahhaf correlation which results in a constant value of normal boiling point for high carbon numbers (Figure 4-3). This figure also indicates that the Sancet (2007) correlation predicts the normal boiling point of each carbon number higher than the Twu (1984) correlation does which is in good agreement with Rodriguez and Hamouda (2010) results.

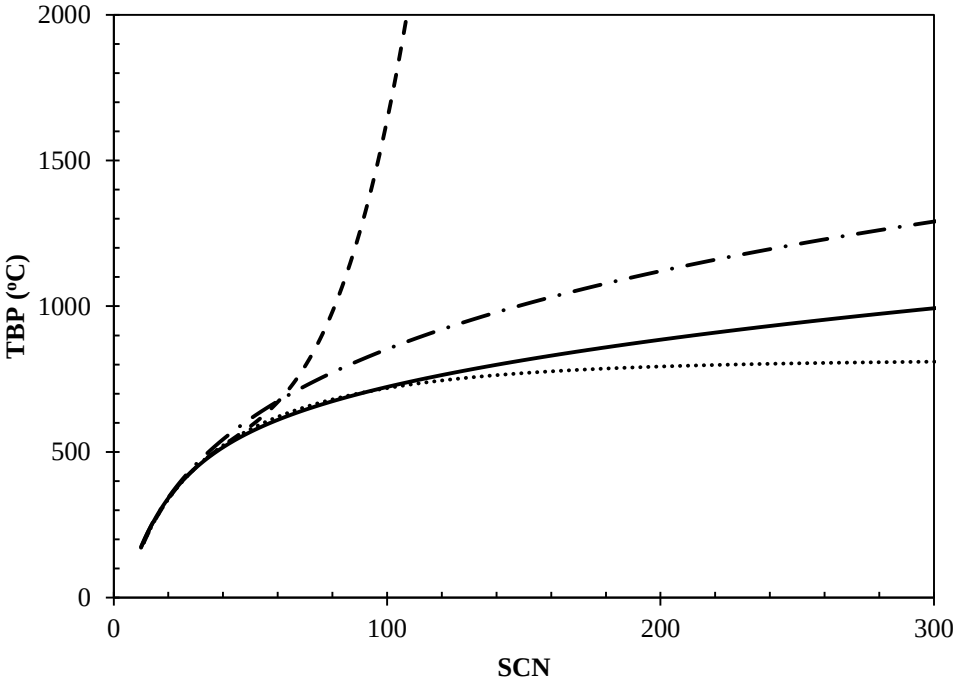

Figure 4-3: TBP prediction versus carbon number for different correlation. Different correlations are shown by — Twu (1984), - - - Ahmed (1985), … Riazi and Al-Sahhaf (1996) , and ·−·− Sancet correlations(2007).

The experimental data and predicted normal boiling point for Athabasca bitumen is shown in Figure 4-4. As this figure shows, the Ahmed (1985) correlation cannot predict the normal boiling point curve with sufficient accuracy. Due to its exponential form, the Riazi and Al-Sahhaf (1996) correlation extends the TBP curve linearly and leads to a constant value of 1090 K for high carbon numbers. In spite of superior prediction in low carbon numbers, the Riazi and Al-Sahhaf (1996) correlation is not suitable for high carbon number regions. Accuracy of these correlations in normal boiling point prediction is summarized in Table 4-2. In this table AARDs of TBP are calculated based on difference of experimental and calculated values up to 80% weight percent.

$$AARD(TBP) = \frac{100}{np}\sum_{i=1}^{n_p}\frac{\left|TBP_{\exp} - TBP_{cal}\right|}{TBP_{\exp}} \qquad 4\text{-}1$$

Table 4-2: Average absolute relative deviation of TBP data for different correlations.

Correlation	AARD(TBP)
Twu (1984)	1.54
Ahmed (1985)	4.14
Riazi and Al-Sahhaf (1996)	0.47
Sancet (2007)	1.40

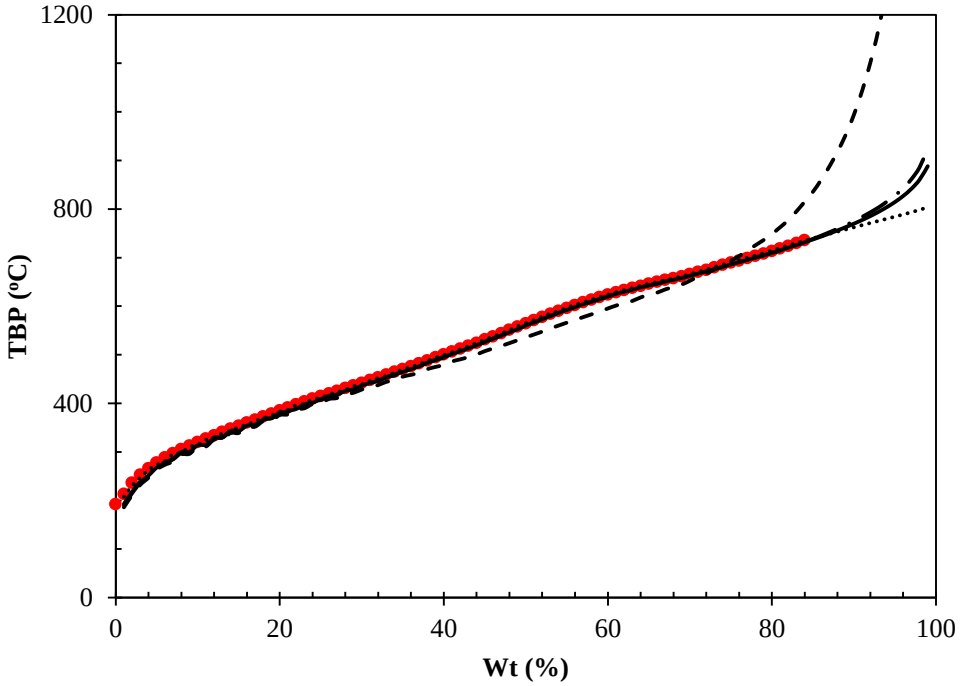

Figure 4-4: TBP curve extension of Athabasca bitumen by different correlation. Different correlation are shown by — Twu (1984), - - - Ahmed (1985), … Riazi and Al-Sahhaf (1996), and ·—·— Sancet (2007) and dots are experimental data (Nourozieh 2013).

4.1.2. Gamma Distribution Function

In the next step, the experimental or calculated SCN data is modeled by means of the gamma distribution function. The shape factor is calculated by matching the molecular weight with the highest mole fraction. It should be mentioned that the molecular weight of the SCN with the highest weight fraction is considered as a first guess. However, the SCN with the highest weight fraction may not be the SCN with highest mole fraction (Figure 4-5). For this reason, the

molecular weight of the SCN with the highest mole fraction is compared with the initial guess and is modified until they are equal following each run.

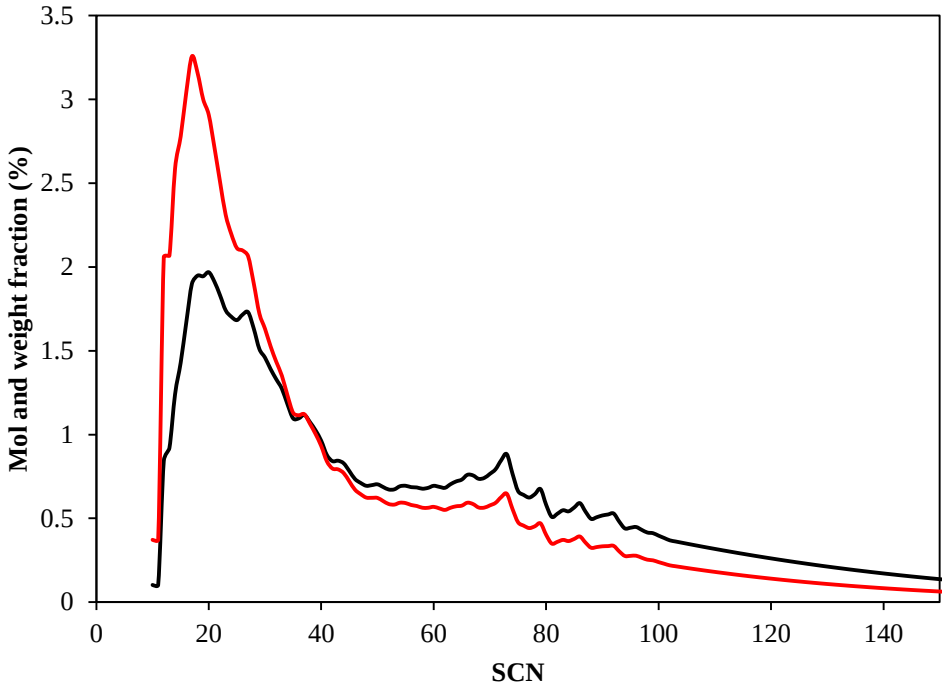

Figure 4-5: Weight and mole distribution of Athabasca bitumen. The red and black lines show mole and weight fraction respectively (The experimental data are plotted up to C_{100}).

With this method, values of 1.87 and 1.98 were obtained for the shape factor of Athabasca and Cold Lake bitumen respectively. The limiting molecular weight was used to model the SCN data. As outlined in the previous chapter, the limiting molecular weight of each SCN was calculated by a step of dM. While decreasing dM can increase the execution time, it can also affect the accuracy of matching data. The different values of dM and corresponding number of iteration and AARDs are reported in Table 4-3. In this study, the dM is considered as a variable instead of a constant value which can be large in regions far from transition zone between two different SCNs and can be small near changing area. With this method in addition to keep the high accuracy of small dM, the number of iterations and execution time decreases.

By using limiting molecular weight, the distribution is forced to match the experimental data which are shown in Figure 4-6. As the figure indicates the results are in good agreement with the experimental results.

Table 4-3: Effect of different step size of limiting molecular weight on number of iterations and AARD for Athabasca bitumen

dM	Iteration	AARD(wt%)
0.1	12175	0.478
0.01	121015	0.049
0.001	1209399	0.005

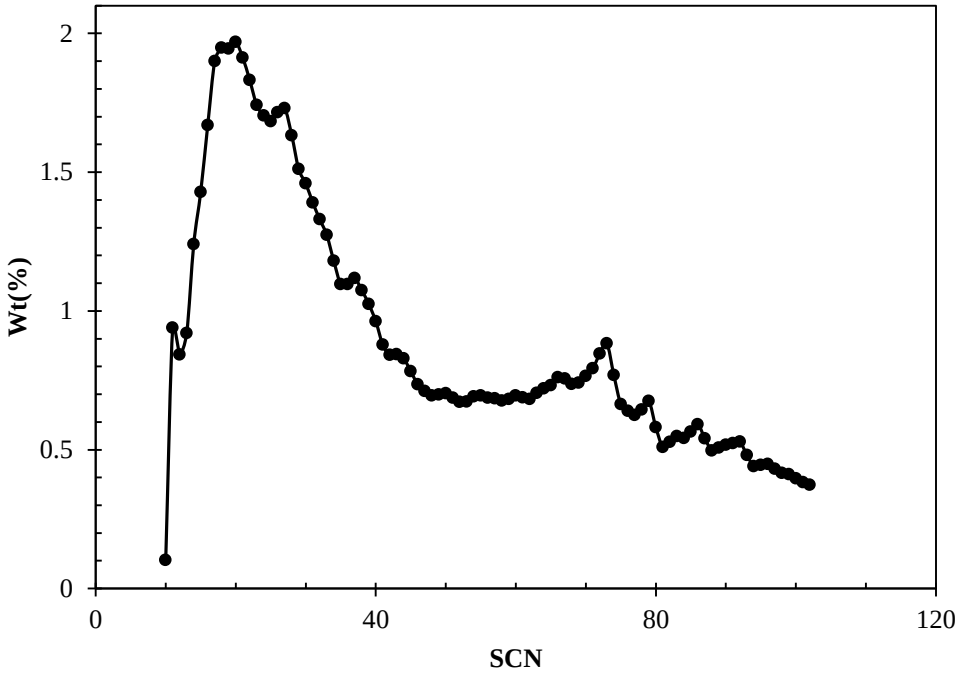

Figure 4-6: Predicted and experimental values of SCN distribution. The line is modeling and the dots show experimental data (Nourozieh 2013)

4.1.3. Prediction of Petrochemical Properties

After extrapolating L_{Mw} and obtaining the molecular weight and normal boiling point for each SCN, the specific gravity, critical properties, and acentric factors must be determined. The specific gravity of bitumen must be calculated and modified considering the specific gravity of whole bitumen. The physical properties of Athabasca and Cold Lake bitumens are summarized in Table 4-4.

Table 4-4: Molecular weight, density and asphaltene mass percent of Athabasca and Cold Lake bitumen.

Sample	Molar Mass (g/mol)	Density (g/cm^3)
Athabasca Bitumen	539	1.010
Cold Lake Bitumen	577	0.995

The specific gravity and molecular weight of bitumen are used to calculate the critical properties and acentric factors. A sensitivity test has been done to investigate the accuracy of the solubility prediction with respect to the critical pressure, temperature, and acentric factor. The acentric factor did not have a significant effect on the solubility prediction, and the deviation of critical pressure and temperature from the appropriate value can affect accuracy (Figure 4-7). By increasing critical temperature, the critical pressure would decrease however in this sensitivity test the bitumen considered as one pseudo-component and critical property changed while the other remains constant. The same trend has been reported by Fu et al. (1987) for carbon dioxide and methane with Athabasca and Cold Lake bitumen. They follow the same procedure for sensitivity test and found out the VLE and volumetric prediction is more sensitive to critical temperature. After critical temperature, critical pressure and acentric factor have the highest effect which is in good agreement with our study.

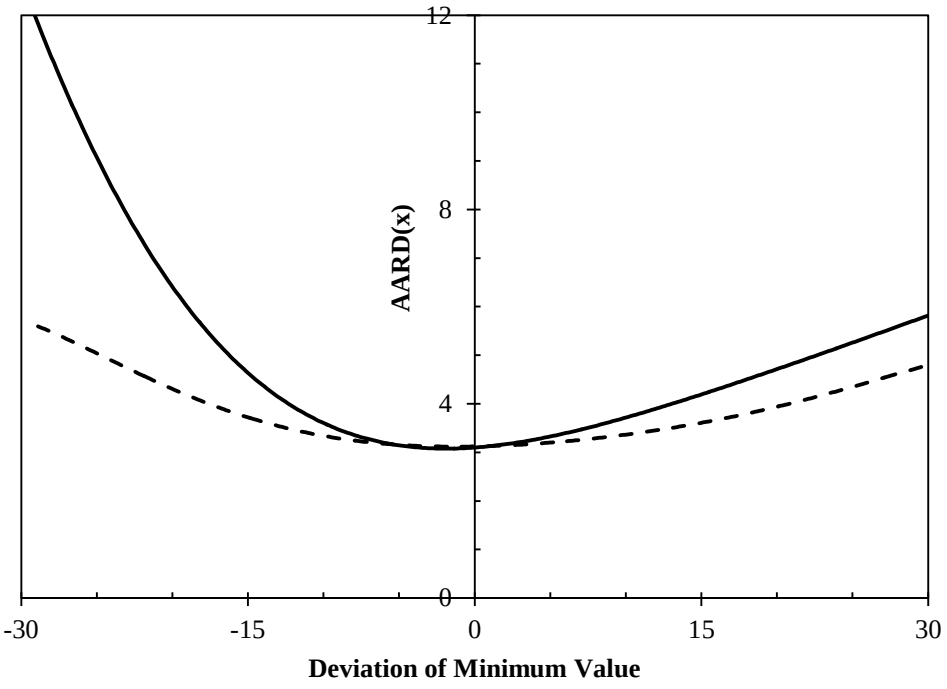

Figure 4-7: Effect of deviation of critical properties on solubility prediction of methane for Cold Lake bitumen. — and − − show T_c and P_c respectively.

Four different correlations for critical pressure and temperature including Lee-Kesler (1976), Twu (1984), Ahmed (1985) and Sancet (2007) correlations were investigated. As Figure 4-8 and

Figure 4-9 indicate, the Ahmed (1985) correlation does not accurately predict the critical pressure and temperature. Duan et al. (2013) indicates that the Ahmed (1985) critical pressure and temperature correlations are valid in the carbon number range of 7-40 and 7-60 respectively while our results confirm their statement. The correlation by Sancet (2007) for the calculation of critical pressure does not perform well for high carbon numbers, which may be due to its exponential form, which leads to a constant value of 571 kPa for high carbon numbers.

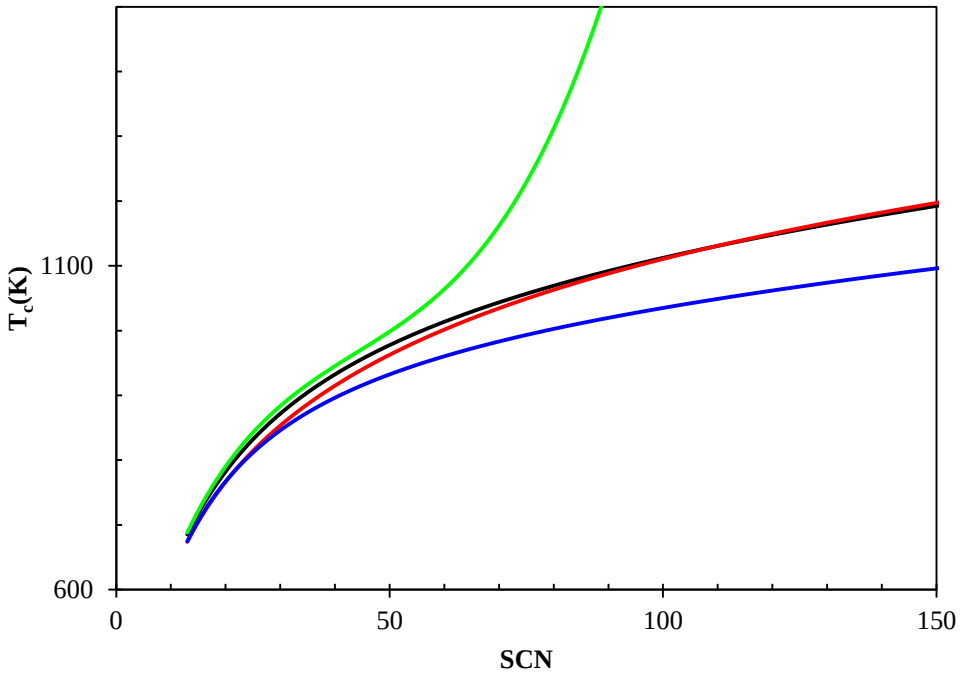

Figure 4-8: Critical temperature versus carbon number. Black, blue, green and red lines are Lee-Kesler (1976), Twu (1984), Ahmed (1985) and Sancet (2007)correlations respectively

Figure 4-10 compares the correlation by Edmister (1958) for the calculation of acentric factor in conjunction with other critical pressure and temperature correlations. As the figure shows, in carbon numbers less than 20, all of the correlations are sufficiently accurate but in the higher carbon numbers they show different predictions. Therefore, the Lee-Kesler (1976) correlation is the best correlation for modeling of solvent/bitumen systems. This finding agrees with previous studies (Svrcek and Mehrotra (1982 and 1989), Kariznovi et al. (2010) and Diaz et al. (2011)).

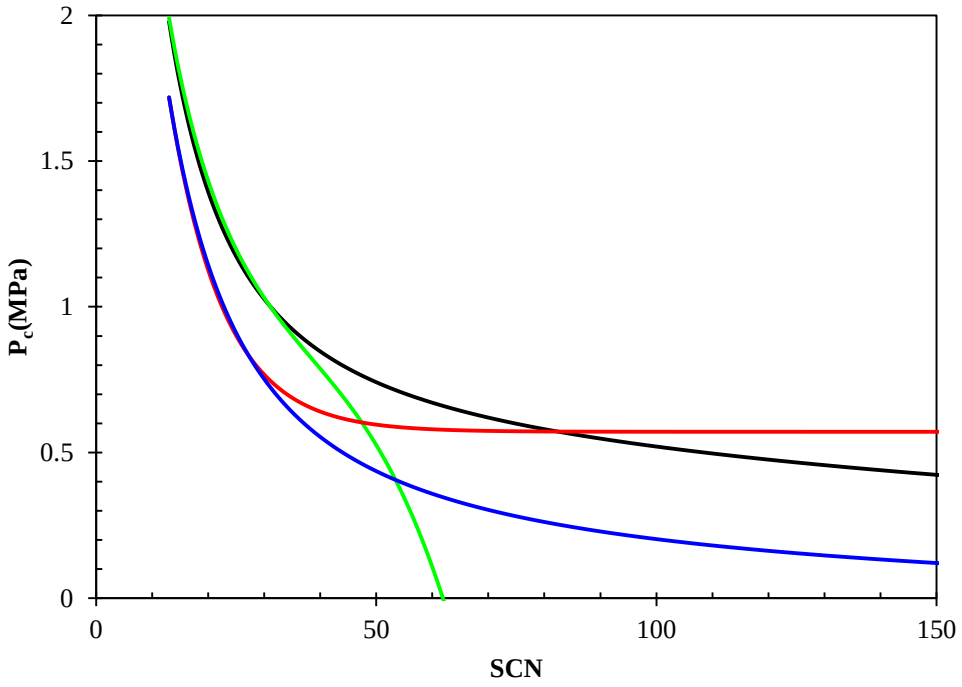

Figure 4-9: Critical pressure versus carbon number. Black, blue, green and red lines are Lee-Kesler (1976), Twu (1984), Ahmed (1985) and Sancet (2007) correlations respectively

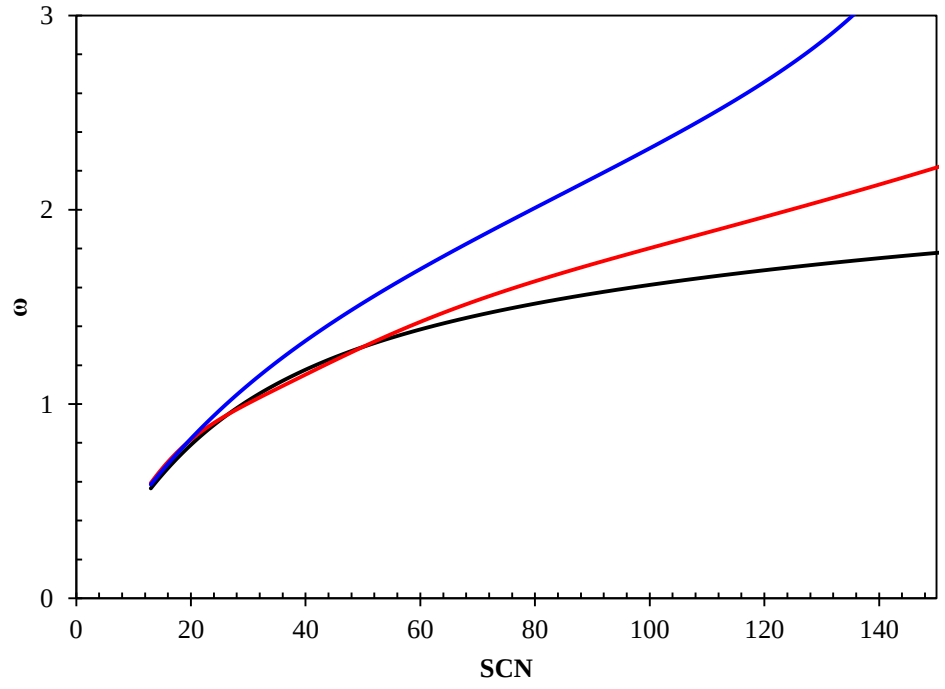

Figure 4-10: Acentric factor versus carbon number. Black, blue and red lines are Edmister (1958) input data correlations which are Lee-Kesler (1976), Twu (1984) and Sancet (2007) correlations respectively

4.1.4. Lumping Scheme

Finally, Lee's (1981) and Whitson's (1983) characterization schemes were used to lump the pseudo-components. In Lee's method, the criterion for fraction closeness is the deviation of their properties with regards to the normal boiling point. A different number of pseudo-components are obtained when different values for closeness are considered. While decreasing the number of pseudo-components can reduce accuracy, it can also reduce the execution time and complexity of the regression process. The one-parameter mixing rule was chosen in conjunction with Gao's (1992) model binary interaction coefficient and temperature dependent volume shifts to compare the effect of reducing the number of pseudo-components. The system of methane/Cold Lake bitumen was investigated using Kays's (1982) combining rule for the critical properties and acentric factor of pseudo-component. Table 4-5 lists the AARD of the methane solubility in Cold Lake bitumen and its saturated density. The table indicates, decreasing the number of pseudo-components, decrease the accuracy of the prediction.

Table 4-5: Effect of reducing number of pseudo-components on VLE and saturated density prediction of methane + Cold Lake bitumen

Number of PCs	θ	AARD(x)	AARD(ρ)
100	0.137	4.08	0.329
87	0.137	4.08	0.329
46	0.130	4.16	0.330
17	0.102	4.44	0.333
7	0.023	5.22	0.348
3	-0.022	5.69	0.370
2	-0.029	5.78	0.372
1	-0.037	5.88	0.375

Figure 4-11 shows the experimental and predicted values for methane solubility in Cold Lake bitumen at four different isotherms (300K, 319K, 350K, and 376K). As Figure 4-11 indicates, decreasing the number of pseudo-components decreases accuracy of the prediction. This issue is more pronounced near the critical region. The experimental and predicted liquid densities are plotted in Figure 4-12. As the figure indicates lumping pseudo-components does not have a significant effect on the prediction of saturated pressure.

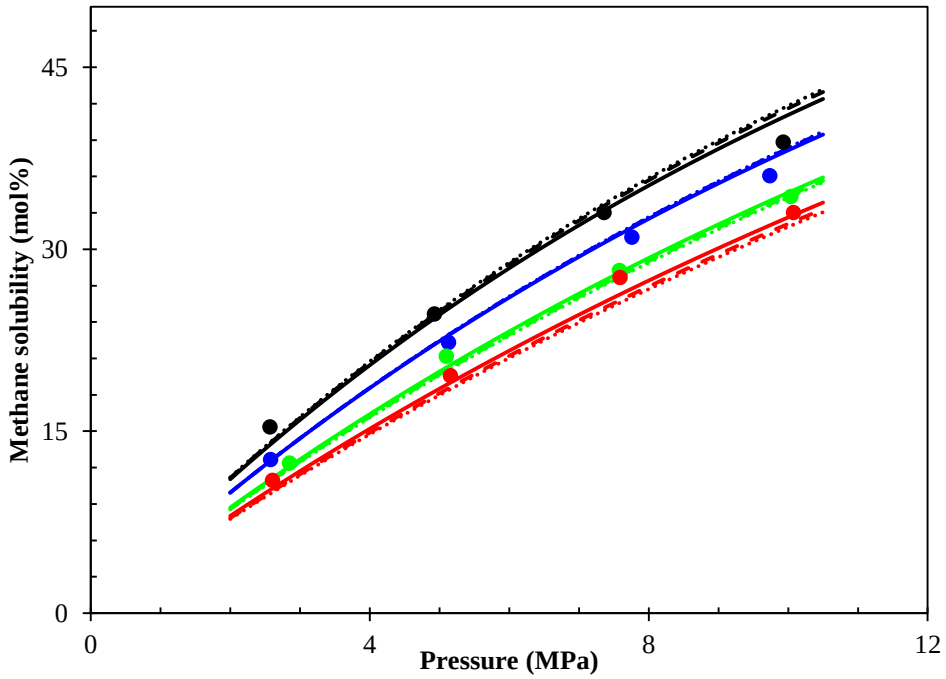

Figure 4-11: Mole fraction of methane in Cold Lake bitumen. Data has been taken from Mehrotra and Svrcek (1988a). Black, blue, green and red lines are 300K, 319K, 350K and 376K respectively. —, ·—·— and … are 1, 7 and 96 PCs respectively.

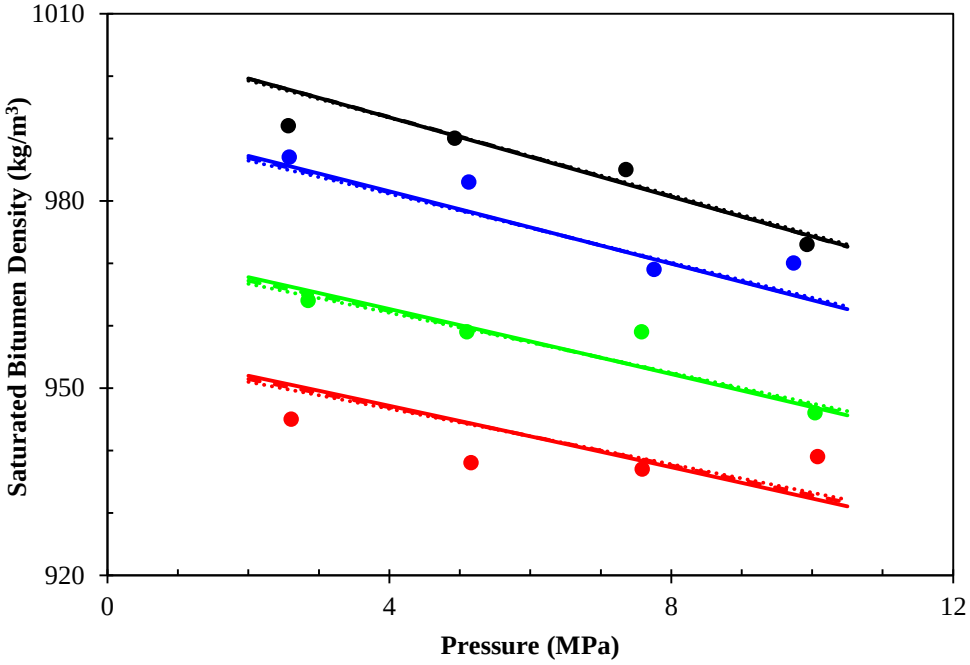

Figure 4-12: Saturated density of methane + Cold Lake bitumen. Data has been taken from Mehrotra and Svrcek (1988a). Black, blue, green and red lines are 300K, 319K, 350K and 376K respectively. —, ·—·— and … are 1, 7 and 96 PCs respectively.

In Whitson's scheme (1983), the number of pseudo-components was found as a function of the first and last SCN generated by the characterization. However, in the continuous distribution schemes, the cumulative mole fraction never reaches to 100%. Therefore, by this method 8 pseudo-components are obtained before 99% distillation achieved plus one, the last fraction, results to 9 pseudo-components. This characterization is compared with Lee's lumping method (1981) using 9 pseudo-components. As Table 4-6 indicates Whitson's method (1983) is more efficient for solubility and density prediction.

Table 4-6: Comparing efficiency of different lumping schemes for prediction of methane solubility in Cold Lake bitumen and saturated density

Lumping's method	**Number of PCs**	**AARD(*x*)**	**AARD(*ρ*)**
Lee et al. (1981)	9	5.065	0.345
Whitson (1983)	9	4.184	0.324

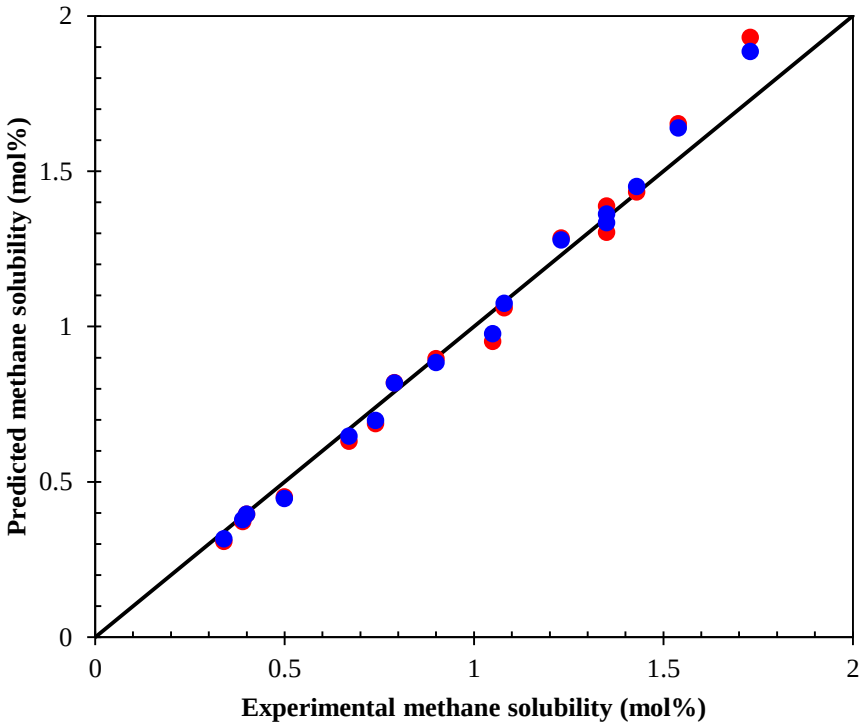

Figure 4-13: Comparison of Lee's (1981) and Whitson (1983) lumping method. Data has been taken from Mehrotra and Svrcek (1988a). The blue and red dots are Whitson (1983) and Lee (1981) lumping method respectively.

The critical properties and acentric factors were calculated for each pseudo-component using the Hong's (1982) and Kay's (1936) mixing rules. As Table 4-7 indicates, mass average method

of Hong (1982) is more accurate than a molar average over the critical properties and acentric factors.

Table 4-7: Effect of different properties mixing rule on VLE and saturated density prediction of methane + Cold Lake bitumen

Number of Pseudo-components	Hong's (1982) Mixing Rule		Kay's (1936) Mixing Rule	
	AARD(*x*)	AARD(*ρ*)	AARD(*x*)	AARD(*ρ*)
1 PC	5.49	0.321	5.88	0.375
9 PCs	4.17	0.323	4.18	0.324

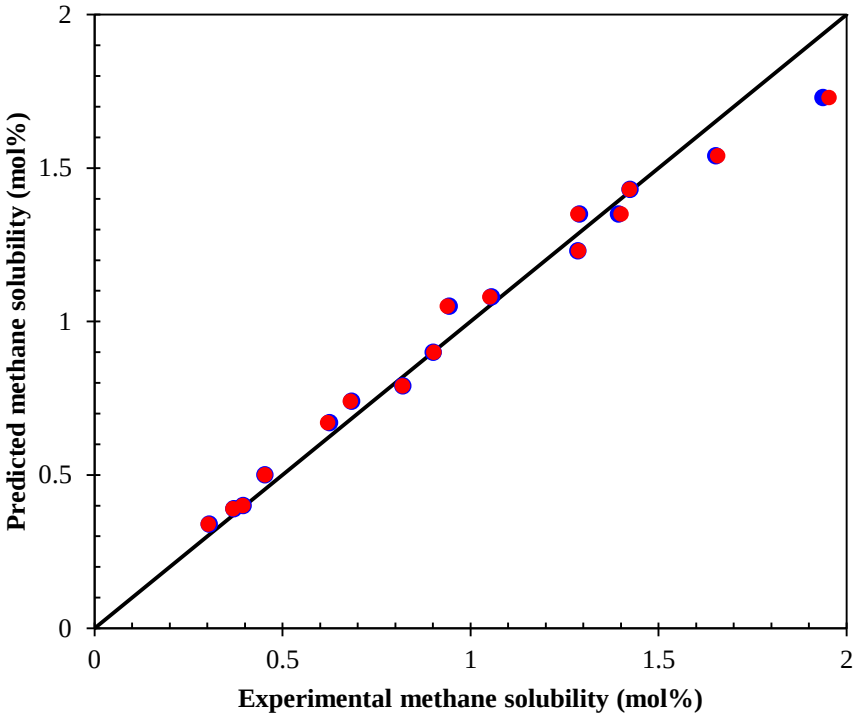

Figure 4-14: The experimental and predicted methane solubility in Cold Lake bitumen. Data has been taken from Mehrotra and Svrcek (1988a). Line is experimental data and red and blue dots are Hong (1982) and Kay (1936) mixing rules.

In conclusion, the Twu (1984) and Sancet (2007) correlations for extrapolating normal boiling point were the most appropriate models. The Lee-Kesler (1976) correlation was the best correlation for the calculation of critical pressure and temperature. The Whitson's (1983) lumping method was determined to be more efficient than Lee's method (1981) and Hong (1982) mass averaging method performs better than Kay's (1936) for the calculation of the critical properties and acentric factors of pseudo-components. The characterization scheme for

Athabasca and Cold Lake bitumens was found with the best correlation mentioned in this chapter. This characterization method is used for all of the VLE calculations in this chapter.

Table 4-8: Mole fraction and critical properties of Cold Lake bitumen

PC	Mole fraction (%)	Molecular weight	T_c (K)	P_c(kPa)	ω	T_b
1	2.49	232.1	700.4	1872.1	0.599	522.8
2	11.63	298.2	726.1	1707.3	0.656	552.5
3	16.50	385.3	770.9	1454.3	0.762	613.0
4	24.60	493.4	842.2	1138.0	0.942	701.0
5	23.41	642.1	946.5	818.1	1.213	823.6
6	14.48	838.1	1053.1	606.6	1.478	947.6
7	5.31	1087.9	1136.7	489.9	1.664	1072.3
8	1.23	1401.9	1209.7	404.6	1.809	1126.6
9	0.313	1842.9	1281.0	329.0	1.934	1191.1

Table 4-9: Mole fraction and critical properties of Athabasca bitumen

PC	Mole fraction(%)	Molecular weight	T_c(K)	P_c(kPa)	ω	T_b
1	15.95	270.3	721.5	2430.5	0.523	520.3
2	31.61	409.3	839.9	1701.3	0.752	646.9
3	26.72	564.8	983.6	1150.7	1.044	806.0
4	22.52	789.7	1130.2	822.9	1.302	967.0
5	2.38	1130.9	1253.0	631.9	1.473	1101.4
6	0.42	1293.3	1306.9	558.1	1.533	1161.3
7	0.40	1343.1	1343.5	510.0	1.569	1203.2

4.2. Non-Condensable Gases/Athabasca Bitumen Systems

Three non-condensable gases were chosen for VLE and saturated density modeling. Three gases of methane, ethane, and carbon dioxide were studied in four isotherms (50, 100, 150 and 190 ^{o}C). The VLE data of methane and carbon dioxide with Athabasca bitumen were taken from Kariznovi (2013) and the ethane with Athabasca bitumen data was from Nourozieh (2013). Different mixing rules and combining rules were tested for these systems and different binary interactions and volume shift correlations were evaluated.

4.2.1. Methane/Athabasca Bitumen

Bitumen characterization with seven pseudo-components was used to model methane solubility and saturated bitumen density. Twenty data points for four different isotherms and over a pressure range of 1 MPa to 8 MPa were used to determine the best binary interaction coefficients and volume shifts. The application of different α correlations was investigated using this system and the results are reported in Table 4-10. As the results indicate, Li and Yang (2010) correlation improves the accuracy of the solubility prediction.

Table 4-10: Different α correlations and corresponding AARDs for methane solubility in Athabasca bitumen

α correlation	**Temperature independent**	**Temperature dependent**
	AARD(*x*)	**AARD(*x*)**
Peng-Robinson(1976)	15.78	11.81
Peng-Robinson (1978)	16.50	11.85
Twu et al. (1995)	15.36	11.87
Nji et al. (2009)	16.89	11.89
Li and Yang (2010)	16.41	11.24

4.2.1.1. Methane Solubility

Different approaches for combining rules, mixing rules and functionality of binary interaction coefficient were tested. The importance of the interactions between pseudo-components was evaluated and the different binary interaction functionality was compared. Finally, the efficiency of the van der Waals mixing rule with one and two regression parameters is investigated.

4.2.1.1.1. Pseudo-Components/Pseudo-Component Binary Interaction Coefficient

The Gao et al. (1992) correlation was used to investigate the interaction between pseudo-components with the following equation.

$$k_{ij} = 1 - \left(\frac{2\sqrt{T_{c_i} T_{c_j}}}{T_{c_i} + T_{c_j}} \right)^{\frac{Z_{c_i} + Z_{c_j}}{2}} \qquad 4\text{-}2$$

This correlation was tested coupling with the one parameter van der Waals mixing rule. For the binary interaction coefficients between pseudo-components, the AARD for methane solubility

was 15.41% and 11.79% for temperature independent and dependent respectively. These results are the same as those reported in Table 4-10. Therefore, the binary interaction coefficient between pseudo-components does not have a significant effect for bitumen systems and can be disregarded. The interaction between pseudo-components is considered in all cases.

4.2.1.1.2. Solvent/Pseudo-Components Binary Interaction Coefficient

Binary interaction coefficients can be used as regression parameters to match the saturation pressure or solubility data. A common method is to find the binary interaction coefficient for each pseudo-component at each isotherm or for the whole range. For heavy oil and bitumen, which consist of many pseudo-components this method is not practical because the large number of regression parameters significantly increases the execution time and renders the regression scheme incapable of finding the global minimum. For this reason, different correlations have been proposed which define the interaction parameters as a function of the critical properties or other parameters such as carbon numbers. These correlations contain some constants, which are found by matching the VLE data. The Chueh and Parusnitz (1967) correlation includes critical volume functionality and is used frequently. This correlation has been compared with the Gao et al. (1992) model, which has a critical temperature functionality. It has been determined that the Gao et al. (1992) model with an AARD of 15.36% predicts more accurately than Chueh and Prusnitz (1976) model with an AARD of 15.56%. However, the accuracy can improve significantly by considering the binary interaction coefficients as a function of temperature. The temperature dependent binary interaction coefficient of Agrawal (2012) which contains a temperature dependent and a temperature independent section was selected. Either of the mentioned temperature independent correlations (Chueh and Prausnitz (1967) and Gao et al. (1992)) can be used for the temperature independent section of the interaction parameters.

The correlations by Chueh and Prausnitz (1967) and Gao et al. (1992) indicates that while the pseudo-components become heavier and the critical volume or critical temperature increase, the

absolute value of the interaction coefficient also increases. If two components are similar to each other, the binary interaction is lesser than that of two non-similar components. In this case, when the pseudo-component becomes heavier, the difference between methane and the pseudo-component and the absolute value of binary interaction increase. The binary interaction graphs for all systems of methane, ethane, and carbon dioxide with bitumen follow this trend. Agrawal (2012) used a temperature dependent binary interaction correlation with the following form:

$$k_{ij} = k_{ij}{}^{0}\left(1+\frac{k_{ij}{}^{1}}{T}+k_{ij}{}^{2}\ln(T)\right) \qquad 4\text{-}3$$

Their correlation is a special case of the general binary interaction coefficients form used in commercial software such as ProMax:

$$k_{ij} = a_{ij} + b_{ij}T + \frac{c_{ij}}{T} + d_{ij}T^{2} \qquad 4\text{-}4$$

$$k_{ij} = \frac{a_{ij}}{T} + b_{ij} + c_{ij}T + d_{ij}\ln(T) \qquad 4\text{-}5$$

Equations 4-4 and 4-5 are appropriate for nonpolar and polar systems, respectively. Equation 4-5 is used for binary interaction of different solvents with bitumen because bitumen is a complex component. Agrawal (2012) indicates that there is no unique solution when three regression parameters are used. Therefore, a constant value of 0.27 is considered for the parameter of the temperature independent section.

In the present study, the Gao et al. (1992) correlation was used to match the data with one regression parameter *(θ)*. In the temperature dependent approach, two different cases for the parameter θ are considered. In the first case, θ is constant and equal to 0.27. In the second case θ is equal to the value of the first case. The same approach is considered in the van der Waals mixing rule for K_{ij} and I_{ij}. In total six different approaches are considered.

The binary interaction parameters are reported in Table 4-11. As the table indicates the van der Waals mixing rule with two parameters (VDW2P) while binary interaction coefficients are as a

function of temperature and critical temperature, leads to the minimum deviation. In addition, the regression has been done when all parameters considered. In this case, the resulting AARD is the same as when θ is considered to be constant. This is an evident to Agrawal (2012) statement, which indicates that there is no unique solution.

The first and second binary interaction coefficients for VDW2P are plotted in Figure 4-15 and Figure 4-16. As the figures indicate, the binary interaction coefficients increase with temperature as it increases with increasing molecular weight or in other words critical temperature. The difference in binary interaction coefficients for heavy components decreases while the pseudo-component becomes heavy. This trend was also reported by Fu and Puttagunta (1986b). They found that as temperature increases, the binary interaction coefficient of methane/Athabasca bitumen increases. The temperature dependent section can change the sign and make a binary interaction coefficient negative while the absolute value of binary interaction coefficient will increase with increasing the molecular weight. Different temperature dependency trends have been seen for different systems which are in good agreement with previous reported trends. These trends are a function of the accuracy of the experimental data and may have no physical meaning. The experimental and predicted values for methane solubility with two methods are plotted in Figure 4-17. The proposed method is compared with VDW1P which is a popular method in literature. The picture depicted the solubility of methane increases as pressure increases and temperature decreases. As the pressure increases toward the critical point, the accuracy decreases in the VDW1P approach.

Table 4-11: Binary interaction coefficient parameters for methane/Athabasca bitumen

	BI functionality	**K_{ij}^0**	**K_{ij}^1**	**K_{ij}^2**	**I_{ij}^0**	**I_{ij}^1**	**I_{ij}^2**	**AARD(Wt)%**
VDW1P	$f(T_C)$	-0.361	-	-	-	-	-	15.36
	f(T)	(-0.361)	-818.4	0.391	-	-	-	11.87
	$f(T_c,T)$	(0.27)	1076	-0.903	-	-	-	11.87
VDW2P	$f(T_C)$	0.493	-	-	0.133	-	-	7.78
	f(T)	(0.493)	-461.1	0.239	(0.133)	-579.4	0.258	3.55
	$f(T_c,T)$	(0.27)	-950.1	0.533	(0.27)	-320.6	0.060	3.41

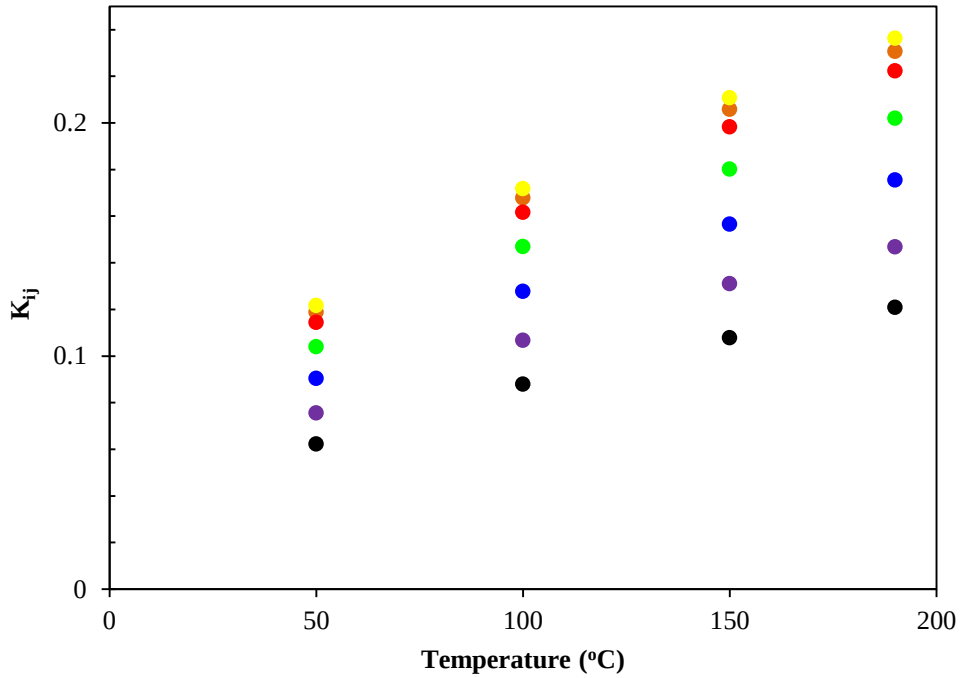

Figure 4-15: First binary interaction coefficient (k_{ij}) for methane/Pesudo-component. Black, violet, blue, green, red, orange and yellow dots are PC1 to PC7.

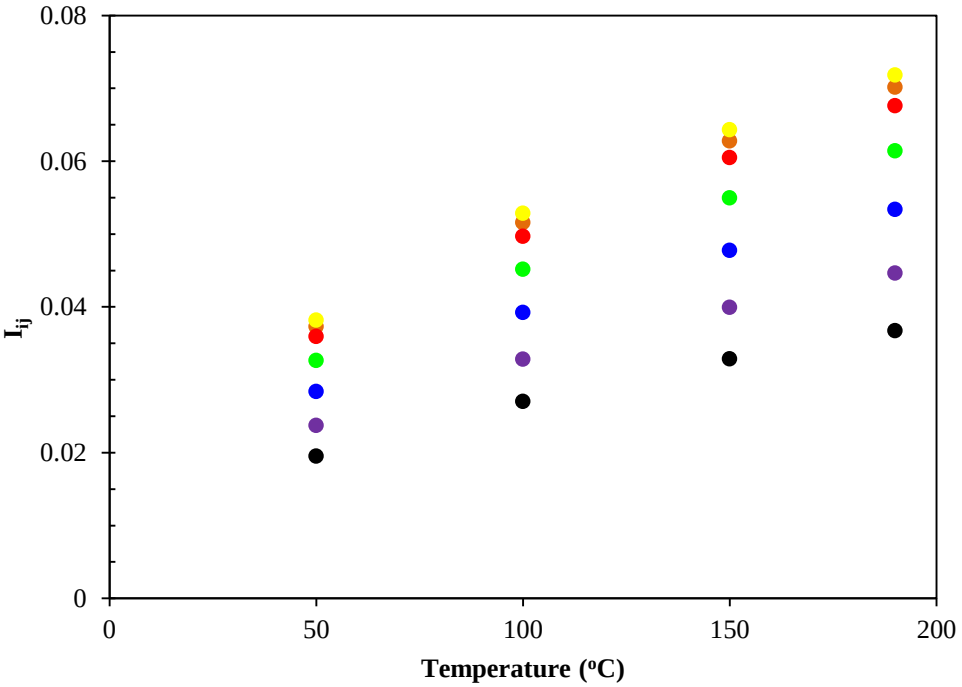

Figure 4-16: Second binary interaction (I_{ij}) coefficients for methane/pseudo-components. Black, violet, blue, green, red, orange and yellow dots are PC1 to PC7.

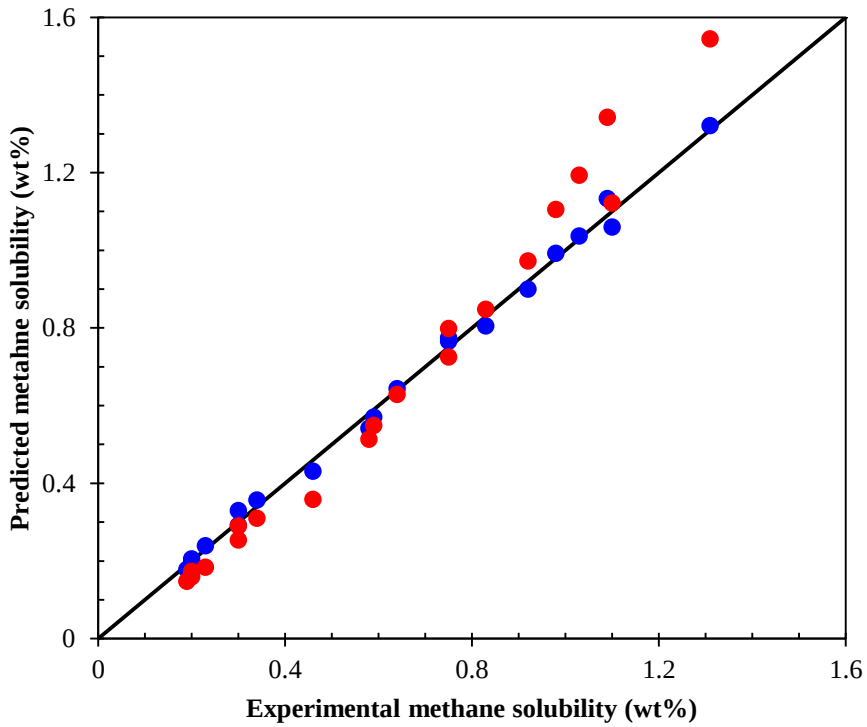

Figure 4-17: Experimental and predicted methane solubility (wt.%) in Athabasca bitumen. The line is experimental data and blue and red are VDW1P case 1 and VDW2P respectively.

The Nikos (1986) correlation was also tested. This correlation can predict solubility data with an AARD of 3.39% when the correlation applies to both binary interaction coefficients. This correlation can improve the solubility prediction slightly because it increases the number of regression parameters. The best approach is VDW2P when the binary interaction coefficients are functions of temperature and critical temperature and four regression parameters are used.

4.2.1.2. Saturated Bitumen Density

The predicted density shows a significant deviation compared to the experimental data. Thus, the volume shift concept has been used to match the data. Different correlations were generated to match the density data and the authors correlated the volume shifts as a function of the molecular weight (Danesh 1998):

$$S_E = 1 - \frac{\Psi}{M^{\chi}} \quad 4\text{-}6$$

Where Ψ and χ are positive constants that can be used as regression parameters for heavy fractions. Similar to the Agrawal (2012) model for the binary interaction coefficient, the following temperature dependent volume shift correlation is proposed.

$$S_E = \left(1 - \frac{\Psi}{M^{\chi}}\right)\left(1 + \frac{SE^1}{T} + SE^2 \ln(T)\right) \quad 4\text{-}7$$

This correlation can also be defined regarding to reference temperature:

$$S_E = \left(1 - \frac{\Psi}{M^{\chi}}\right)\left(1 + \frac{SE^1}{T_f}(T - T_f) + SE^2 \ln(\frac{T}{T_f})\right) \quad 4\text{-}8$$

The reference temperature in above correlation can be ambient temperature, however since the ambient temperature data is not available, different temperature points were tested and found out the reference temperature can be different for each solvent/bitumen systems. The critical temperature has been tested as reference temperature and good agreement has been found with experimental data which leads to the following equation:

$$S_E = \left(1 - \frac{\Psi}{M^{\chi}}\right)\left(1 + SE^1(T_r - 1) + SE^2 \ln(T_r)\right) \quad 4\text{-}9$$

As Agrawal (2012) mentioned, this type of correlation does not have a unique solution therefore the parameters Ψ and χ must be kept constant. Danesh (1998) suggested considering χ as a regression parameter for the heavy component with a constant value for Ψ. Values of Ψ are 2.258, 3.004 and 2.516 for Paraffins, Naphtenes and Aromatics. The PNA analysis of bitumen makes it possible to find an accurate value for Ψ. Unfortunately, the PNA data was not available for our study so a value of 2.258 has been used. The matched χ parameters are reported in Table 4-12. As the table indicates, the values are very close to each other.

Table 4-12: Temperature independent volume shift constant and corresponding AARDs for methane/Athabasca bitumen

	BI functionality	χ	AARD(ρ)
VDW1P	Case 1	0.123	1.83
	Case 2	0.123	1.69
	Case 3	0.124	1.69
VDW2P	Case 1	0.122	1.69
	Case 2	0.122	1.79
	Case 3	0.122	1.79

After finding the parameter for the temperature independent section, the parameters for temperature dependent section must be matched. The parameters and corresponding AARDs are reported in Table 4-13. As the table indicates, the two-parameter mixing rule can predict density more accurately than the van der Waals mixing rule with one parameter. The AARD for the density before the volume shift is 2.65%, which demonstrate that the volume shift can improve the density prediction.

Table 4-13: Temperature dependent volume shift parameter and corresponding AARDs for methane/Athabasca bitumen

	BI functionality	SE^1	SE^1	AARD(ρ)
VDW1P	Case 1	-265.1	-0.038	0.269
	Case 2	-246.9	-0.047	0.307
	Case 3	-246.9	-0.047	0.307
VDW2P	Case 1	-245.9	-0.041	0.171
	Case 2	-257.8	-0.036	0.166
	Case 3	-257.8	-0.036	0.165

The volume shifts are shown in Figure 4-18. As the figure indicates, when the component becomes heavier, the value of the volume shift increases. Similarly, increasing the temperature, increases the absolute value of volume shifts. It has been foundthat an increase in the temperature, results in an increase in the deviation from experimental data before the volume shift applies. The experimental and predicted values for density are shown in Figure 4-19.

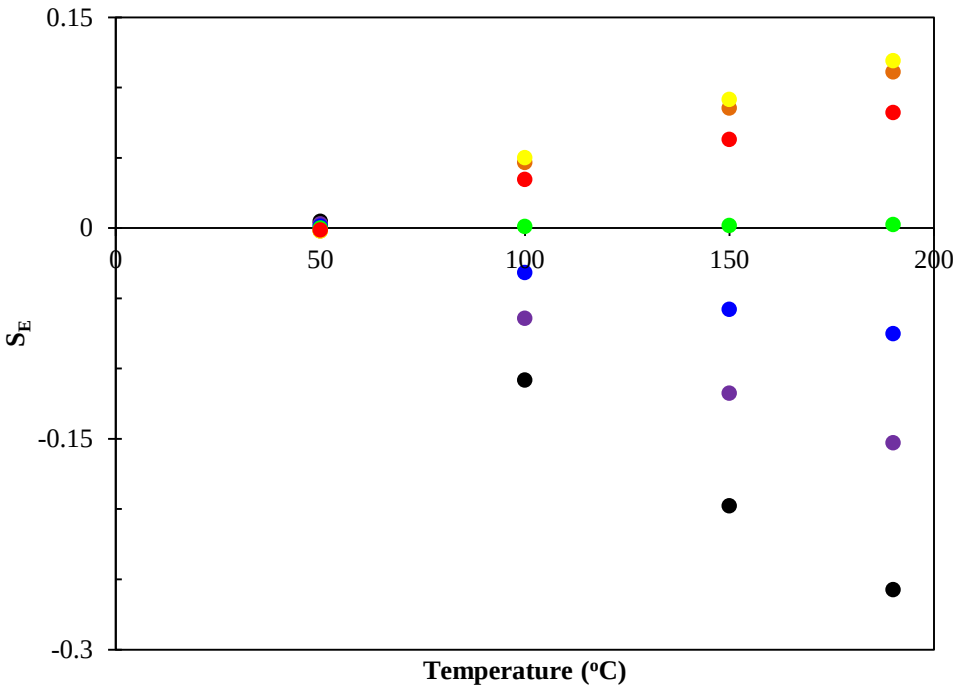

Figure 4-18: Volume shifts of pseudo-components for methane/Athabasca bitumen system. Black, violet, blue, green, red, orange and yellow dots are PC1 to PC7.

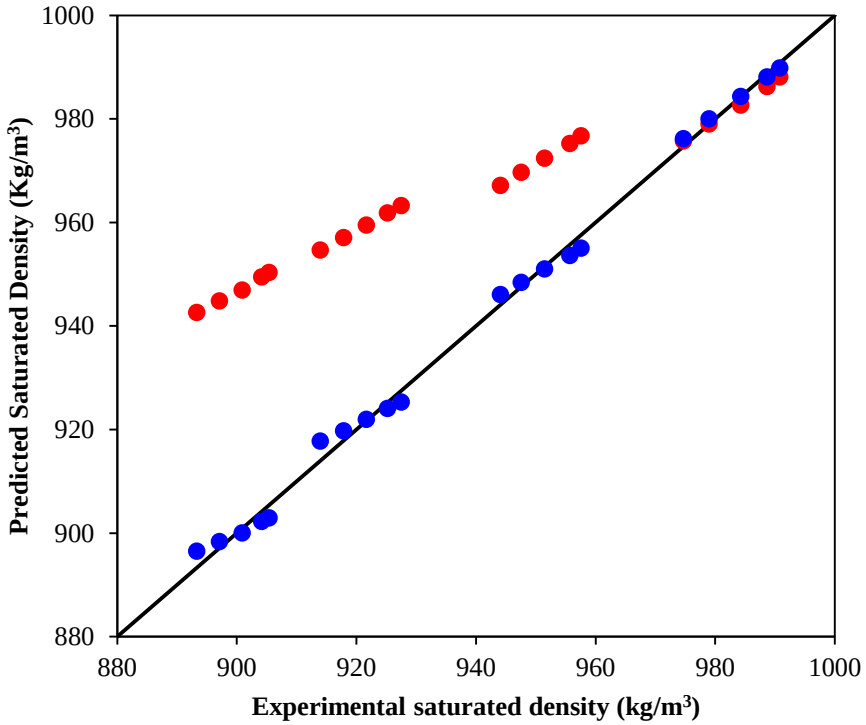

Figure 4-19: Experimental and predicted saturated density for methane/Athabasca bitumen mixtures, Line is experimental data, red and blue dots are predicted values before and after applying volume shift.

4.2.2. Ethane/Athabasca Bitumen

For the ethane/Athabasca bitumen system, 18 points were considered at four different temperatures (50, 100, 150 and 190 ^{o}C). The previously discussed characterization is used and the efficiency of different α correlations is compared. As Table 4-14 indicates, the Twu et al. (1995) correlation is sufficiently accurate for ethane/Athabasca bitumen system. This correlation was used in further modeling for the ethane/Athabasca bitumen system.

Table 4-14: Different α correlations and corresponding AARDs

α correlation	**Temperature independent**	**Temperature dependent**
	AARD*(x)*	**AARD*(x)***
Peng-Robinson(1976)	11.11	8.39
Peng-Robinson (1978)	11.80	8.29
Twu et al. (1995)	10.25	8.07
Nji et al. (2009)	12.25	8.31
Li and Yang (2010)	13.21	8.97

Different binary interaction coefficient forms in conjunction with the van der Waals mixing rules are used to model the solubility data of ethane in Athabasca bitumen. The resulting parameters are reported in Table 4-15. The van der Waals mixing rule with two binary interaction coefficients predicted the ethane solubility with sufficient accuracy. The table also illustrates that the binary interaction parameters as a function of the critical properties and temperature can improve the prediction. The experimental and predicted solubilities are also shown in Figure 4-20. As the graph shows the deviation from the experimental data increases near the critical point. The first binary interaction coefficients are shown in Figure 4-21. As the figure indicates the binary interaction parameter for each pseudo-component decreases as the temperature increases. Fu and Puttagunta (1986) reported the same trend for the ethane/Athabasca bitumen. The figure also indicates that the interactions between pseudo-components and ethane increase as the pseudo-components become heavier which has been seen in methane/Athabasca bitumen as well.

Table 4-15: Binary interaction coefficient parameters for ethane/Athabasca bitumen

	BI functionality	K_{ij}^0	K_{ij}^1	K_{ij}^2	I_{ij}^0	I_{ij}^1	I_{ij}^2	AARD*(Wt)*
VDW1P	$f(T_C)$	-0.111	-	-	-	-	-	10.23
	f(T)	(-0.111)	-1867	0.869	-	-	-	8.17
	$f(T_c,T)$	(0.27)	721.7	-0.577	-	-	-	8.16
VDW2P	$f(T_C)$	0.065	-	-	0.092	-	-	5.79
	f(T)	(0.065)	2093	-1.05	(0.092)	-41.93	-0.012	3.28
	$f(T_c,T)$	(0.27)	473.9	-0.368	(0.27)	-50.55	-0.098	3.28

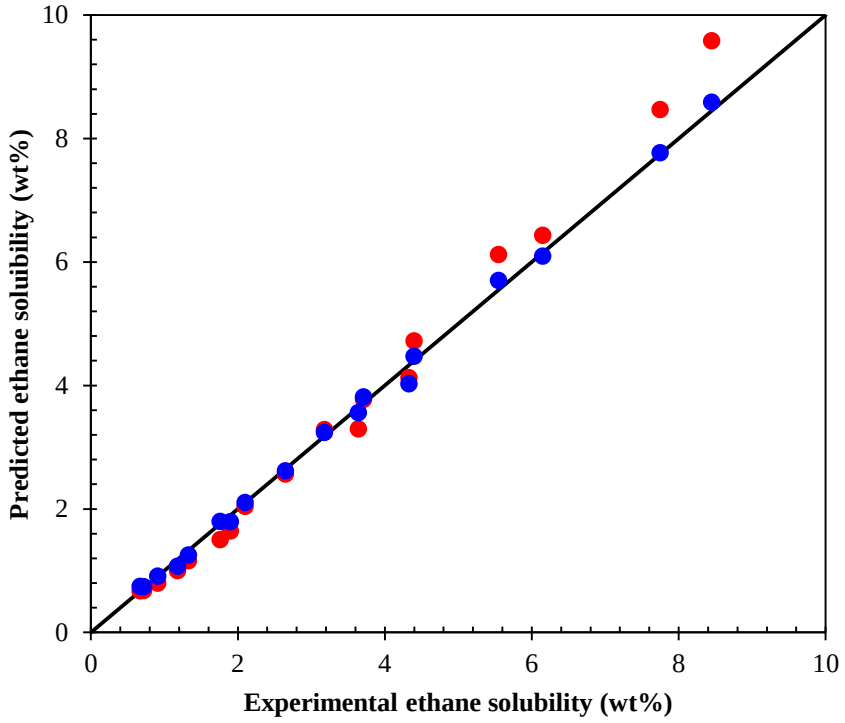

Figure 4-20: Experimental and predicted ethane solubility in Athabasca bitumen. The line is experimental data and blue and red are VDW1P case 1 and VDW2P respectively.

The second binary interaction coefficients are shown in Figure 4-22. As the figure shows the interaction between pseudo-component and ethane increases when the molecular weight increases. The binary interaction coefficient of ethane with pseudo-component is less than methane. The behaviour of ethane is more similar to that of the bitumen components because it is heavier than methane and therefore it has a lesser binary interaction coefficient.

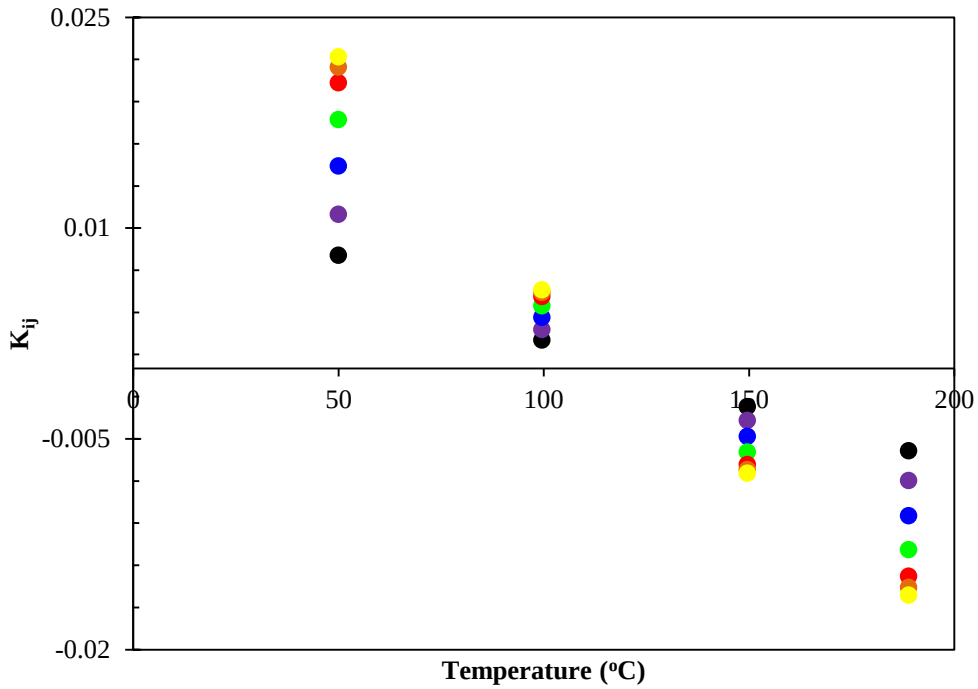

Figure 4-21: First binary interaction coefficient for ethane/pseudo-components. Black, violet, blue, green, red, orange and yellow dots are PC1 to PC7.

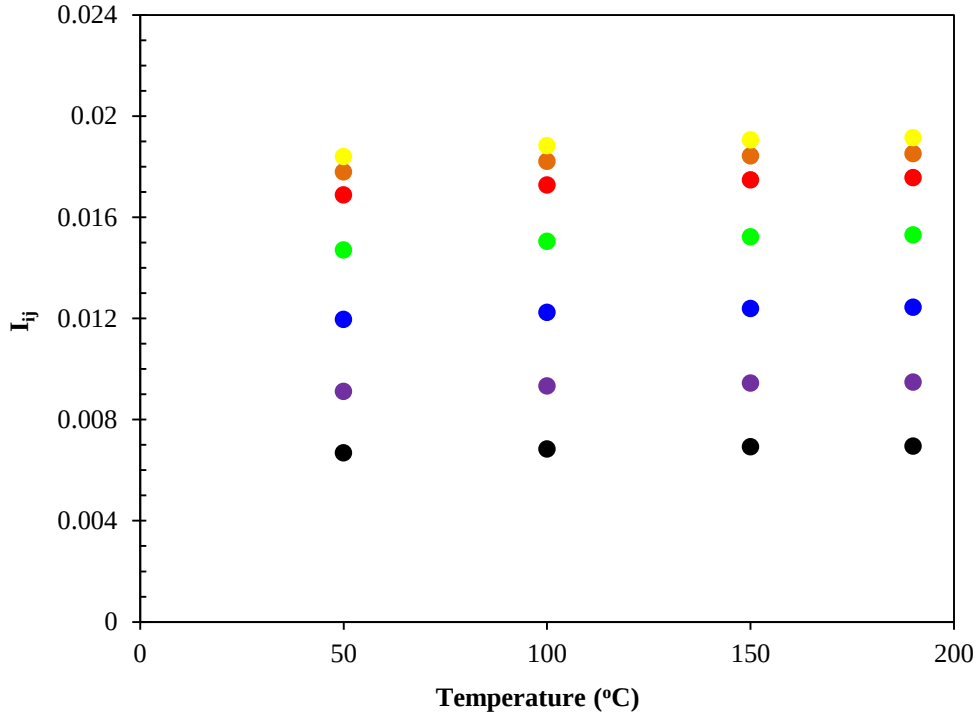

Figure 4-22: Second binary interaction coefficient of ethane/pseudo-components. Black, violet, blue, green, red, orange and yellow dots are PC1 to PC7.

As with methane/Athabasca bitumen the temperature independent section of volume shift was matched for different cases. As Table 4-16 indicates the values for parameter χ are very close to each other. These values are used to determine the coefficients for the temperature dependent section.

Table 4-16: Temperature independent volume shift and corresponding AARDs for ethane/Athabasca bitumen

	BI functionality	χ	**AARD(ρ)**
VDW1P	Case 1	0.128	1.66
	Case 2	0.129	1.43
	Case 3	0.129	1.43
VDW2P	Case 1	0.122	1.38
	Case 2	0.122	1.29
	Case 3	0.122	1.29

In the next step, the volume shifts are matched as a function of temperature. The results are shown in Table 4-17 and that indicates the van der Waals mixing rule with two interaction coefficients predicts the density data with the greatest accuracy. The results are in good agreement with Agrawal (2012), who asserts that there is no unique answer. For example, in case 5 and 6 while the binary interaction coefficient constants are different, the AARDs and the volume shift parameters are the same. The results are reported in Figure 4-23 and Figure 4-24. As Figure 4-24 indicates, the volume shift can significantly improve the saturated density prediction. It also demonstrates that without volume shift, the density prediction at higher temperatures is poor, resulting in greater volume shifts at higher temperatures.

Table 4-17: Temperature dependent volume shift and corresponding AARDs for ethane/Athabasca bitumen

	BI functionality	SE^1	SE^2	**AARD(ρ)**
VDW1P	Case 1	-556.7	0.107	0.420
	Case 2	-468.1	0.068	0.480
	Case 3	-468.1	0.068	0.480
VDW2P	Case 1	-1518	0.554	0.160
	Case 2	-1392	0.583	0.086
	Case 3	-1392	0.582	0.086

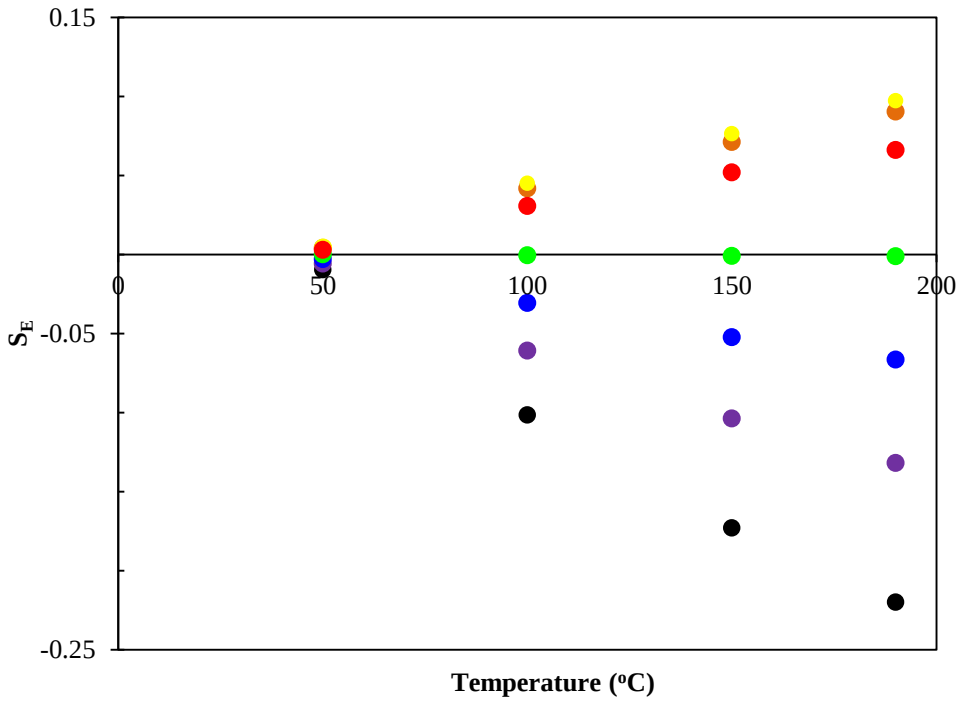

Figure 4-23: Volume shifts of pseudo-components of ethane/Athabasca bitumen system. Black, violet, blue, green, red, orange and yellow dots are PC1 to PC7.

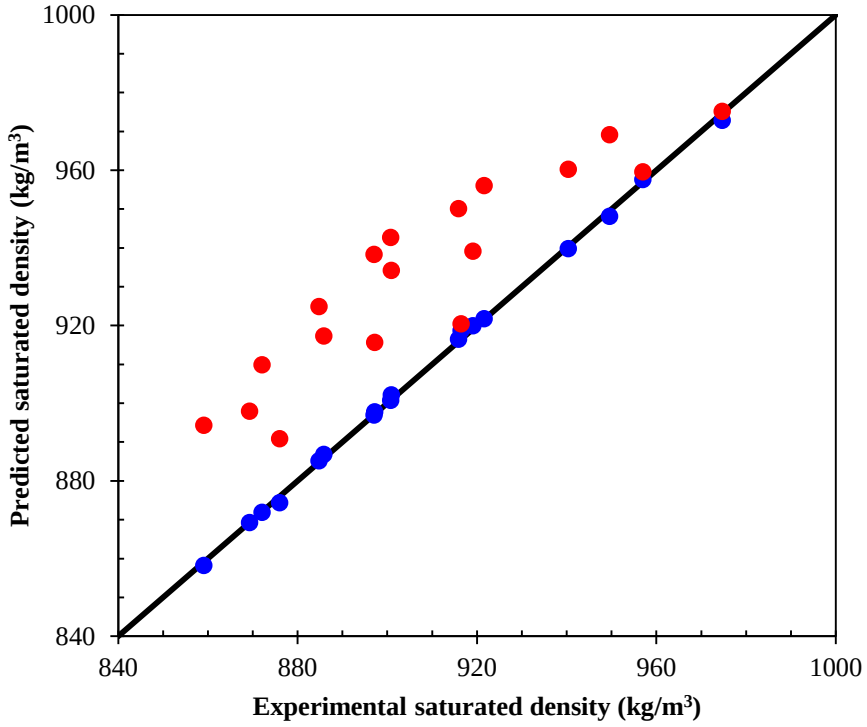

Figure 4-24: Experimental and predicted saturated density for ethane/Athabasca bitumen, Line is experimental data, red and blue dots are predicted values before and after applying volume shift

4.2.3. Carbon Dioxide/Athabasca Bitumen

The previous characterization which contains seven pseudo-components was used to model this system. Six approaches were used to match the solubility data of carbon dioxide in Athabasca bitumen. The van der Waals mixing rules with one and two binary interaction coefficients were employed. The binary interaction coefficients were considered as a function of temperature, critical temperature and dependents on both temperature and critical property. The carbon dioxide data consisted of 23 different points over four different temperatures (50, 100, 150 and 190 ^{o}C). Different α correlations were tested for this system. The data reported in Table 4-18 indicates Twu et al. (1995) correlation improves the prediction in temperature independent approach.

Table 4-18: Different α correlations and corresponding AARDs

α correlation	**Temperature independent**	**Temperature dependent**
	AARD(x)	**AARD(x)**
Peng-Robinson(1976)	18.22	7.05
Peng-Robinson (1978)	19.29	7.06
Twu et al. (1995)	16.65	7.06
Nji et al. (2009)	18.22	7.07
Li and Yang (2010)	18.22	7.05

The parameters of the binary interaction coefficients and their AARDs are reported in Table 4-19. As the table indicates, the temperature dependent binary interaction coefficients can significantly improve the solubility prediction. This table also confirms that one parameter must be constant to produce a unique solution.

Table 4-19: Binary interaction coefficient parameters for carbon dioxide/Athabasca bitumen

	BI functionality	$\mathbf{K_{ij}^0}$	$\mathbf{K_{ij}^1}$	$\mathbf{K_{ij}^2}$	$\mathbf{I_{ij}^0}$	$\mathbf{I_{ij}^1}$	$\mathbf{I_{ij}^2}$	**AARD(Wt)**
VDW1P	$f(T_C)$	0.161	-	-	-	-	-	16.65
	f(T)	(0.161)	3254	-1.58	-	-	-	7.00
	$f(T_c,T)$	(0.27)	1944	-1.02	-	-	-	7.02
VDW2P	$f(T_C)$	0.997	-	-	0.218	-	-	6.43
	f(T)	(0.997)	459.6	-0.273	(0.218)	83.21	-0.099	3.04
	$f(T_c,T)$	0.27	1714	-0.583	0.27	54.44	-0.107	3.04

The experimental and predicted carbon dioxide solubility in Athabasca bitumen is displayed in Figure 4-25. The solubility of the bitumen decreased with increasing temperature and decreasing pressure. The greater solubility, the deviation from the experimental data increases. This means that the accuracy of the prediction decreases near the critical pressure. The binary interaction coefficients in VDW2P are shown in Figure 4-26. As the figure shows, when the component becomes heavier, the interaction coefficient increases. This has also demonstrated for other systems. This graph also indicates that increasing the temperature results in a decrease in the binary interaction coefficient. Fu and Puttagunta (1986) also reported this issue.

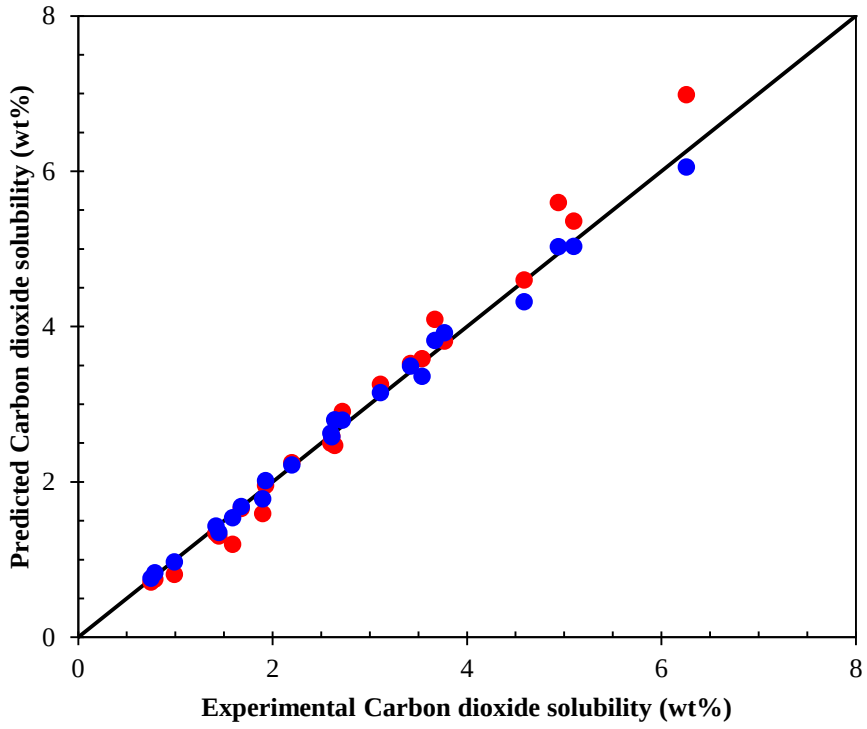

Figure 4-25: Experimental and predicted carbon dioxide solubility in Athabasca bitumen. The line is experimental data and blue and red are VDW1P case 1 and VDW2P respectively.

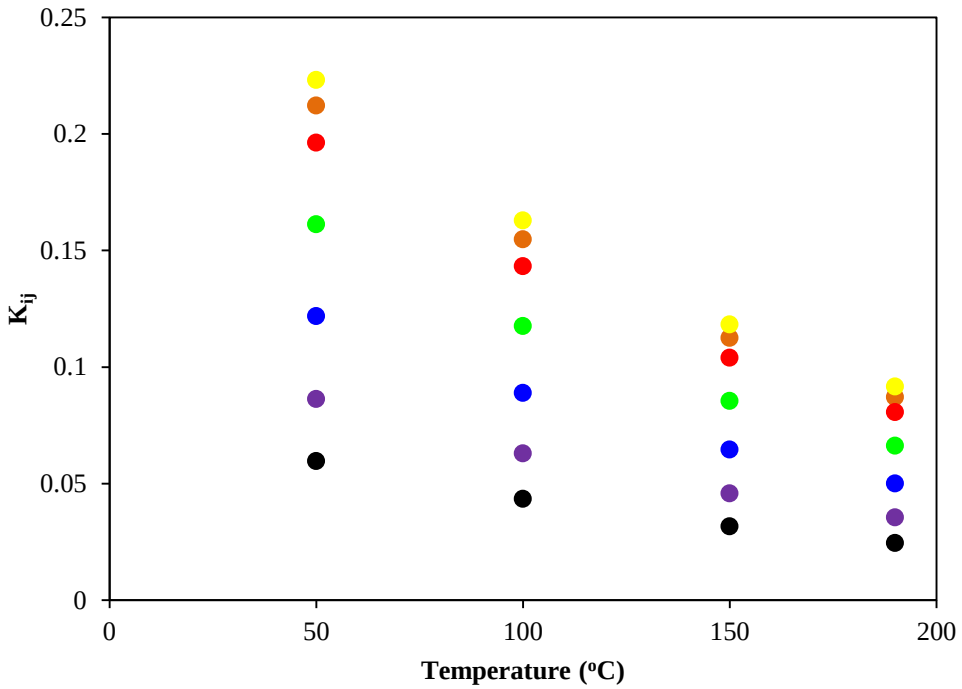

Figure 4-26: K_{ij} for pseudo-components in carbon dioxide/Athabasca bitumen mixtures, Black, violet, blue, green, red, orange and yellow dots are PC1 to PC7.

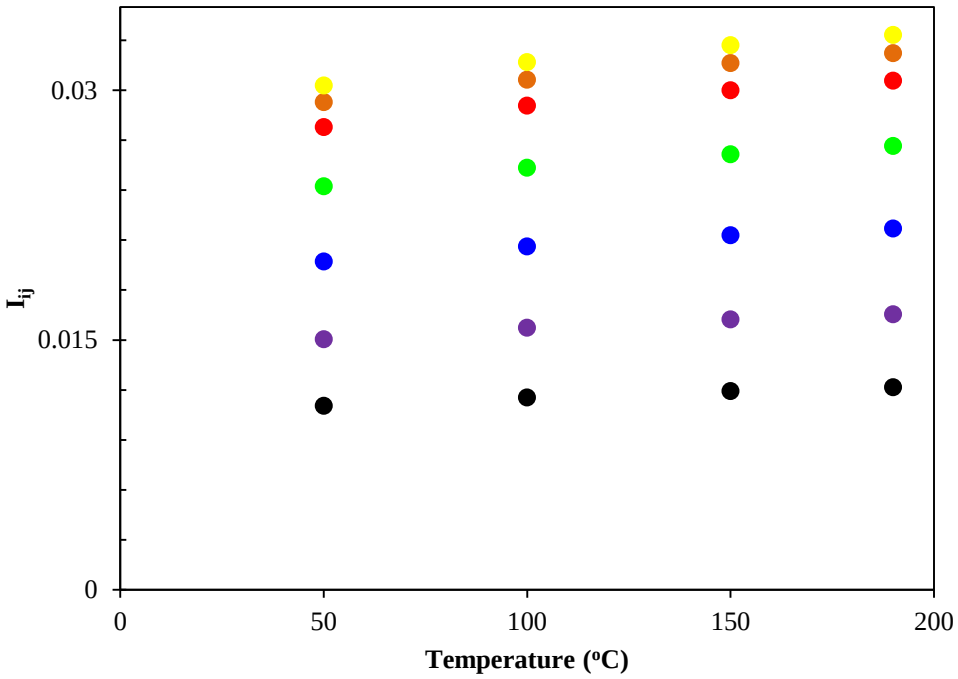

Figure 4-27: I_{ij} for pseudo-components in carbon dioxide/Athabasca bitumen mixtures, Black, violet, blue, green, red, orange and yellow dots are PC1 to PC7.

The second binary interaction coefficient is shown in Figure 4-27. This coefficient also increases as the pseudo-components become heavier. The binary interaction coefficients are higher than ethane and lower than the methane systems. The molecular weight of carbon dioxide is higher than the molecular weight of methane making its behaviour more similar to that of the bitumen pseudo-components. However, the dipolar behaviour of carbon dioxide makes its interaction parameters higher than that of ethane, which is not a polar molecule and its behaviour is more similar to that of a bitumen system. The parameters for the molecular weight dependent volume shift parameter and its corresponding AARD are reported in Table 4-20. As the table indicates, more accurate solubility matching does not lead to a better prediction of saturated density. In the next step the volume shift parameters are correlated as a function of temperature (Table 4-21). As the table indicates the van der Waals mixing rule with two binary interaction parameters is extremely successful at matching the saturated density data. The results for saturated density in the absence of volume shift are also reported in Figure 4-28. The figure indicates that at high temperatures, the deviation of the experimental data is higher in the absence of the volume shift. Therefore at higher temperature, the value of the volume shift is higher.

Table 4-20: Temperature independent volume shift constant and corresponding AARDs for carbon dioxide/Athabasca bitumen

	BI functionality	χ	**AARD(ρ)**
VDW1P	Case 1	0.129	1.56
	Case 2	0.129	1.48
	Case 3	0.129	1.48
VDW2P	Case 1	0.122	1.34
	Case 2	0.122	1.44
	Case 3	0.122	1.36

Table 4-21: Temperature dependent volume shift parameter and corresponding AARDs for carbon dioxide/Athabasca bitumen

	BI functionality	S_E^1	S_E^2	**AARD(ρ)**
VDW1P	Case 1	-1912	0.821	0.157
	Case 2	-1904	0.810	0.178
	Case 3	-1904	0.810	0.178
VDW2P	Case 1	-1188	0.509	0.201
	Case 2	-1359	0.581	0.138
	Case 3	-1359	0.581	0.138

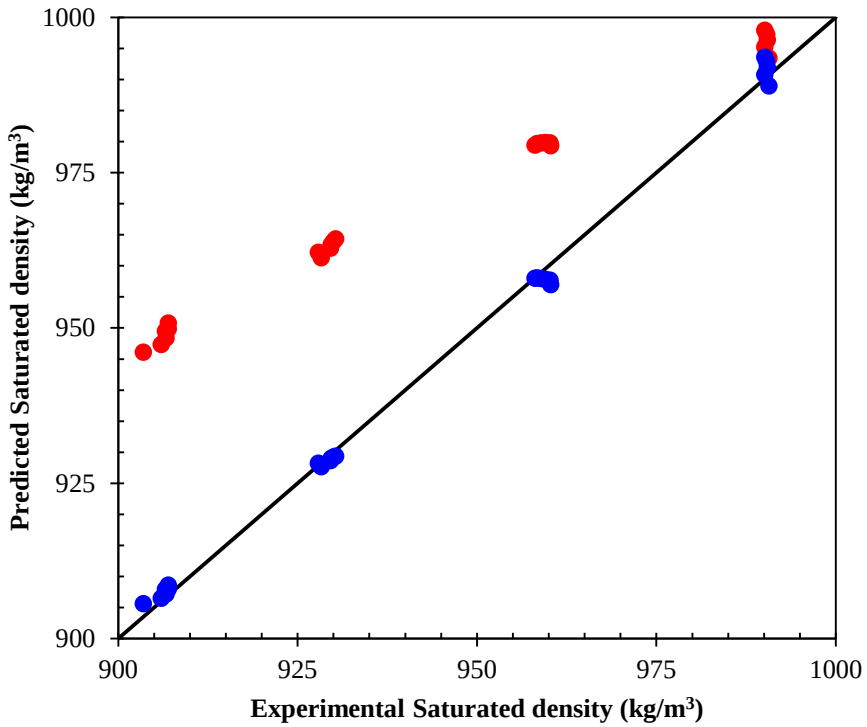

Figure 4-28: Experimental and predicted saturated carbon dioxide/bitumen density. Line is experimental data, red and blue dots are predicted values before and after applying volume shift

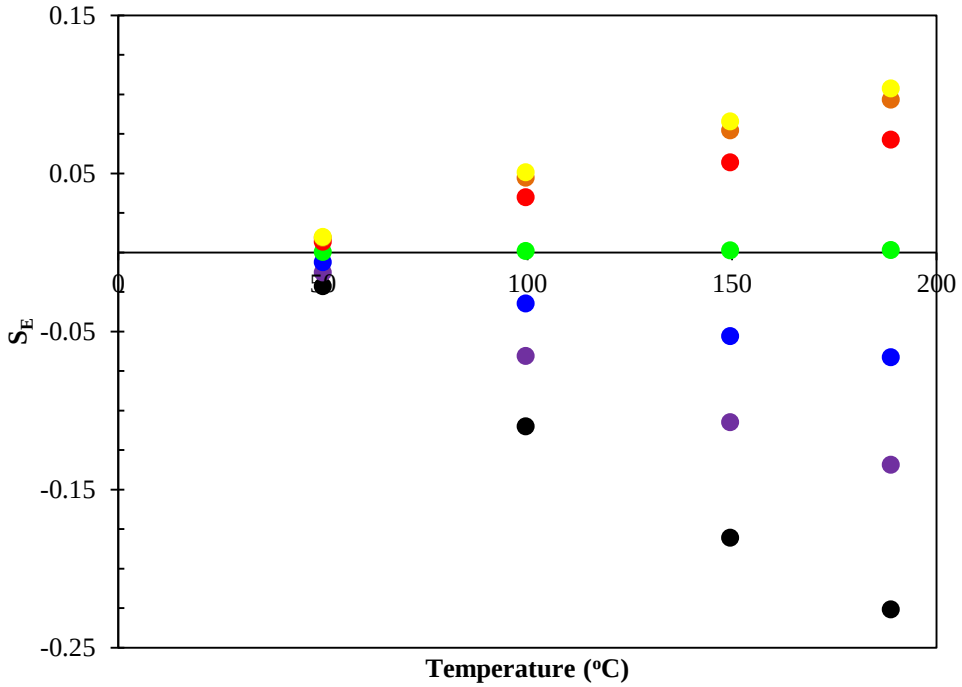

Figure 4-29: Volume shift of pseudo-components at different temperatures for carbon dioxide/Athabasca bitumen system. Black, violet, blue, green, red, orange and yellow dots are PC1 to PC7.

4.3. Solvent/Cold Lake Bitumen Systems

This section presents models of the Cold Lake bitumen systems. For this part, the characterization of Cold Lake bitumen was used (Table 4-8). The van der Waals mixing rule was tested with both one and two parameters. The binary interaction coefficient has been used as a function of temperature therefore two and four regression parameters were used for the one and two parameter van der Waals mixing rules, respectively. The results were compared with the literature data and significant improvements were observed.

4.3.1. Methane/Cold Lake Bitumen

The methane solubility in Cold Lake bitumen is shown in Figure 4-30. The deviation from the experimental data increased approaching to the critical point. The figure also demonstrates that the deviation is higher at low temperatures. The AARD of the predicted methane solubility in Cold Lake bitumen is compared with the literature data in Table 4-22 . As the table shows, this method accurately predicts the methane solubility. The saturated density has an AARD of 0.357% and 0.35% for the van der Waals mixing rule with one and two binary interaction coefficients, respectively. The predicted and experimental values for methane solubility and saturated density are shown in Figure 4-30 and Figure 4-31.

Table 4-22: AARD of methane solubility in Cold Lake bitumen

Predictive Models	AARDs
Mehrotra and Svrcek (1988b)	2.70
Kariznovi et al. (2010)	3.69
VDW1P	2.35
VDW2P	2.07

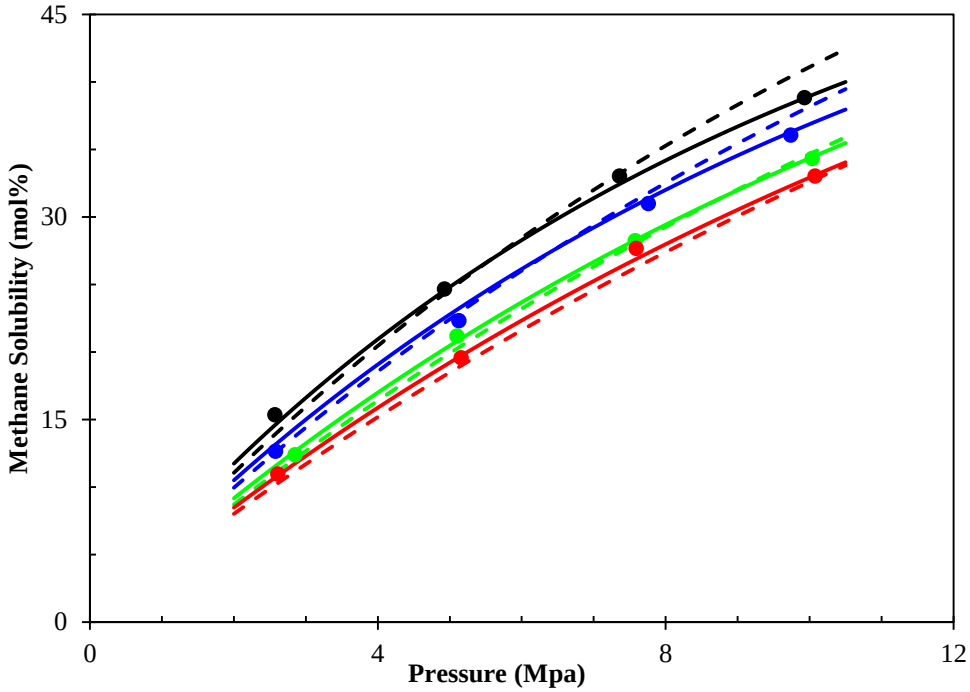

Figure 4-30: Methane solubility in Cold Lake bitumen, data has been taken from Mehrotra and Svrcek (1988a). The dots are experimental data, — and - - - are VDW2P and VDW1P respectively. Black, blue, green and red are 300K, 319K, 350K and 376K respectively.

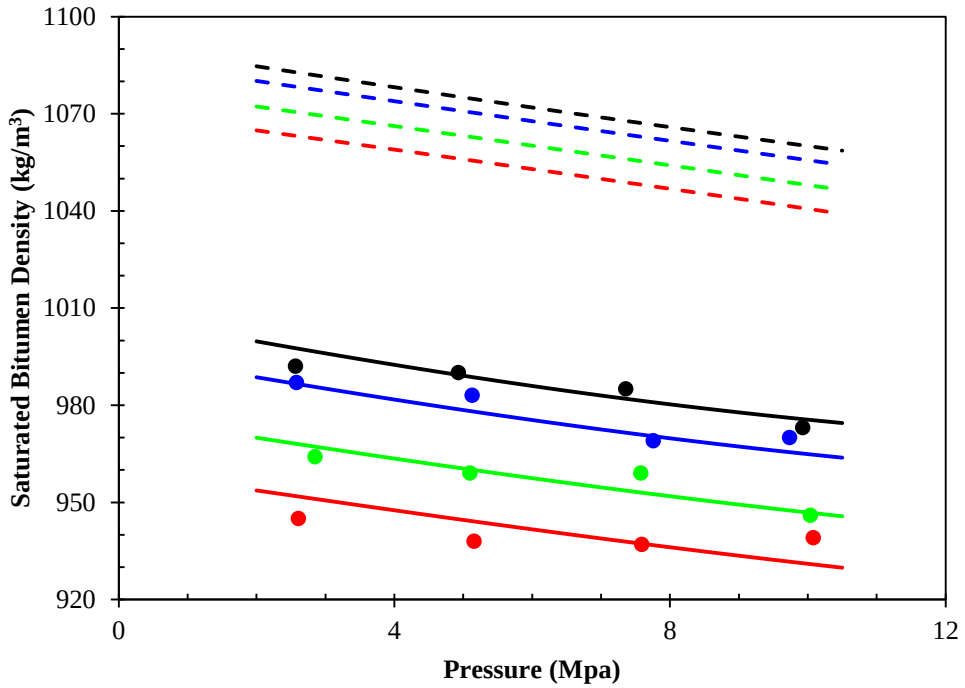

Figure 4-31: Saturated density of methane/Cold Lake bitumen. Data has been taken from Mehrotra and Svrcek (1988a). The dots are experimental data, — and - - - are results with volume shift and without volume shift respectively. Black, blue, green and red are 300K, 319K, 350K and 376K respectively.

4.3.2. Ethane/Cold Lake Bitumen

The system of ethane/Cold Lake bitumen was predicted by the characterization presented for Cold Lake bitumen. The ethane solubility and saturated density of ethane and Cold Lake bitumen systems are presented in Figure 4-32 and Figure 4-33. As Figure 4-32 indicates, the van der Waals mixing rule was not able to predict ethane solubility but the van der Waals with two parameters matched the experimental data with sufficient accuracy.

Table 4-23: AARD of ethane solubility in Cold Lake bitumen

Predictive Models	AARDs
Mehrotra and Svrcek (1988b)	5.70
Kariznovi et al. (2010)	8.14
VDW1P	11.23
VDW2P	2.49

Figure 4-33 indicates that the van der Waals mixing rule with two parameters is more appropriate for density prediction than the van der Waals mixing rule with one parameter. The AARDs for the saturated density are 0.37% and 0.32 % for the van der Waals mixing rule with one and two interaction parameters respectively.

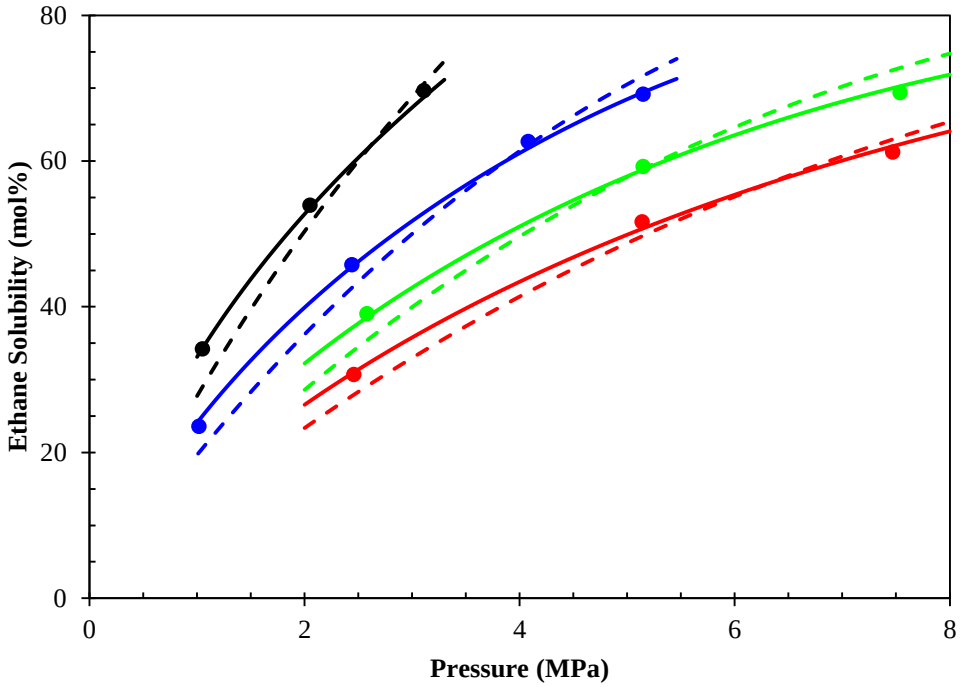

Figure 4-32: Ethane solubility in Cold Lake bitumen. Data has been taken from Mehrotra and Svrcek (1988a). The dots are experimental data, — and - - - are VDW2P and VDW1P respectively. Black, blue, green and red are 298K, 325K, 349K and 374K respectively.

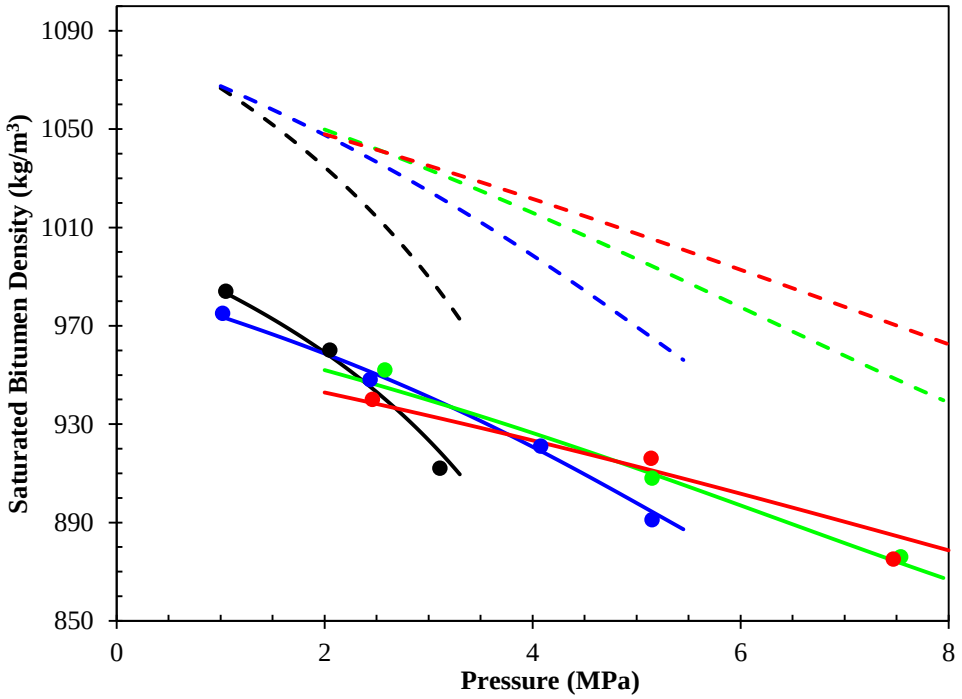

Figure 4-33: Saturated density of ethane/Cold Lake bitumen. Data has been taken from Mehrotra and Svrcek (1988a). The dots are experimental data, — and - - - are results with volume shift and without volume shift respectively. Black, blue, green and red are 298K, 325K, 349K and 374K respectively.

4.3.3. Carbon Dioxide/Cold Lake Bitumen

The carbon dioxide/Cold Lake data was modeled using the proposed characterization. The appropriate α correlation was selected and the results are plotted in Figure 4-34 and Figure 4-35. As the figure shows, the van der Waals mixing rule with two binary interaction coefficients is more successful at predicting the solubility and saturated density. The results were compared with the literature in the table below. As the table indicates, my model predicts solubility more accurately sufficient accuracy. The density prediction had an AARD of 0.78% and 0.56% for the van der Waals mixing rule with one and two binary interaction coefficients, respectively.

Table 4-24: AARD of carbon dioxide solubility in Cold Lake bitumen

Predictive Models	AARDs
Mehrotra and Svrcek (1988b)	1.9
Eastick et al. (1992)	6.8
Kariznovi et al. (2010)	7.16
VDW1P	6.21
VDW2P	2.07

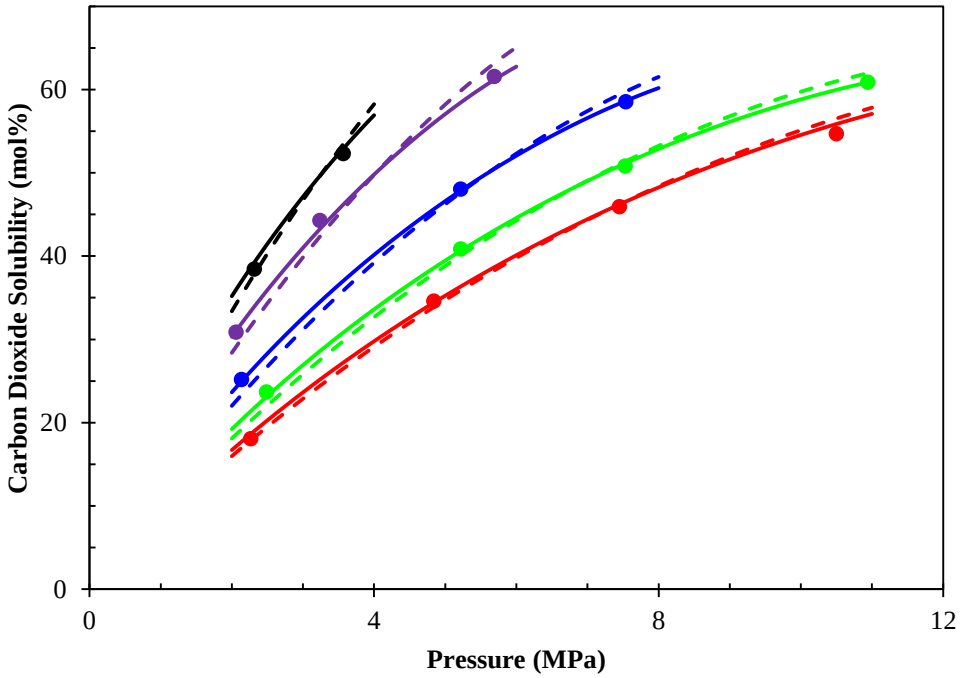

Figure 4-34: Carbon dioxide solubility in Cold Lake bitumen. Data has been taken from Mehrotra and Svrcek (1988a). The dots are experimental data, — and - - - are VDW2P and VDW1P respectively. Black, violet, blue, green and red are 287K, 300K, 325K, 350K and 370K respectively.

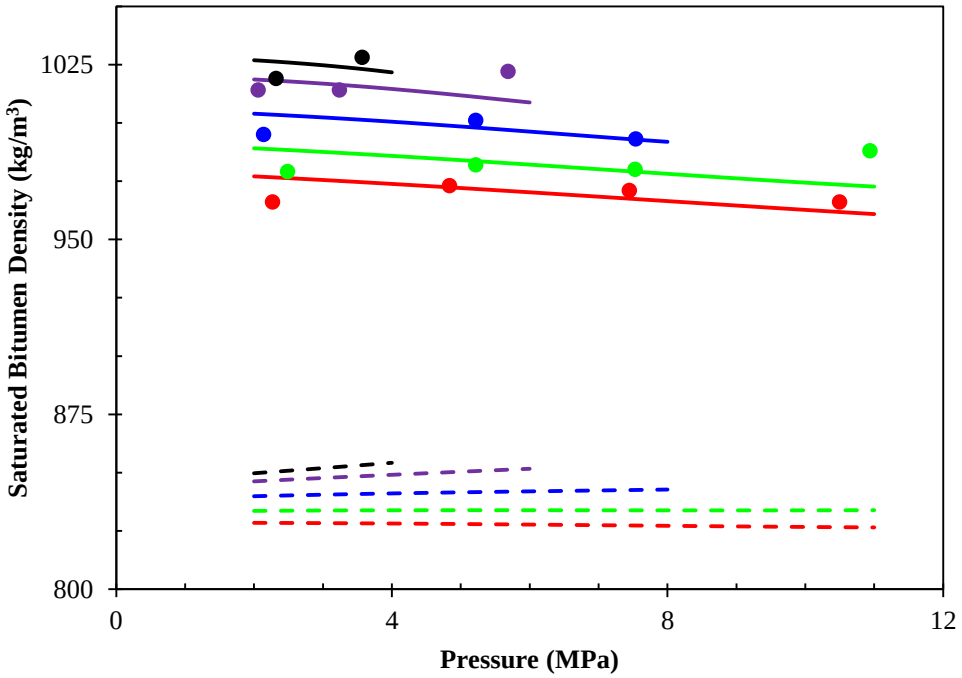

Figure 4-35: Saturated density of carbon dioxide/Cold Lake bitumen. Data has been taken from Mehrotra and Svrcek (1988a). The dots are experimental data, — and - - - are are results with volume shift and without volume shift respectively. Black, violet, blue, green and red are 287K, 300K, 325K, 350K and 370K respectively.

4.3.4. Nitrogen/Cold Lake Bitumen

The system of nitrogen/Cold Lake bitumen was also modeled by the characterization proposed for Cold Lake bitumen. The Li and Yang (2010) correlation was determined to be the best α correlation for this system. The experimental and predicted values for nitrogen solubility and saturated density are plotted in Figure 4-36 and Figure 4-37. As the graphs show, the van der Waals mixing rule with two parameters is more successful than van der Waals mixing rule with one interaction coefficient. The results are also compared with literature in the table. Our characterization and model predicted the solubility more accurately than previous attempts (Mehrorta and Svrcek 1988b and Kariznovi et al. 2010).

Table 4-25: AARDs of nitrogen solubility in Cold Lake bitumen

Predictive Models	AARDs
Mehrotra and Svrcek (1988b)	8.1
Kariznovi et al. (2010)	5.32
VDW1P	4.73
VDW2P	4.30

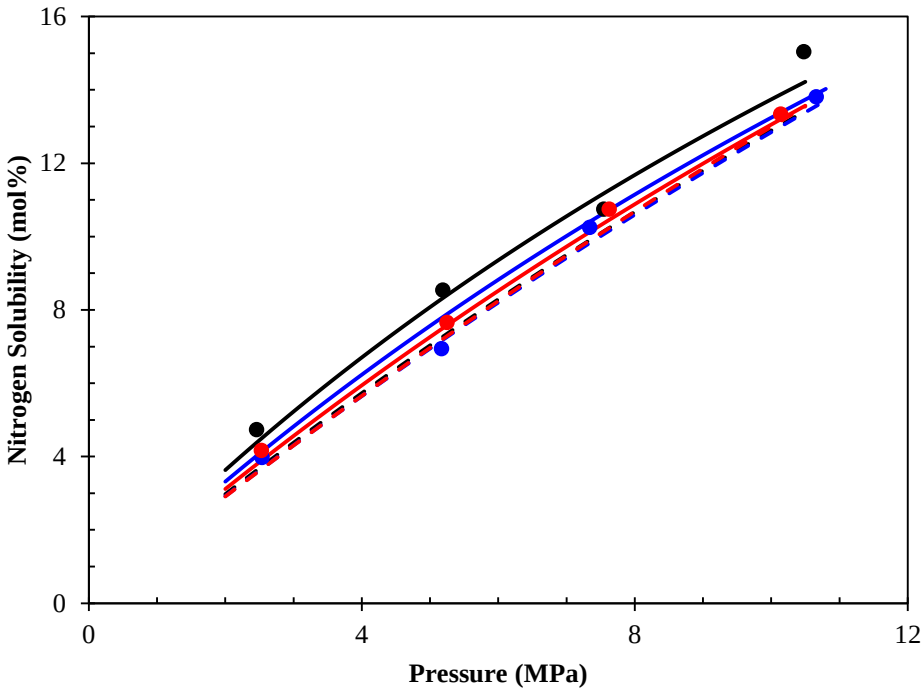

Figure 4-36: Nitrogen solubility in Cold Lake bitumen. The data has been taken from Mehrotra and Svrcek (1988a), the dots are experimental data, — and - - - are VDW2P and VDW1P respectively. Black, blue and red are 304K, 330K and 370K respectively.

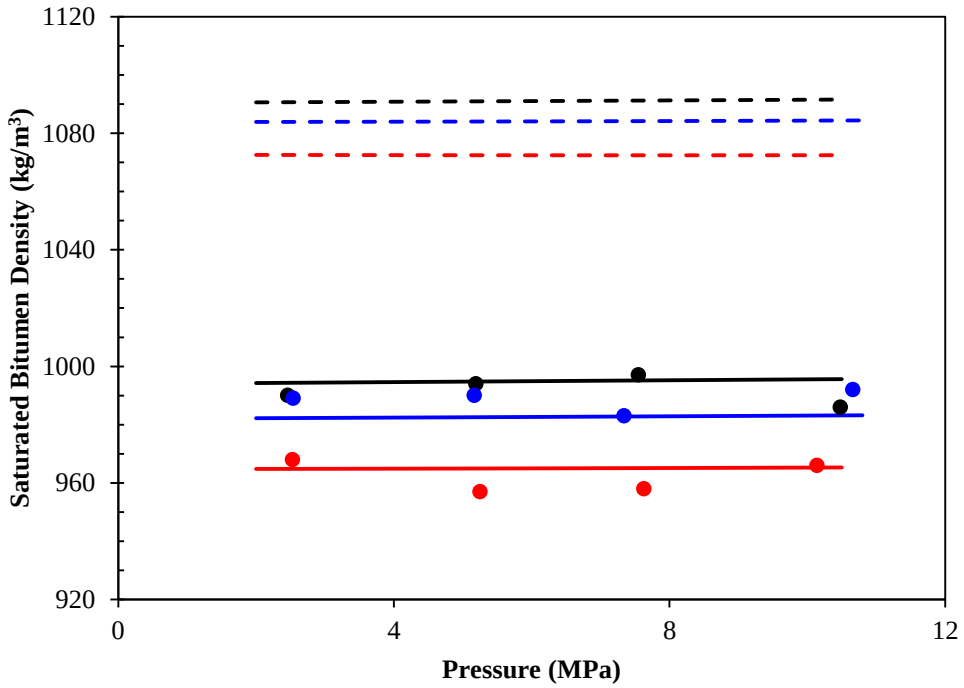

Figure 4-37: Saturated density of nitrogen/Cold Lake bitumen. The data has been taken from Mehrotra and Svrcek (1988a). The dots are experimental data, — and - - - are results with volume shift and without volume shift respectively. Black, blue and red are 304K, 330K and 370K respectively.

4.4. Wong-Sandler Mixing Rule for Bitumen Systems

The complexity of the Wong-Sandler mixing rule for multi component systems makes it impossible to use for systems with more than three components. In order to apply the Wong-Sandler mixing rule, the bitumen is considered as one pseudo-component. The properties of the bitumen are reported in Table 4-26.

Table 4-26: Chemo physical properties of Athabasca bitumen

PC	Mole fraction(%)	Molecular weight	T_c(K)	P_c(kPa)	ω	V_c	T_b(K)
1	100	539.0	938.63	1437.6	0.941	2.120	756.57

To compare the flexibility of the Wong-Sandler mixing rule with other mixing rules, the one-component bitumen system was also modeled with the van der Waals mixing rule with one and two parameters. In the Wong-Sandler mixing rule, the objective function defines the K-values and following the regression, the AARD is calculated from the weight percent solubility. The results are summarized in the following tables:

Table 4-27: AARD of methane solubility in Athabasca bitumen for different mixing rules

Mixing Rule	BI functionality	Number of Regression parameters	AARD(wt%)
VDW1P	T_c	1	17.14
VDW1P	T,T_c	2	11.98
VDW2P	T_c	2	9.57
VDW2P	T,T_c	4	3.57
WS	-	3	3.23

Table 4-28: AARD of ethane solubility in Athabasca bitumen for different mixing rules

Mixing Rule	BI functionality	Number of Regression parameters	AARD(wt%)
VDW1P	T_c	1	11.76
VDW1P	T,T_c	2	7.99
VDW2P	T_c	2	7.54
VDW2P	T,T_c	4	3.35
WS	-	3	4.69

Table 4-29: AARD of carbon dioxide solubility in Athabasca bitumen for different mixing rules

Mixing Rule	BI functionality	Number of Regression parameters	AARD(wt%)
VDW1P	T_c	1	20.78
VDW1P	T,T_c	2	7.14
VDW2P	T_c	2	8.35
VDW2P	T,T_c	4	3.29
WS	-	3	3.147

The obtained binary interaction coefficients and NRTL model parameters are summarized in below table:

Table 4-30: Interaction coefficients, NRTL parameters and AARDs of different solvents with Athabasca bitumen

T(°C)	Solvents											
	Methane				Ethane				Carbon Dioxide			
	k_{12}	τ_{12}	τ_{21}	AARD	k_{12}	τ_{12}	τ_{21}	AARD	k_{12}	τ_{12}	τ_{21}	AARD
50	0.669	13.9	-0.673	2.98	0.831	70.8	-0.379	1.23	0.911	6.59	-0.904	4.43
100	0.871	7.36	-1.55	2.48	0.608	11.2	-0.559	2.14	0.837	6.88	-0.965	3.11
150	0.960	7.43	-1.68	4.49	0.566	9.74	-0.781	10.4	0.410	8.66	-0.149	1.63
190	0.496	22.8	-0.303	2.97	0.567	13.3	-0.393	3.56	0.894	13.9	-0.383	3.40

The experimental and predicted solvent solubility of Athabasca bitumen is plotted in Figure 4-38 to Figure 4-40. As the figures show, the predicted values demonstrate good agreement with the experimental data. Despite its high accuracy, this method is not applicable for bitumen systems. The high number of regression parameters for each isotherm and its limited application to binary systems diminish its usefulness.

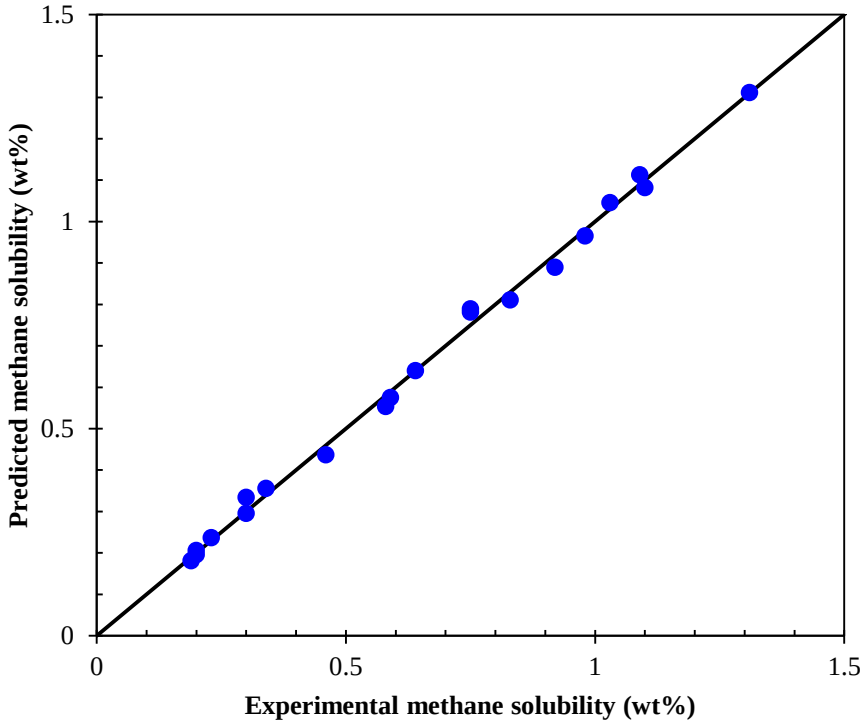

Figure 4-38: Experimental and predicted methane solubility in Athabasca bitumen. The solid line is the experimental data and dots are predicted values by WS mixing rule.

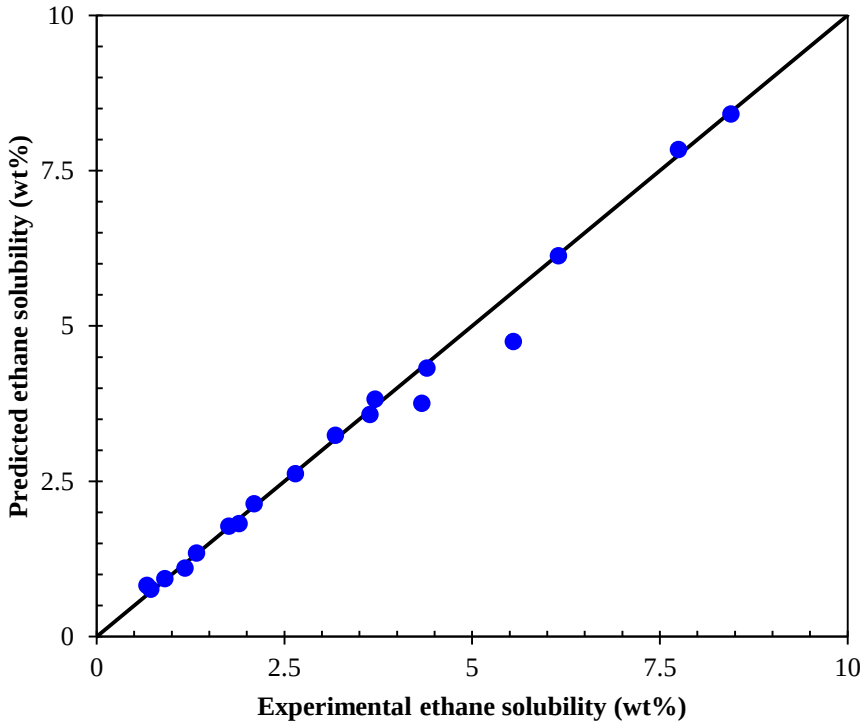

Figure 4-39: Experimental and predicted ethane solubility in Athabasca bitumen. The solid line is the experimental data and dots are predicted values by WS mixing rule.

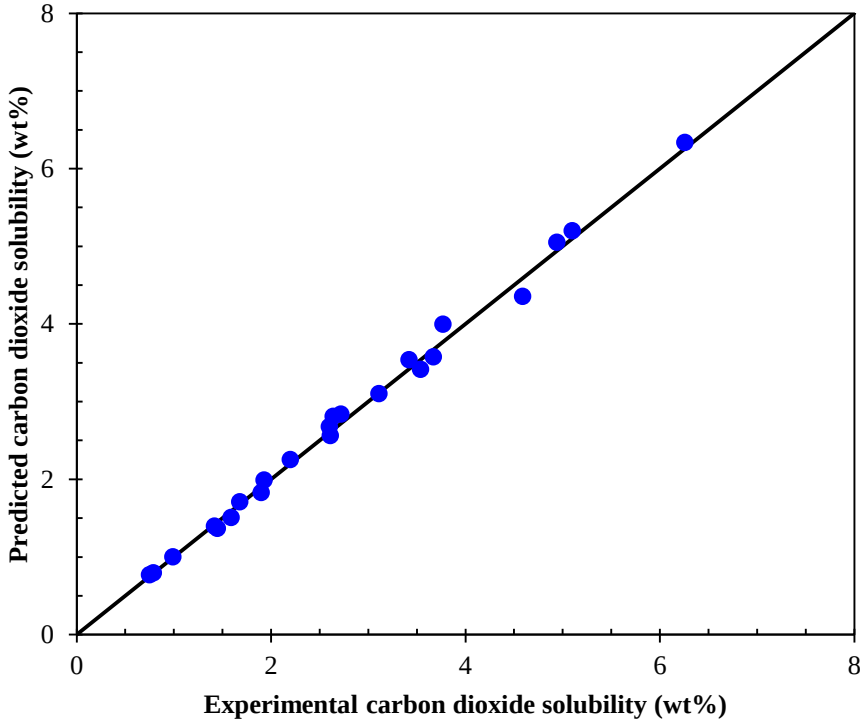

Figure 4-40: Experimental and predicted carbon dioxide solubility in Athabasca bitumen. The solid line is the experimental data and dots are predicted values by WS mixing rule.

Chapter 5: Conclusions and Recommendations

The goal of this study was a better understanding of phase behaviour modeling for solvent/bitumen systems. A comprehensive code was developed for the bitumen characterization and cubic equation of state modeling of the complex systems. A stepwise scheme was developed for bitumen characterization and the results were used for VLE study. The proposed characterization method provides a practical and straightforward bitumen characterization using limited experimental data. In this method the SCN curve was generated from the TBP curve to characterize bitumen. The effect of different lumping schemes and mixing rules was investigated and the accuracy of different correlations for critical temperature, pressure, and acentric factor were considered. In this characterization scheme gamma distribution has been considered as probability function which can model a wide range of crude oils from light and condensate to heavy oils and bitumen. In this method, the pseudo-component properties have been calculated through a schematic approach comparing to other characterization method, provide consistency for different oils and bitumen.

In this study, different mixing rules for attractive and repulsive terms have been compared. It was found that the van der Waals mixing rule with two regression parameters successfully improves the accuracy of the solvent solubility predictions. It was observed that the temperature dependency of the binary interaction coefficient also improves the prediction significantly. A temperature and molecular weight dependent correlation was used for volume shift and saturated liquid density and was matched to the literature data with sufficient accuracy. These new correlations for volume shifts and binary interaction coefficients reduce the number of regression parameters and improve the capability of optimization schemes. With this method, the number of pseudo-components does not affect the number of regression parameters and different sensitivity and test runs can be executed more simply. The Wong-Sandler mixing rule was also tested for solvent solubility and successfully matched to the experimental data. The results showed the

capability of Wong-Sandler mixing rule in polar and non polar mixture even while bitumen considered as one pseudo-component.

In the future, a universal characterization scheme for different heavy oils and bitumen will be developed. Investigating different random and non-random mixing rules for solvent/bitumen systems modeling is another opportunity for further research. Different correlations for binary interaction coefficient, NRTL model parameters, and volume shifts can be tested to improve the prediction and reduce the regression parameters.

Modeling the phase behaviour of different cuts with bitumen would allow us to create a more realistic phase behaviour model to study the effect of different chemo physical properties on the predictive accuracy. In addition, this data could be used in the Wong-Sandler mixing rule and its parameters can be found with regards to each pseudo-component.

References

Abbott, M. M. 1979. Cubic equation of state: an interpretive review. *Equations of State in Engineering and Research*, Adv. in Chemistry Ser., 182, K. C. Chao and R. L. Robinson eds., American Chemical Society, Washington, DC, p. 47.

Adachi, Y., and Sugie, H. 1986. A new mixing rule—modified conventional mixing rule. *Fluid Phase Equilibria*, 28(2): 103-118.

Agrawal, P. 2012. Measurement and modeling of the phase behavior of solvent diluted bitumens. MSc thesis, University of Calgary, Calgary, Alberta, Canada.

Ahmed, T. H. 1989. *Hydrocarbon phase behavior* (Vol. 7). Gulf publishing company.

Anderko, A. 1990. Equation-of-state methods for the modelling of phase equilibria. *Fluid Phase Equilibria*, 61(1): 145-225.

Atilhan, M. 2004. A new cubic equation of state. PhD thesis, Texas A&M University, Texas, United States.

Badamchi-Zadeh, A., Yarranton, H.W., and Maini, B. 2013. Phase behavior and physical property modeling for vapex solvents: propane, carbon dioxide, and Athabasca bitumen. *SPE Heavy Oil Conference*, Calgary, Alberta, Canada, 11-13 June.

Beattie, J. A., and Bridgeman, O. C. 1927. A new equation of state for liquids. I. Application to gaseous ethyl ether and carbon dioxide. *Journal of the American Chemical Society*, 49(7): 1665-1667.

Behrens, R. A., and Sandler, S. I. 1988. The use of semicontinuous description to model the C7+ fraction in equation of state calculations. *SPE reservoir engineering*, 3(3): 1041-1047.

Benedict, M., Webb, G. B., and Rubin, L. C. 1940. An empirical equation for thermodynamic properties of light hydrocarbons and their mixtures I. Methane, ethane, propane and n-butane. *The Journal of Chemical Physics*, 8: 334-345.

Beret, S., and Prausnitz, J. M. 1975. Perturbed hard-chain theory: An equation of state for fluids containing small or large molecules. *AIChE Journal*, 21(6): 1123-1132.

Bergman, D. F. 1976. Predicting the phase behavior of natural gas in pipelines. PhD thesis, University of Michigan, United States.

Bishnoi, P. R., Heidemann, R. A., and Shah, M. K. 1977. Calculation of thermodynamic properties of bitumen systems. *CZM Special Volume*, *17*.

Carnahan, N. F., and Starling, K. E. 1969. Equation of state for non-attracting rigid spheres. *The Journal of Chemical Physics*, 51: 414-417.

Carnahan, N. F., and Starling, K. E. 1972. Intermolecular repulsions and the equation of state for fluids. *AIChE Journal*, 18(6): 1184-1189.

Cavett, R. H. 1962. Physical data for distillation calculations, Vapor-liquid equilibria. *API Proc., Sec. III, 42*.

Chao, K. C., and Seader, J. D. 1961. A general correlation of vapor-liquid equilibria in hydrocarbon mixtures. *AIChE Journal*, 7(4): 598-605.

Chapman, W. G., Gubbins, K. E., Jackson, G., and Radosz, M. 1990. New reference equation of state for associating liquids. *Industrial & Engineering Chemistry Research*, 29(8): 1709-1721.

Chou, G. F., and Prausnitz, J. M. 1989. A phenomenological correction to an equation of state for the critical region. *AIChE Journal*, 35(9): 1487-1496.

Christoforakos, M., and Franck, E. U. 1986. An equation of state for binary fluid mixtures to high temperatures and high pressures. *Berichte der Bunsengesellschaft für physikalische Chemie*, 90(9): 780-789.

Chueh, P. L., and Prausnitz, J. M. 1967a. Vapor-liquid equilibria at high pressures. Vapor-phase fugacity coefficients in nonpolar and quantum-gas mixtures. *Industrial & Engineering Chemistry Fundamentals*, 6(4): 492-498.

Chueh, P. L., and Prausnitz, J. M. 1967b. Vapor-liquid equilibria at high pressures: Calculation of partial molar volumes in nonpolar liquid mixtures.*AIChE Journal*, 13(6): 1099-1107.

Danesh, A. 1998. PVT and phase behaviour of petroleum reservoir fluids (Vol. 47). Elsevier.

Dennis, J. J. E., and Schnabel, R. B. 1983. Numerical methods for unconstrained optimization and nonlinear equations (Vol. 16). Siam.

Deo, M. D., Wang, C. J., and Hanson, F. V. 1991. Solubility of carbon dioxide in tar sand bitumen: experimental determination and modeling. *Industrial & Engineering Chemistry Research*, 30(3): 532-536.

Dhulesia, H. 1984. Equation fits ASTM distillations. *Hydrocarbon processing*, 62(9): 179-180.

Díaz, O. C., Modaresghazani, J., Satyro, M. A., and Yarranton, H. W. 2011. Modeling the phase behavior of heavy oil and solvent mixtures. *Fluid Phase Equilibria*, 304(1): 74-85.

Donohue, M. D., and Prausnitz, J. M. 1978. Perturbed hard chain theory for fluid mixtures: thermodynamic properties for mixtures in natural gas and petroleum technology. *AIChE Journal*, 24(5): 849-860.

Duan, J., Wang, W., Liu, H., and Gong, J. 2013. Modeling the characterization of the plus fractions by using continuous distribution function. *Fluid Phase Equilibria* 345: 1-10.

Eastick, R. R. 1989. Phase behaviour and viscosity of bitumen fractions saturated with CO_2. MSc thesis, University of Calgary, Calgary, Alberta, Canada.

Eastick, R. R., Svrcek, W. Y., and Mehrotra, A. K. 1992. Phase behaviour of CO2-bitumen fractions. *The Canadian Journal of Chemical Engineering*, 70(1): 159-164.

Edmister, W.C. 1958. Applied hydrocarbon thermodynamics, part 4, compressibility factors and equations of state, *Petroleum Refinery* 37: 173–179

Elizalde-Solis, O., Galicia-Luna, L. A., and Camacho-Camacho, L. E. 2007. High-pressure vapor–liquid equilibria for CO_2 alkanol systems and densities of *n*-dodecane and *n*-tridecane. *Fluid Phase Equilibria*, 259(1): 23-32.

Fink, J. 2011. Petroleum engineer's guide to oil field chemicals and fluids. Access Online via Elsevier.

Firoozabadi, A. 1999. Thermodynamics of hydrocarbon reservoirs. New York: McGraw-Hill.

Flory, P. J. 1965. Statistical thermodynamics of liquid mixtures. *Journal of the American Chemical Society*, 87(9): 1833-1838.

Frauenfeld, T., Gerald, K., and Zhou, S. 2002. PVT and viscosity measurements for Lloydminster-Aberfeldy and Cold Lake blended oil systems. In *SPE International Thermal Operations and Heavy Oil Symposium and International Horizontal Well Technology Conference*.

Frey, K. 2009. Improving thermodynamic property estimation through volume translation. PhD thesis, Massachusetts Institute of Technology, USA.

Fu, C. T., Puttagunta, V. R., and Hsi, C. 1987. Sensitivities in representing the phase behaviour of gas-bitumen systems. *The Canadian Journal of Chemical Engineering*, 65(2): 308-313.

Fu, C., Puttagunla, R., and Vilcsak, G. 1986a. Vapor-liquid equilibrium properties for gas-Cold Lake bitumen. *Annual Technical Meeting* Calgary Canada.

Fu, C. T., Puttagunta, R., Baumber, L., and Hsi, C. 1986b. Pseudo-critical properties of heavy oils and bitumens. *Fluid Phase Equilibria*, 30: 281-295.

Fu, C., and Puttagunta, R. 1986c. Binary interaction coefficients of the modified Soave-Redlich-Kwong equation of state for bitumen-containing systems at in-situ conditions. *Journal of Canadian Petroleum Technology*, 25(5): 38-43.

Gao, G., Daridon, J. L., Saint-Guirons, H., Xans, P., and Montel, F. 1992. A simple correlation to evaluate binary interaction parameters of the Peng-Robinson equation of state: binary light hydrocarbon systems. *Fluid phase equilibria*, 74: 85-93.

Gates, I. D. 2010. Solvent-aided Steam-Assisted Gravity Drainage in thin oil sand reservoirs. *Journal of Petroleum Science and Engineering*, 74(3): 138-146.

Ghasemi, M., Alavian, S. A., and Whitson, C. 2011. C7+ Characterization of Heavy Oil Based on Crude Assay Data. In *SPE Heavy Oil Conference and Exhibition*.

Gonzales, E., Colonomos, P., and Rusinek, I. 1986. A New Approach For Characterizing Oil Fractions, And For Selecting Pseudo-Components Of Hydrocarbons. *Journal of Canadian Petroleum Technology*, 25(2): 78-84.

Guggenheim, E. A. 1965. Variations on van der Waals' equation of state for high densities. *Molecular Physics*, 9(2): 199-200.

Han, S.J., Lin, H.M., and Chao, K.C. 1988. Vapour-Liquid Equilibrium of Molecular Fluid Mixtures by Equation of State. Chem. Eng. Sci. 43: 2327-2367.

Hong, K. C. 1982. Lumped-component characterization of crude oils for compositional simulation. In *SPE Enhanced Oil Recovery Symposium*.

Huang, H., and Sandler, S. I. 1993. Prediction of vapor-liquid equilibria at high pressures using activity coefficient parameters obtained from low-pressure data: a comparison of two equation of state mixing rules. *Industrial and Engineering Chemistry Research*, 32(7): 1498-1503.

Huang, S. H., and Radosz, M. 1990. Phase behavior of reservoir fluids II: Supercritical carbon dioxide and bitumen fractions. *Fluid Phase Equilibria*, 60(1): 81-98.

Huang, S. H., and Radosz, M. 1991a. Phase behavior of reservoir fluids IV: Molecular weight distributions for thermodynamic modeling. *Fluid Phase Equilibria*, 66(1): 23-40.

Huang, S. H., and Radosz, M. 1991b. Phase behavior of reservoir fluids III: Molecular lumping and characterization. *Fluid Phase Equilibria*, 66(1): 1-21.

Huron, M. J., and Vidal, J. 1979. New mixing rules in simple equations of state for representing vapour-liquid equilibria of strongly non-ideal mixtures. *Fluid Phase Equilibria*, 3(4): 255-271.

International Energy Agency, World Energy Outlook 2008

Iwai, Y., Margerum, M. R., and Lu, B. C. Y. 1988. A new three-parameter cubic equation of state for polar fluids and fluid mixtures. *Fluid Phase Equilibria*, 42: 21-41.

Jabr, N.M. 1990. Study of naphtha stabilization system with view to control naphtha product quality. MSc. Thesis, Kuwait University

Jamaluddin, A. K. M., Kalogerakis, N. E., and Chakma, A. 1991. Predictions of CO_2 solubility and CO_2 saturated liquid density of heavy oils and bitumens using a cubic equation of state. *Fluid phase equilibria*, 64: 33-48.

James, N. E., and Mehrotra, A. K. 1988. V-L-S multiphase equilibrium in bitumen-diluent systems. *The Canadian Journal of Chemical Engineering*, 66(5): 870-878.

Jhaveri, B., and Youngren, G. 1988. Three-parameter modification of the Peng-Robinson equation of state to improve volumetric predictions. *SPE reservoir engineering*, 3(3): 1033-1040.

Kariznovi, M. 2013. Phase behavior study and physical properties measurement for Athabasca bitumen/solvent systems applicable for thermal and hybrid solvent recovery processes. PhD thesis, University of Calgary, Calgary, Alberta, Canada.

Kariznovi, M., Nourozieh, H., and Abedi, J. 2011a. Experimental and modeling study of vapor-liquid equilibrium for propane/heavy crude systems at high temperature conditions. In *SPE Annual Technical Conference and Exhibition*, Denver, Colorado, USA, 30 October-2 November.

Kariznovi, M., Nourozieh, H., and Abedi, J. 2009. Bitumen characterization and pseudocomponents determination for equation of state modeling. *Energy & Fuels*, 24(1): 624-633.

Kariznovi, M., Nourozieh, H., and Abedi, J. 2010. Bitumen characterization and pseudocomponents determination for equation of state modeling. *Energy & Fuels*, 24(1): 624-633.

Kariznovi, M., Nourozieh, H., and Abedi, J. 2011b. Measurement and modeling of liquid saturated properties (solubility, density, and viscosity) of (ethane+ n-tetradecane) binary systems. *Journal of Chemical & Engineering Data*, 56(9): 3669-3672.

Kariznovi, M., Nourozieh, H., and Abedi, J. 2012. Measurement and equation of state prediction of vapor–liquid equilibrium and physical properties for the system methane + *n*-octadecane. *Fluid Phase Equilibria*, 314: 102-106.

Kariznovi, M., Nourozieh, H., and Abedi, J. 2013a. Experimental measurements and predictions of density, viscosity, and carbon dioxide solubility in methanol, ethanol, and 1-propanol. *The Journal of Chemical Thermodynamics*, 57: 408-415.

Kariznovi, M., Nourozieh, H., and Abedi, J. 2013a. Experimental results and thermodynamic investigation of carbon dioxide solubility in heavy liquid hydrocarbons and corresponding phase properties. *Fluid Phase Equilibria* 339: 105-111.

Kariznovi, M., Nourozieh, H., and Abedi, J. 2013b, Phase Composition and Saturated Liquid Properties in Binary and Ternary Systems Containing Carbon Dioxide, *n*-Decane, and *n*-Tetradecane. *J. Chem. Thermodynamics* 57: 189-196

Katz, D. 1983. Overview of phase behavior in oil and gas production. *Journal of Petroleum Technology*, *35*(6): 1205-1214.

Katz, D. L., & Firoozabadi, A. 1978. Predicting phase behavior of condensate/crude-oil systems using methane interaction coefficients. *Journal of Petroleum Technology*, 30(11): 1649-1655.

Kay, W. 1936. Gases and vapors at high temperature and pressure-density of hydrocarbon. *Industrial & Engineering Chemistry*, 28(9): 1014-1019.

Kesler, M. G., and Lee, B. I. 1976. Improve prediction of enthalpy of fractions. *Hydrocarbon Processing*, 55(3): 153-158.

Kokal, S., and Sayegh, S. 1990. Phase behavior and physical properties of CO-saturated heavy oil and its constitutive fractions. *Annual Technical Meeting*, Calgary, Alberta, Canada, 10-13 June.

Kordas, A., Magoulas, K., Stamataki, S., and Tassios, D. 1995. Methane-hydrocarbon interaction parameters correlation for the Peng-Robinson and the t-mPR equation of state. *Fluid Phase Equilibria*, 112(1): 33-44.

Kumar, A., and Okuno, R. 2012. Fluid characterization using an EOS for compositional simulation of enhanced heavy-oil recovery. In *SPE Annual Technical Conference and Exhibition*, San Antonio, Texas, USA, 8-10 October.

Kutney, M. C., Dodd, V. S., Smith, K. A., Herzog, H. J., and Tester, J. W. 1997. A hard-sphere volume-translated van der Waals equation of state for supercritical process modeling 1. Pure components. *Fluid Phase Equilibria*, 128(1): 149-171.

Lee, S.T., R.H. Jacoby, W.H. Chen, W.E. Culham, and Gulf Research and Development Co., 1981. Experimental and theoretical studies on the fluid properties required for simulation of thermal processes. *SPE Journal*., 21(5): 535-550.

Levenberg, K. 1944. A method for the solution of certain problems in least squares. *Quarterly of Applied Mathematics*, 2: 164-168.

Li, H., and Yang, D. 2010. Modified α function for the Peng− Robinson equation of state to improve the vapor pressure prediction of non-hydrocarbon and hydrocarbon compounds. *Energy & Fuels*, 25(1): 215-223.

Lin, H. M., and Chao, K. C. 1984. Correlation of critical properties and acentric factor of hydrocarbons and derivatives. *AIChE Journal*, 30(6): 981-983.

Lohrenz, J., Bray, B., and Clark, C. 1964. Calculating viscosities of reservoir fluids from their compositions. *Journal of Petroleum Technology*, 16(10): 1171-1176.

López, J. A., Trejos, V. M., and Cardona, C. A. 2009. Parameters estimation and VLE calculation in asymmetric binary mixtures containing carbon dioxide+*n*-alkanols. *Fluid Phase Equilibria*, 275(1): 1-7.

Magoulas, K., and Tassios, D. 1990. Thermophysical properties of *n*-alkanes from C_1 to C_{20} and their prediction for higher ones. *Fluid Phase Equilibria*, 56: 119-140.

Marquardt, D. W. 1963. An algorithm for least-squares estimation of nonlinear parameters. *Journal of the Society for Industrial & Applied Mathematics*, 11(2): 431-441.

Martin, J. J. 1967. Equations of state-applied thermodynamic symposium. *Industrial & Engineering Chemistry*, 59(12): 34-52.

Mathias, P. M., Naheiri, T., and Oh, E. M. 1989. A density correction for the Peng—Robinson equation of state. *Fluid Phase Equilibria*, 47(1): 77-87.

Mehra, R., Heidemann, R., Aziz, K., and Donnelly, J. 1982. A statistical approach for combining reservoir fluids into pseudo components for compositional model studies. In *SPE Annual Technical Conference and Exhibition*, New Orleans, Louisiana, USA, 26-29 September.

Mehrotra, A. K., and Svrcek, W. Y. 1985. Viscosity, density and gas solubility data for oil sand bitumens. Part I: Athabasca bitumen saturated with CO and C_2H_6. *AOSTRA J. Res*, 1(4): 263-268.

Mehrotra, A. K., and Svrcek, W. Y. 1988a. Properties of Cold Lake bitumen saturated with pure gases and gas mixtures. *The Canadian Journal of Chemical Engineering*, 66(4): 656-665.

Mehrotra, A. K., and Svrcek, W. Y. 1988b. Correlation and prediction of gas solubility in Cold Lake bitumen. *The Canadian Journal of Chemical Engineering*, 66(4): 666-670.

Mehrotra, A., Patience, G., and Svrcek, W. 1989. Calculation of gas solubility in Wabasca bitumen. *Journal of Canadian Petroleum Technology*, 28(3): 81-83.

Memon, A., Gao, J., Taylor, S., Engel, T., and Jia, N. 2010. A Systematic Workflow Process for Heavy Oil Characterization: Experimental Techniques and Challenges. In *Canadian*

Unconventional Resources and International Petroleum Conference, Calgary, Alberta, Canada, 19-21 October.

Montel, F., and Gouel, P. L. 1984. A new lumping scheme of analytical data for compositional studies. *In SPE Annual Technical Conference and Exhibition*, Houston, Texas, USA, 16-19 September.

Foster, N.R., Bezanehtak, K., and Dehghani, F. Retrieved from http://www.isasf.net/fileadmin/files/Docs/Versailles/Papers/PTs15.pdf

Nikos, V., Stewart, G., Todd, A.C., and Clancy, M. 1986. Phase behavior of systems comprising North Sea reservoir fluids and injection gases. *Journal of Petroleum Technology* 38: 1221‑1233.

Nji, G. N., Svrcek, W. Y., Yarranton, H., and Satyro, M. A. 2009. Characterization of heavy oils and bitumens 2. Improving the prediction of vapor pressures for heavy hydrocarbons at low reduced temperatures using the Peng− Robinson equation of state. *Energy & Fuels*, 23(1): 366-373.

Nourozieh, H. 2013. Phase Partitioning and thermo-physical properties of Athabasca bitumen/solvent mixtures. PhD thesis, University of Calgary, Calgary, Alberta, Canada.

Nourozieh, H., Kariznovi, M., and Abedi, J. 2012a. Phase equilibrium measurements and thermodynamic modeling of methane alcohol systems at ambient temperature. *The Journal of Chemical Thermodynamics*, 54: 165-170.

Nourozieh, H., Kariznovi, M., and Abedi, J. 2012b. Vapor–liquid equilibrium measurement and thermodynamic modeling of binary systems (methane+ *n*-tetradecane). *Fluid Phase Equilibria*, 318: 96-101.

Nourozieh, H., Kariznovi, M., and Abedi, J. 2012c. Experimental measurement and equation of state modeling of liquid saturated properties (solubility, density, and viscosity) of (ethane+ *n*-octadecane) binary systems. *Journal of Chemical & Engineering Data*, 57(1): 137-141.

Nourozieh, H., Kariznovi, M., and Abedi, J. 2013. Measurement and correlation of saturated liquid properties and gas solubility for decane, tetradecane and their binary mixtures saturated with carbon dioxide. *Fluid Phase Equilibria* 237: 246-254.

Onnes, H. K. 1901. Expression of the equation of state of gases and liquids by means of series. In *KNAW, Proceedings* 4: 1901-1902: 125-147.

Orbey, N., and Sandler, S. I. 1994. Vapor-liquid equilibrium of polymer solutions using a cubic equation of state. *AIChE journal*, 40(7): 1203-1209.

Panagiotopoulos, A. Z., and Reid, R. C. 1986. Multiphase high pressure equilibria in ternary aqueous systems. *Fluid Phase Equilibria*, 29: 525-534.

Patel, N. C., and Teja, A. S. 1982. A new cubic equation of state for fluids and fluid mixtures. *Chemical Engineering Science*, 37(3): 463-473.

Pedersen, K. S., Blilie, A. L., and Meisingset, K. K. 1992. PVT calculations on petroleum reservoir fluids using measured and estimated compositional data for the plus fraction. *Industrial & Engineering Chemistry Research*, 31(5): 1378-1384.

Pedersen, K. S., Thomassen, P., and Fredenslund, A. 1983. SRK-EOS calculation for crude oils. *Fluid Phase Equilibria*, 14: 209-218.

Pedersen, K. S., Thomassen, P., and Fredenslund, A. 1984. Thermodynamics of petroleum mixtures containing heavy hydrocarbons. 1. Phase envelope calculations by use of the Soave-Redlich-Kwong equation of state. *Industrial & Engineering Chemistry Process Design and Development*, 23(1): 163-170.

Péneloux, A., Rauzy, E., and Fréze, R. 1982. A consistent correction for Redlich-Kwong-Soave volumes. *Fluid Phase Equilibria*, 8(1): 7-23.

Peng, D. Y., and Robinson, D. B. 1976. A new two-constant equation of state.*Industrial & Engineering Chemistry Fundamentals*, 15(1): 59-64.

Prausnitz, J. M., Lichtenthaler, R. N., and de Azevedo, E. G. 1999. *Molecular thermodynamics of fluid-phase equilibria*. Pearson Education.

Prigogine, I., Bellemans, A., and Mathot, V. 1957. The molecular theory of solutions (Vol. 4). Amsterdam: North-Holland.

Quiñones-Cisneros, S. E., Zéberg-Mikkelsen, C. K., and Stenby, E. H. 2003. Friction theory prediction of crude oil viscosity at reservoir conditions based on dead oil properties. *Fluid Phase Equilibria*, 212(1): 233-243.

Quiñones-Cisneros, S. E., Zéberg-Mikkelsen, C. K., Baylaucq, A., and Boned, C. 2004. Viscosity modeling and prediction of reservoir fluids: From natural gas to heavy oils. *International Journal of Thermophysics*, 25(5): 1353-1366.

Rachford Jr, H. H., and Rice, J. D. 1952. Procedure for use of electronic digital computers in calculating flash vaporization hydrocarbon equilibrium. *Journal of Petroleum Technology*, 4(10): 327-328.

Redlich, O., and Kwong, J. N. S. 1949. On the Thermodynamics of Solutions. V. An Equation of State. Fugacities of Gaseous Solutions. *Chemical Reviews*, 44(1): 233-244.

Riazi, M. R. 1989. Distribution model for properties of hydrocarbon-plus fractions. *Industrial & Engineering Chemistry Research*, 28(11): 1731-1735.

Riazi, M. R. 1997. A continuous model for C7+ fraction characterization of petroleum fluids. *Industrial & Engineering Chemistry Research*, 36(10): 4299-4307.

Riazi, M. R. 2005. Characterization and properties of petroleum fractions (Vol. 50). West Conshohocken, PA: ASTM international.

Riazi, M. R., and Al-Sahhaf, T. A. 1996. Physical properties of heavy petroleum fractions and crude oils. *Fluid Phase Equilibria*, 117(1): 217-224.

Riazi, M. R., and Daubert, T. E. 1980. Simplify property predictions. *Hydrocarbon Process*, 59(3): 115-116.

Robinson, D. B., and Peng, D. Y. 1978. The characterization of the heptanes and heavier fractions for the GPA Peng-Robinson programs. Gas Processors Association.

Robinson, D.B., and Associates (1981). "EQUI-PHASE" Computer Software Package. Edmonton, Alberta, Canada.

Rodgers, P. A., Creagh, A. L., Prange, M. M., and Prausnitz, J. M. 1987. Molecular weight distribution for heavy fossil fuels from gel-permeation chromatography and characterization data. *Industrial & Engineering Chemistry Research*, 26(11): 2312-2318.

Rodriguez, I., and Hamouda, A. 2010. An approach for characterization and lumping of plus fractions of heavy oil. *SPE Reservoir Evaluation & Engineering*, 13(2): 283-295.

Rowlinson, J.S. and Swinton, F.L. 1982. Liquids and Liquid Mixtures. 3rd edition. Butterworths, Wolhom, MA

Salim, P.H., and Trebble, M. A., 1995. A generalized equation of state approach to the prediction of phase behavior in CO_2-bitumen systems," *The Journal of Supercritical Fluids*, 8: 6-14

Sigmund, P. M., and Trebble, M. A. 1992. Phase behaviour prediction in supercritical systems using generalized solute critical properties. *The Canadian Journal of Chemical Engineering*, 70(4): 814-817.

Sancet, G. N. 2007. Heavy fraction C7+ characterization for PR-EOS. In *SPE Annual Technical Conference and Exhibition*.

Sánchez, S., Ancheyta, J., & McCaffrey, W. C. (2007). Comparison of probability distribution functions for fitting distillation curves of petroleum. *Energy & Fuels*, *21*(5), 2955-2963.

Sandoval, R., Wilczek-Vera, G., and Vera, J. H. 1989. Prediction of ternary vapor-liquid equilibria with the PRSV equation of state. *Fluid Phase Equilibria*, 52: 119-126.

Schlijper, A. G. 1986. Simulation of compositional processes: the use of pseudo components in equation-of-state calculations. *SPE Reservoir Engineering*, 1(5): 441-452.

Schwartzentruber, J., Galivel-Solastiouk, F., and Renon, H. 1987. Representation of the vapor-liquid equilibrium of the ternary system carbon dioxide- propane- methanol and its binaries with a cubic equation of state: a new mixing rule. *Fluid Phase Equilibria*, 38(3): 217-226.

Sim, W. J., and Daubert, T. E. 1980. Prediction of vapor-liquid equilibria of undefined mixtures. *Industrial & Engineering Chemistry Process Design and Development*, 19(3): 386-393.

Smith, J.M., Van Ness, H., and Abbott, M. 2005. Introduction to Chemical Engineering Thermodynamics. The Mcgraw-Hill Chemical Engineering Series

Soave, G. 1972. Equilibrium constants from a modified Redlich-Kwong equation of state. *Chemical Engineering Science*, 27(6): 1197-1203.

Soreide, I. 1989. Improved phase behavior predictions of petroleum reservoir fluids from a cubic equation of state. PhD thesis, The Norwegian Institute of Technology.

Spear, R. R., Robinson Jr, R. L., and Chao, K. C. 1971. Critical states of ternary mixtures and equations of state. *Industrial & Engineering Chemistry Fundamentals*, 10(4): 588-592.

Speight, J. G. 2010. The chemistry and technology of petroleum. CRC press.

Stryjek, R., and Vera, J. H. 1986. PRSV: An improved Peng—Robinson equation of state for pure compounds and mixtures. *The Canadian Journal of Chemical Engineering*, 64(2): 323-333.

Svrcek, W., and Mehrotra, A. K. 1982. Gas solubility, viscosity and density measurements for Athabasca bitumen. *Journal of Canadian Petroleum Technology*, 21(4): 31-38.

Tsai, J. C., and Chen, Y. P. 1998. Application of a volume-translated Peng-Robinson equation of state on vapor-liquid equilibrium calculations. *Fluid phase equilibria*, 145(2): 193-215.

Tsonopoulos, C., and Prausnitz, J. M. 1969. A review for engineering applications. *Cryogenics*, 9(5): 315-327.

Twu, C. H. 1983. Prediction of thermodynamic properties of normal paraffins using only normal boiling point. *Fluid Phase Equilibria*, 11(1): 65-81.

Twu, C. H. 1984. An internally consistent correlation for predicting the critical properties and molecular weights of petroleum and coal-tar liquids. *Fluid Phase Equilibria*, 16(2): 137-150.

Twu, C. H., and Chan, H. S. 2009. Rigorously universal methodology of volume translation for cubic equations of state. *Industrial & Engineering Chemistry Research*, 48(12): 5901-5906.

Twu, C. H., Coon, J. E., and Cunningham, J. R. 1995. A new generalized alpha function for a cubic equation of state Part 1. Peng-Robinson equation. *Fluid Phase Equilibria*, 105(1): 49-59.

USGS FS2006-3133_508, web PDF file: http://pubs.usgs.gov/fs/2006/3133/pdf/FS2006-3133_508.pdf

van der Waals, J.D. 1873 "On the Continuity of the Gaseous and Liquid States," PhD Thesis, Leiden.

Voros, N. G., and Tassios, D. P. 1993. Vapor-liquid equilibria in nonpolar/weakly polar systems with different types of mixing rules. *Fluid Phase Equilibria*, 91(1): 1-29.

Voros, N., Stamataki, S., and Tassios, D. 1994. Effect of translation on the prediction of saturated densities of binary mixtures with a Peng-Robinson equation of state. *Fluid Phase Equilibria*, 96: 51-63.

Wang, J. L. 2012. Global phase diagram and critical phenomena of binary mixtures.PhD Thesis, Swinburne University of Technology.

Watson, K. M., and Nelson, E. F. 1933. Improved methods for approximating critical and thermal properties of petroleum fractions. *Industrial & Engineering Chemistry*, 25(8): 880-887.

Watson, P., Cascella, M., May, D., Salerno, S., and Tassios, D. 1986. Prediction of vapor pressures and saturated molar volumes with a simple cubic equation of state: Part II: The Van der Waals-711 EOS. *Fluid Phase Equilibria*, 27: 35-52.

Wei, Y. S., and Sadus, R. J. 2000. Equations of state for the calculation of fluid-phase equilibria. *AIChE Journal*, 46(1): 169-196.

Whitson, C. 1983. Characterizing hydrocarbon plus fractions. *SPE Journal*, 23(4): 683-694.

Whitson, C. H., and Brulé, M. R. 2000. *Phase behavior*. Richardson, Tex.: Henry L. Doherty Memorial Fund of AIME, Society of Petroleum Engineers.

Whitson, C., and Ghasemi, M. 2013. Phase behavior and viscosity modeling of Athabasca bitumen and light solvent mixtures. In *2013 SPE Heavy Oil Conference-Canada*.

Willman, B., and Teja, A. S. 1987. Prediction of dew points of semicontinuous natural gas and petroleum mixtures. 1. Characterization by use of an effective carbon number and ideal solution predictions. *Industrial & Engineering Chemistry Research*, 26(5): 948-952.

Wilson, G. M. 1968. A modified Redlich-Kwong equation of state, application to general physical data calculations. In *65th National AIChE Meeting, Cleveland, OH*.

Wong, D. S. H., and Sandler, S. I. 1992. A theoretically correct mixing rule for cubic equations of state. *AIChE Journal*, 38(5): 671-680.

Xavier, G. M., Boaventura, K. M., and Peixoto, F. C. 2011. On the use of continuous distribution models for characterization of crude oils. *Latin American Applied Research*, 41(4): 325-329.

Yazdani, A., and Maini, B. 2007. Measurements and modeling of phase behaviour and viscosity of a heavy oil-butane system. In *Canadian International Petroleum Conference*.

Yu, J. M., Huang, S. H., and Radosz, M. 1989. Phase behavior of reservoir fluids: supercritical carbon dioxide and cold lake bitumen. *Fluid Phase Equilibria*, 53: 429-438.

Zabel, F., Law, D., Taylor, S., and Zuo, J. 2008. Impact of uncertainty of heavy oil fluid property measurement. *In Canadian International Petroleum Conference*, Calgary, Alberta, Canada, 17-19 June.

Appendix I

(Development of Fugacity Coefficient Expression)

The PR EoS is given by:

$$P = \frac{RT}{v-b} - \frac{a}{v(v+b)+b(v-b)} = \frac{RT}{v-b} - \frac{a}{v^2+2vb-b^2}$$

The mixing rules are defined like:

$$a = \sum_{i=1}^{m}\sum_{j=1}^{m} x_i x_j a_{ij} = \frac{1}{n_T{}^2}\sum_{i=1}^{m}\sum_{j=1}^{m} n_i n_j a_{ij}$$

$$b = \sum_{i=1}^{m}\sum_{j=1}^{m} x_i x_j b_{ij} = \frac{1}{n_T{}^2}\sum_{i=1}^{m}\sum_{j=1}^{m} n_i n_j b_{ij}$$

The fugacity can be defined as a function of Helmholtz free energy:

$$\ln \phi_i = \left(\frac{\partial}{\partial n_i} \frac{\left(A - A^{IG}\right)}{RT} \right)_{T,V,n_j} - \ln Z$$

While by having expression of residual Helmholtz free energy we have:

$$\frac{\left(A - A^{IG}\right)}{RT} = -n_T \ln(1-b\rho) - \frac{a n_T{}^2}{\sqrt{8}bRTn_T}\left[\ln\left(1+(1+\sqrt{2})b\rho\right) - \ln\left(1+(1-\sqrt{2})b\rho\right)\right]$$

$$\left(\frac{\partial\left(A-A^{IG}\right)/RT}{\partial n_i}\right)_{T,V,n_j} = -\ln(1-b\rho)\left(\frac{\partial(b\rho)}{\partial n_i}\right) - \frac{\partial n^2{}_T}{\sqrt{8}bRTn_T}\left[\frac{\left(1+\sqrt{2}\right)\left(\frac{\partial(b\rho)}{\partial n_i}\right)}{1+(1+\sqrt{2})b\rho} - \frac{\left(1-\sqrt{2}\right)\left(\frac{\partial(b\rho)}{\partial n_i}\right)}{1+(1-\sqrt{2})b\rho}\right]$$

$$-\ln\left[\frac{1+(1+\sqrt{2})b\rho}{1+(1-\sqrt{2})b\rho}\right]\left[\frac{\left(\frac{\partial\left(an^2{}_T\right)}{\partial n_i}\right)}{\sqrt{8}bRTn_T} - \frac{an^2{}_T}{\sqrt{8}RT}\frac{\left(\frac{\partial(n_Tb)}{\partial n_i}\right)}{\left(n_Tb\right)^2}\right]$$

And the derivatives are calculated with following equations:

$$\left(\frac{\partial\left(n_T^2a\right)}{\partial n_i}\right)_{n_j} = \left(\frac{\partial\left[\sum_{i=1}^{m}\sum_{j=1}^{m}n_in_ja_{ij}\right]}{\partial n_i}\right)_{n_j} = \left(\frac{\partial\left[\sum_{i=1}^{m}n_i\sum_{j=1}^{m}n_ja_{ij}\right]}{\partial n_i}\right)_{n_j} = 2\sum_{k=1}^{m}n_ka_{ik}$$

$$\left(\frac{\partial(n_Tb)}{\partial n_i}\right)_{n_j} = \left(\frac{\partial\left[\frac{1}{n_T}\sum_{i=1}^{m}\sum_{j=1}^{m}n_in_jb_{ij}\right]}{\partial n_i}\right)_{n_j} = \frac{1}{n_T}\left(\frac{\partial\left[\sum_{i=1}^{m}\sum_{j=1}^{m}n_in_jb_{ij}\right]}{\partial n_i}\right) - \frac{1}{n_T^2}\sum_{i=1}^{m}\sum_{j=1}^{m}n_in_jb_{ij}$$

$$= \frac{1}{n_T}\left(\frac{\partial\left[\sum_{i=1}^{m}n_i\sum_{j=1}^{m}n_jb_{ij}\right]}{\partial n_i}\right) - b = 2\sum_{k=1}^{m}x_kb_{ik} - b$$

For single summation mixing rule we have:

$$\left(\frac{\partial(n_Tb)}{\partial n_i}\right)_{n_j} = b_i$$

Plugging these equations in fugacity coefficient equation, we will have:

$$\ln \varphi_i = -\ln Z - \ln(1-b\rho) + \frac{\rho a\left(2\sum_{k=1}^{m} x_k b_{ik} - b\right)}{\sqrt{8}bRT} - \frac{\rho a\left(2\sum_{k=1}^{m} x_k b_{ik} - b\right)}{\sqrt{8}bRT}\left[\frac{\left(1+\sqrt{2}\right)}{1+(1+\sqrt{2})b\rho} - \frac{\left(1-\sqrt{2}\right)}{1+(1-\sqrt{2})b\rho}\right]$$

$$- \frac{a}{\sqrt{8}bRT}\ln\left[\frac{1+(1+\sqrt{2})b\rho}{1+(1-\sqrt{2})b\rho}\right]\left[\frac{2\sum_{k=1}^{m} x_k a_{ik}}{a} - \frac{\left(2\sum_{k=1}^{m} x_k b_{ik} - b\right)}{b}\right]$$

$$Z = \frac{1}{1-b\rho} - \frac{a\rho}{RT}\frac{1}{1+2b\rho-b^2\rho^2}$$

$$b\rho = \frac{B}{Z}$$

$$\frac{a}{bRT} = \frac{A}{B}$$

Therefore the final correlation would be:

$$\ln \varphi_i = -\ln(Z-B) - \frac{\left(2\sum_{k=1}^{m} x_k b_{ik} - b\right)P}{RTB}(Z-1) - \frac{A}{\sqrt{8}B}\ln\left[\frac{Z+(1+\sqrt{2})B}{Z+(1-\sqrt{2})B}\right]$$

$$\left[\frac{\left(2\sum_{k=1}^{m} x_k a_{ik}\right)P}{\left(R^2T^2\right)A} - \frac{\left(2\sum_{k=1}^{m} x_k b_{ik} - b\right)P}{RTB}\right]$$

Appendix II

(Wong-Sandler Mixing Rule)

Wong and Sandler (1992) developed their mixing rule by equivalence of excess Helmholtz energy of an equation of state by an activity coefficient model. At a given temperature, pressure and composition, the Helmholtz free energy for PR EOS will be

$$\frac{\left(\overline{A}-\overline{A}^{IGM}\right)}{RT}=-\ln\left[\frac{P(\overline{V}-b)}{RT}\right]+\frac{a}{2\sqrt{2}bRT}\ln\left[\frac{\overline{V}+(1-\sqrt{2})b}{\overline{V}-(1-\sqrt{2})b}\right]$$

Where $\bar{A}$ is the molar Helmholtz free energy and superscript *IGM* refers to ideal gas mixture. When the pressure goes to infinity, the equation will be

$$\lim_{p\to\infty}\frac{\left(\overline{A}-\overline{A}^{IG}\right)}{RT}=\frac{a}{bRT}C$$

Superscript *IG* denotes to ideal gas. Where

$$C=\frac{1}{\sqrt{2}}\ln(\sqrt{2}-1)$$

Therefore, the excess Helmholtz free energy at infinite pressure will be written as,

$$\frac{\overline{A}_{\infty}^{E}}{CRT}=\frac{a_m}{b_mRT}-\sum_i x_i\frac{a_i}{b_iRT}$$

$\overline{A}_{\infty}^{E}$ is excess molar Helmholtz free energy at infinite energy state. Wong and Sandler [9] showed that

$$b_m = \frac{Q}{1-D}$$

$$\frac{a_m}{RT} = Q\frac{D}{(1-D)}$$

where D and Q defined as,

$$Q = \sum_i \sum_j x_i x_j \left(b - \frac{a}{RT} \right)_{ij}$$

and

$$D = \sum_i x_i \frac{a_i}{b_i RT} + \frac{\overline{A}_\infty^E}{CRT}$$

For PR EoS, they calculated fugacity coefficient by,

$$\ln \phi_i = -\ln\left[\frac{P(\overline{V} - b_m)}{RT} \right] + \frac{1}{b_m}\left(\frac{\partial n b_m}{\partial n_i} \right)\left(\frac{P\overline{V}}{RT} - 1 \right)$$
$$+ \frac{1}{2\sqrt{2}}\left(\frac{a_m}{b_m RT} \right)\left[\frac{1}{a_m}\left(\frac{1}{n}\frac{\partial n^2 a_m}{\partial n_i} \right) - \frac{1}{b_m}\frac{\partial n b_m}{\partial n_i} \right] \ln\left[\frac{\overline{V} + b_m(1-\sqrt{2})}{\overline{V} + b_m(1+\sqrt{2})} \right]$$

The partial derivatives of a_m and b_m can be calculated as,

$$\frac{\partial n b_m}{\partial n_i} = \frac{1}{(1-D)}\left(\frac{1}{n}\frac{\partial n^2 Q}{\partial n_i} \right) - \frac{Q}{(1-D)^2}\left(1 - \frac{\partial n D}{\partial n_i} \right)$$

$$\frac{1}{RT}\left(\frac{1}{n}\frac{\partial n^2 a_m}{\partial n_i} \right) = D\frac{\partial n b_m}{\partial n_i} + b_m \frac{\partial n D}{\partial n_i}$$

The partial derivatives of Q and D are:

$$\left(\frac{1}{n}\frac{\partial n^2 Q}{\partial n_i}\right) = 2\sum_j x_j \left(b - \frac{a}{RT}\right)_{ij}$$

$$\frac{\partial nD}{\partial n_i} = \frac{a_i}{b_i RT} + \frac{\ln \gamma_{\infty i}}{C}$$

For the activity coefficient at infinite pressure state we have:

$$\ln \gamma_{\infty i} = \frac{1}{RT}\frac{\partial n\overline{A}_{\infty}^{E}}{\partial n_i}$$

where $\gamma_{\infty}$is the activity coefficient at infinite pressure. For calculating activity coefficient, any model can be used; Wong and Sandler used NRTL model:

$$\frac{\overline{A}_{\infty}^{E}}{RT} = \sum_i x_i \left(\frac{\sum_j x_j \tau_{ji} g_{ji}}{\sum_k x_k g_{ki}}\right)$$

where τ and g are NRTL model binary interaction parameters and local composition factor for NRTL model, respectively, and g is calculated by,

$$g_{ji} = \exp(-\alpha_{ij}\tau_{ij})$$

where α is NRTL model parameter. The activity coefficient of component *i*, is calculated by,

$$\ln \gamma_{\infty i} = \frac{\sum_j x_j \tau_{ji} g_{ji}}{\sum_k x_k g_{ki}} + \sum_j \frac{x_j g_{ij}}{\sum_k x_k g_{kj}} \left(\tau_{ij} - \frac{\sum_l x_l \tau_{lj} g_{lj}}{\sum_k x_k g_{kj}}\right)$$